Award Number: W81XWH-11-1-0242

TITLE: Assessment of Nanobiotechnology-Targeted siRNA Designed to Inhibit NF-kappaB Classical and Alternative Signaling in Breast Tumor Macrophages

PRINCIPAL INVESTIGATOR: Fiona Yull

CONTRACTING ORGANIZATION: The Vanderbilt University, Nashville, TN 37240

REPORT DATE: July 2012

TYPE OF REPORT: Annual

PREPARED FOR: U.S. Army Medical Research and Materiel Command
Fort Detrick, Maryland 21702-5012

REPORT DOCUMENTATION PAGE

Form Approved
OMB No. 0704-0188

1. REPORT DATE *(DD-MM-YYYY)*	2. REPORT TYPE	3. DATES COVERED *(From - To)*
01-07-2012	Annual	1 JUL 2011 - 30 JUN 2012

4. TITLE AND SUBTITLE

Assessment of Nanobiotechnology-Targeted siRNA Designed to Inhibit NF-kappaB Classical and Alternative Signaling in Breast Tumor Macrophages

5a. CONTRACT NUMBER

5b. GRANT NUMBER

W81XWH-11-1-0242

5c. PROGRAM ELEMENT NUMBER

6. AUTHOR(S)

Fiona Yull

E-Mail: fiona.yull@vanderbilt.edu

5d. PROJECT NUMBER

5e. TASK NUMBER

5f. WORK UNIT NUMBER

7. PERFORMING ORGANIZATION NAME(S) AND ADDRESS(ES)

The Vanderbilt University
Nashville, TN 37240

8. PERFORMING ORGANIZATION REPORT NUMBER

9. SPONSORING / MONITORING AGENCY NAME(S) AND ADDRESS(ES)

U.S. Army Medical Research and Materiel Command
Fort Detrick, Maryland 21702-5012

10. SPONSOR/MONITOR'S ACRONYM(S)

11. SPONSOR/MONITOR'S REPORT NUMBER(S)

12. DISTRIBUTION / AVAILABILITY STATEMENT

Approved for Public Release; Distribution Unlimited

13. SUPPLEMENTARY NOTES

14. ABSTRACT

Macrophages have been proposed as a potential target for manipulation of the microenvironment in breast cancer because they are potent effectors of the immune system. NF-kappaB (NF-κB) signaling in macrophages contributes to their impact during breast tumorigenesis. Thus, macrophage-targeted modulation of NF-κB has potential as a novel therapeutic approach for breast cancer. NF-κB signaling is mediated via two major pathways; the canonical/classical pathway and the alternative pathway. Our strategy is designed to develop a nanobiotechnology-based method to target siRNA designed to inhibit NF-κB classical and alternative signaling specifically to tumor associated macrophages to modulate the tumor microenvironment and to test the therapeutic potential of this approach. In this highly collaborative study, we have synthesized and characterized in vitro both mannosylated and untargeted nanoparticles. We have compared the efficiency of transfection of bone marrow derived macrophages between nanoparticles and commercial transfection reagents. We have started to investigate the effects of modulation of the NF-κB pathways on macrophage phenotype. Finally, we have performed initial in vivo studies that suggest that tumor associated macrophage specific targeting will be feasible in the context of primary tumors and metastases in the lung.

15. SUBJECT TERMS

Nanoparticles, NF-kappaB, macrophages, alternative NF-kappaB

16. SECURITY CLASSIFICATION OF:			17. LIMITATION OF ABSTRACT	18. NUMBER OF PAGES	19a. NAME OF RESPONSIBLE PERSON
a. REPORT	b. ABSTRACT	c. THIS PAGE			USAMRMC
U	U	U	UU	916	19b. TELEPHONE NUMBER *(include area code)*

Table of Contents

INTRODUCTION

Macrophages have been proposed as a potential target for manipulation of the microenvironment in breast cancer because they are potent effectors of the immune system, demonstrating the ability to secrete a wide range of intercellular signals from pro-inflammatory cytokines and chemokines, to growth and pro-angiogenic factors [1, 2]. NF-kappaB (NF-κB) signaling in macrophages contributes to their impact during breast tumorigenesis [3-9]. Thus, macrophage-targeted modulation of NF-κB has potential as a novel therapeutic approach for breast cancer. NF-κB signaling is mediated via two major pathways; the canonical/classical pathway and the alternative pathway both of which have been implicated in oncogenesis [10-13] (Figure 1). Our strategy is designed to use siRNA-mediated knockdown of expression of key proteins within each pathway to examine their individual and combined roles with respect to potential breast cancer immunotherapy. We selected as our initial targets the IKKβ activator (canonical) or p52 (alternative) proteins. In order to harness inhibition of these pathways to modulate the tumor microenvironment we intend to deliver siRNA specifically to tumor-associated-macrophages (TAMs). Therefore, the proposed work seeks to synthesize, characterize and assess multifunctional nanoparticles for siRNA delivery specifically to tumor-associated-macrophages (TAMs). The nanoparticles will have the capacity for siRNA association, protection and endosome release combined with tissue/cell specific delivery. They are intended to knockdown protein expression of NF-κB modulators with exceptional specificity for TAMs. TAM-specific nanoparticle targeting offers an innovative approach to enable NF-κB modulation *in vivo* through highly localized siRNA knockdown of critical, pathway-specific proteins that control NF-κB. The proposed approach is a novel combination intended to treat primary and metastatic breast cancer, the phase of this disease with the poorest clinical outcomes.

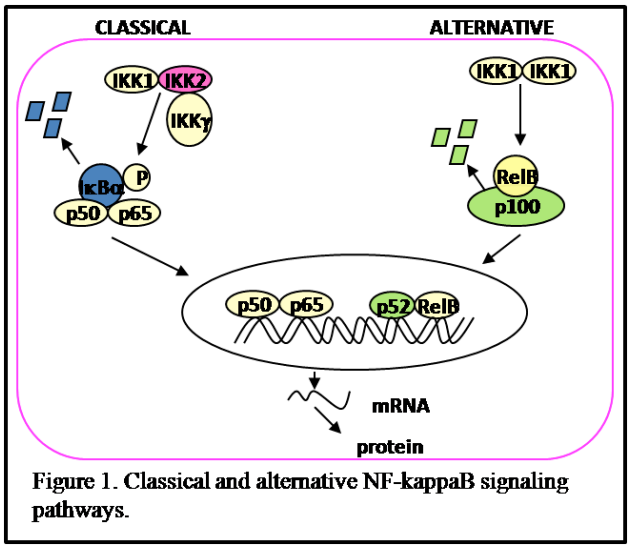

Figure 1. Classical and alternative NF-kappaB signaling pathways.

The ***hypothesis*** to be tested is that siRNA-mediated inhibition of NF-κB signaling in TAMs will decrease primary tumor growth and metastatic potential. Our ***objectives*** are (1) exploration of macrophage response to inhibition of NF-κB activation by the canonical and alternative pathways, separately and in combination using siRNA knockdown *in vitro* and (2) development of a nanobiotechnology delivery vehicle with the capacity for siRNA delivery TAMs for the purpose of pathway-specific NF-κB knockdown *in vivo*.

BODY

Task 1. Generate siRNA-delivering nanoparticles and optimize dosage *in vitro* in cell cultures of murine bone marrow derived macrophages (BMDM):

1a. Synthesize and fluorescently tag copolymer poly-HPMA-bl-DMAEMA-bl-[DMAEMA-co-PAA-co-BMA], and attach macrophage targeting peptide onto the HPMA end.

Completed by the Giorgio lab (see BC102696 annual report for details).

1b. Verify pH-responsive endosomolytic activity of new copolymer in hemolysis assays, and characterize polymer physical properties (light scattering, TEM, siRNA complexation assays).

Completed by the Giorgio lab (see BC102696 annual report for details).

1c. Expose BMDM from NGL reporter transgenics in culture to the nanoparticles. Quantify peptide-specific & dose-dependent delivery of nanoparticles to the BMDMs by fluorescence microscopy and flow cytometry.

As a preliminary step, BMDM's were generated from wild type, FVB mice. Bone marrow derived macrophages (BMDMs) are prepared by isolating bone marrow from the femurs of adult mice on an FVB background. The bone marrow is then plated in BMDM culturing media, which contains a source of colony stimulating factor 1 (CSF-1) for 6 days. After 6 days, the non-adherent cells are discarded and the adherent cells are manually scraped from the plates and re-plated in 6- or 12-well plates. These initialcultures were utilized to demonstrate efficient delivery of FAM-siRNA into BMDMs via mannosylated (targeted) nanoparticles termed ManNPs as determined by flow cytometry and confocal fluorescence analysis. This targeting can be inhibited by the presence of free mannose (see BC102696 annual report, abstracts and Yu *et al* manuscript appendices for additional details).

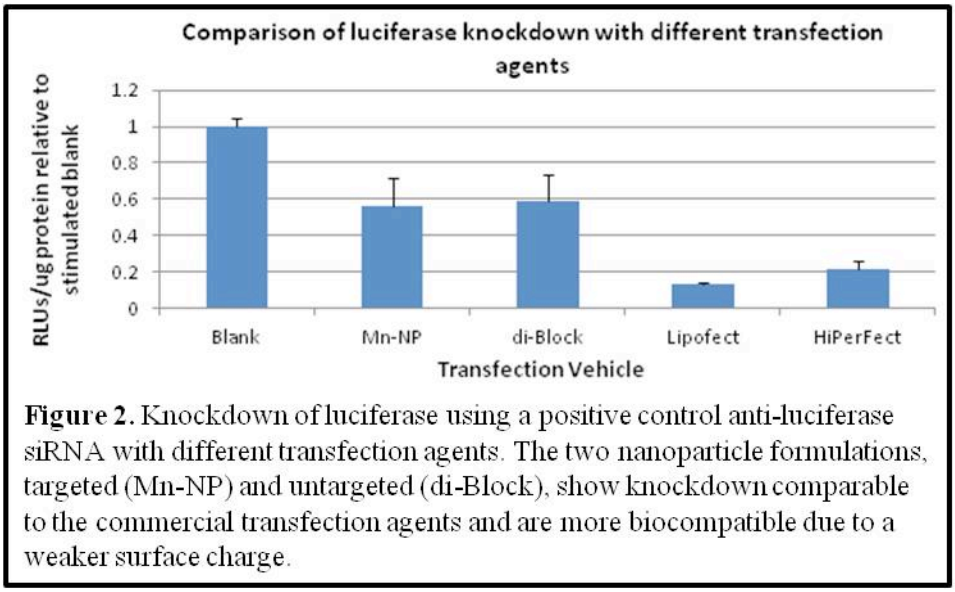

Figure 2. Knockdown of luciferase using a positive control anti-luciferase siRNA with different transfection agents. The two nanoparticle formulations, targeted (Mn-NP) and untargeted (di-Block), show knockdown comparable to the commercial transfection agents and are more biocompatible due to a weaker surface charge.

To further confirm these initial studies, we began using the NGL reporter transgenics to test delivery of nanoparticle encapsulated siRNA. Heterozygous NGL transgenics carry a GFP-Luciferase fusion that is responsive to NF-κB activation and thus acts as a surrogate reporter of NF-κB activation. A breeding colony of NGL transgenics was maintained for studies using BMDMs. Bone marrow was harvested from reporter transgenics and BMDM cultures were generated, as described above. Macrophages were plated in 12-well plates (200,000 cell per well) for luciferase assay experiments and in 6-well plates (2,000,000 cell per well) for RT-PCR experiments. The cells were transfected with positive control siRNA strands against luciferase (luciferase assay) or against GAPDH (RT-PCR) to show the knockdown potential of the nanoparticles as compared to other transfection agents. Lipofectamine and HiPerFect were chosen to represent commercially available agents (please refer below to aim 1d for detailed discussion of the merits of these two agents the protocol used for transfection). An untargeted (di-block-NP) and targeted (Mn-NP) nanoparticle were used as our experimental agents. One initial advantage that our materials have over the commercial materials is that the commercial materials cannot be used *in vivo* while our nanoparticle transfection agents have shown high biocompatibility in hemolysis assays and in *in vivo* murine use. **Figures 2 and 3** show that the targeted nanoparticle formulation appears to be more

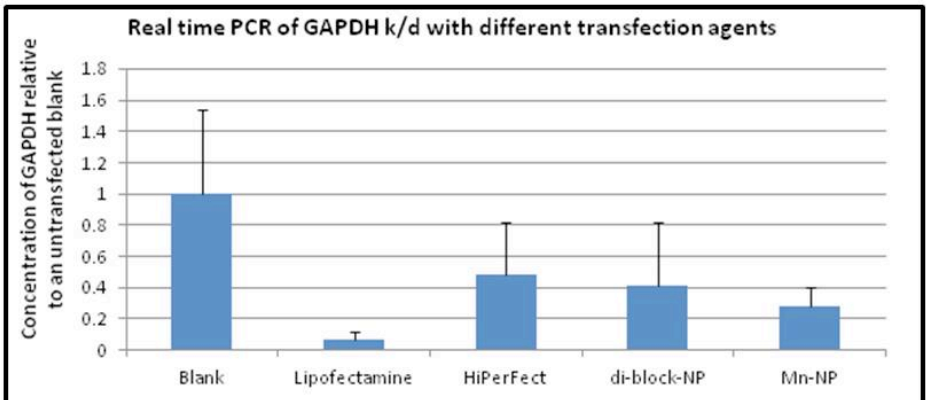

Figure 3. Knockdown of GAPDH using a positive control anti-GAPDH siRNA with different transfection agents. As with the luciferase assay, Lipofectamine is shown to be the most effective transfection agent, but the two nanoparticle formulations also show comparable knockdown, with the targeted Mn-NPs showing approximately 70% knockdown of GAPDH mRNA.

effective at transfecting macrophages than the untargeted nanoparticle. Furthermore, the targeted particles are approximately as effective as the HiPerFect transfection agent, and have proven to be more reliable in repeat experiments. While the Lipofectamine transfection agent has shown the highest transfection efficacy, it must be considered in the context that this agent cannot be used for *in vivo* applications, while the targeted nanoparticles, which show comparable knockdown, can be used *in vivo*.

1d. Deliver IKK2 and p52 siRNA alone and in combination to BMDMs from NGL reporter transgenics in vitro and assess modulation of NF-κB activity by luciferase assay and western analysis of nuclear protein extracts to quantify p65 or p52 translocation to the nucleus as a measure of activation of the canonical and alternative NF-κB pathways. Further, assess resulting phenotype with respect to M2 → M1 markers by RT-PCR to quantify expression of target genes correlated with M1 (iNOS, MIP1-α, IL-12) or M2 (IL-10, CCL17, mannose receptor) phenotypes.

As stated in aim 1c, cells from NGL mice produce luciferase as an indicator of NF-κB pathway activation, allowing for a bioluminescence assay measuring luciferase activity to act as a surrogate measurement of NF-κB activity. In order to represent a biological immunogenic stimulus relevant to an *in vitro* tumor associated macrophage model, the plated cells are stimulated with TNF-α. An initial experiment was performed to verify the effect of the TNF-α on the BMDMs. BMDMs were plated in 6-well plates at a cell density of 2 million cells per well. Cells were exposed to TNF-α at a concentration of 10 ng/ml for 6 hrs. RNA was then isolated from the cells and real time PCR was performed to determine the effect of TNF-α stimulation on expression of key NF-κB proteins and macrophage cell products. **Figure 4** shows the results of this first experiment from which we concluded that our initial supposition that p100/p52 is a good target for knockdown using siRNA was accurate because it is upregulated when BMDMs are stimulated as stated above. These same results also indicated that IKKβ may have less efficacy as a target because levels of mRNA for this protein are unchanged with TNF-α stimulation of cells.

In order to choose efficacious siRNA sequences andachieve knock down of the NF-κB pathways, it was necessary to create a set of controls utilizing commercial transfection agents to deliver siRNAs to BMDMs *in vitro*. The commercial agent transfections serve as both a proving ground for potentially therapeutic siRNA targets and act as a control for the siRNA transfecting ability of the nanoparticles produced for this study.

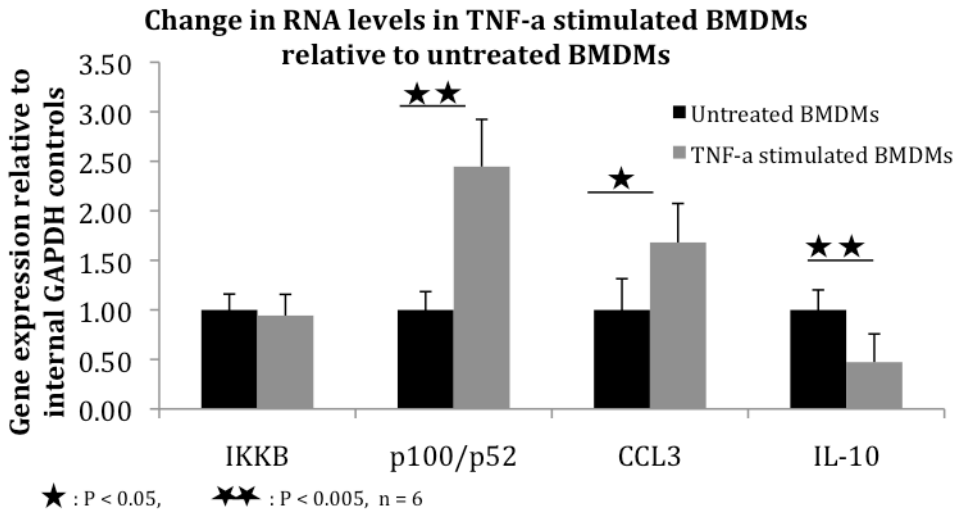

Figure 4: Stimulation with TNF-α increases the amount of alternate NF-κB pathway protein, p100/p52, mRNA in BMDMs while the mRNA levels for classical pathway protein, IKKB remain unchanged. Inflammatory cytokine CCL3 is also upregulated while levels of mRNA for inhibitory cytokine, IL-10, decrease.

However, to best utilize the commercial reagents, we first needed to optimize the manufacturer's suggested protocol in our own hands, using the BMDM's. We chose two well-known transfection agents: HiPerFect and Lipofectamine, and optimized each agent using the NGL BMDM's.

The commercial transfection agent, HiPerFect (Qiagen), was initially selected for use based on manufacturers' claims and previous studies indicating that its formulation was optimal for transfecting macrophages due to the lower cationic charge of the lipids used to from the transfection complexes. To form transfection complexes, siRNA was incubated with HiPerFect for 20 minutes before the transfection solution was added to the cells' media. **Figure 5** shows the result of a 6 hour transfection of BMDMs in 12-well plates (200,000 cells per well) using anti-luciferase siRNA delivered at different concentrations and with different concentrations of HiPerFect. Luciferase activity is used as an indicator of NF-κB activity and is measured by a spectrophotometric assay. The raw number of relative light units (RLUs) is then normalized to sample protein concentrations using a Bradford assay. The reportable quantity of RLUs/ug of protein indicates the amount of NF-κB activation in a sample, controlled for variations in cell plating density. HiPerFect was shown to not induce activation of the NF-κB pathway at concentrations of 10, 20, and 30 ul per well. Knockdown of luciferase using an anti-luciferase positive control siRNA was shown to be more dependent on HiPerFect concentration, rather than siRNA concentration. Based on these results, we chose to use HiPerFect at a concentration of 20 ul per well, with 10 nM siRNA in each well.

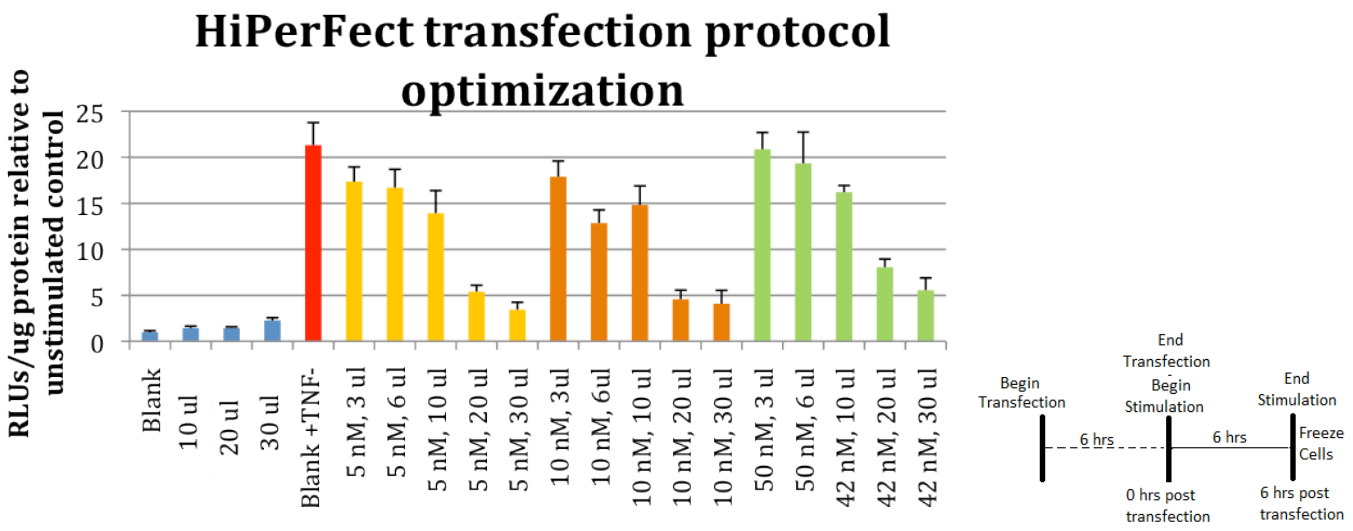

Figure 5: Optimizing the HiPerFect protocol. Cells were transfected with different concentrations of HiPerFect and siRNA for 6 hours. The cells were then stimulated with TNF-α for 6 hours. Knockdown of luciferase was more sensitive to changes in HiPerFect concentration then changes in siRNA concentration. HiPerFect alone did not appreciably stimulate the NF-κB pathway in the macrophages.

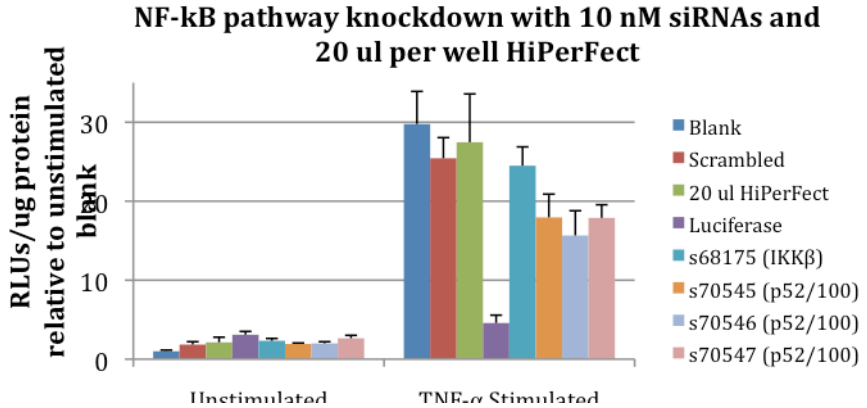

Figure 6: Transfection with various siRNA. Transfecting with siRNA did not activate the NF-κB pathway as shown by the samples unstimulated by TNF-a. The three p52/p100 siRNA were the most effective at knocking down NF-κB activity; however, this effect was not as pronounced as expected. We believe this is due to the fact that each siRNA only targets one of the parallel NF-κB pathways. Knocking down one pathway still leaves the other active.

The next round of transfections tested the efficacy of several experimental siRNA candidate sequences.

BMDMs were cultured in 12-well plates at a density of 200,000 cells per well. The cells were then transfected with the following controls: a negative control for siRNA activity, a scrambled sequence; a positive control for siRNA activity, an anti-luciferase sequence; a control for the effects of the transfection agent, 20 ul of HiPerFect with no siRNA; and a negative control for transfection, no HiPerFect or siRNA (Blank). The experimental siRNAs chosen were: an siRNA for IKKβ, (Ambion, silencer select ®s68175) and three sequences targeting p52/p100 (Ambion, silencer select ® s70545-47). The cells were transfected for 6 hours and then stimulated with TNF-α for 6 hours. **Figure 6** shows that luciferase activity in unstimulated (no TNF-α) samples was approximately uniform. The positive control anti-luciferase siRNA showed very effective knockdown of luciferase expression in the stimulated cells. As expected, the siRNA for IKKβ did not show effective knockdown of NF-κB activity, which may be due to the fact that IKKβ mRNA is not upregulated in response to TNF-α stimulation (as in **Figure 4**). The siRNAs for p52/p100 showed some knockdown of luciferase activity, though they were unable to reproduce knockdown as effective as the siRNA for luciferase. This result is consistent with the fact that only one pathway is being targeted for any given NF-κB targeted-siRNA. The pathway that is not being targeted is free to continue with a normal process of NF-κB activation.

Following the first round of transfections with HiPerFect and siRNAs for IKKβ and p52/p100, more siRNA were tested for efficacy for NF-κB knockdown using the same transfection protocol described above. siRNAs for p65, p50/p105, and IKKα were purchased from Ambion and tested in the next round of transfections. The results of these transfections brought to light significant problems with using HiPerFect as a transfection agent. Several experiments using HiPerFect exhibited little to no knockdown of the NF-κB pathway and little to no knockdown of luciferase using positive control anti-luciferase siRNA. A study using dynamic light scattering (DLS) to examine transfection complex formation showed that while some transfection complexes formed after 20 minutes as indicated by the manufacturer's instructions, complexes continued to form up to an hour after the siRNA was mixed with the HiPerFect. This accounts for the mixed results and questionable efficacy of using this transfection agent. In order to further investigate the ability of the selected siRNAs to knockdown the NF-κB pathway a second commercial agent, Lipofectamine (Invitrogen), was used to

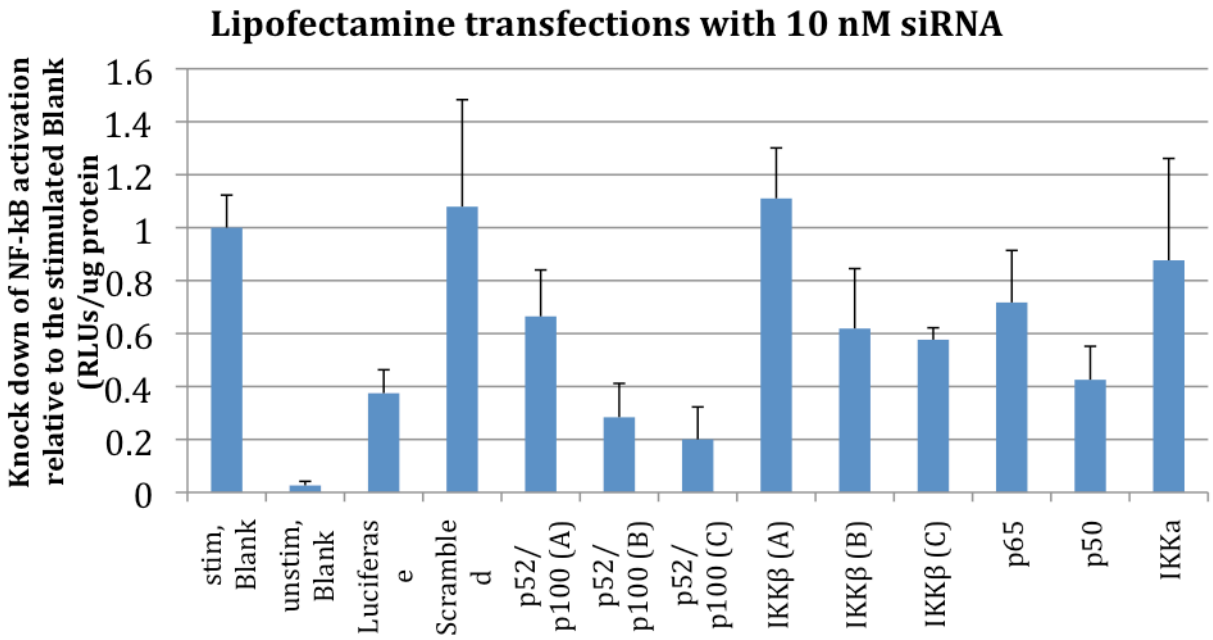

Figure 7: The Lipofectamine transfections confirm the ability of the p52 siRNA to knockdown NF-κB activity. Sequence p52/p100 C demonstrated an 80% knockdown of the luciferase indicating NF-κB activity. Results for other siRNAs are also promising, prompting further experiments with different siRNA sequences and combinations of sequences

transfect the siRNAs. **Figure 7** shows the knockdown of NF-κB activity for each siRNA relative to stimulated cells that were untransfected. The siRNAs, delivered at 10 nM concentrations, showed varied abilities to reduce NF-κB activity. Two of the p52/p100 sequences showed the most effective knockdown of NF-κB activity,

followed by an siRNA for p50/p105. The siRNAs for IKKβ showed mild or no efficacy for knockdown, as did the IKKα siRNA. Currently, we are performing transfection experiments utilizing combined siRNAs and different sequences for p65.

The assessment of BMDM phenotype following inhibition of the NF-κB pathways is imminent and will be performed as soon as the optimal siRNAs for knockdown of expression are defined.

> ***Milestone #1:*** The result of subtasks 1a-1c is the production of a material capable of quantitatively predictable uptake into BMDMs. The result of subtask 1d is the *in vitro* validation and dose-response behavior of siRNA mediated knockdown of the canonical and alternative NF-κB pathways alone and in combination. The interplay of the canonical and alternative NF-κB pathways in modulating BMDM phenotype will be assessed. These methods serve as a baseline to quantitatively evaluate the novel approaches described in the subsequent specific aims.

Task 2. Optimize delivery and efficacy of siRNA-delivering nanoparticles to inhibit canonical and alternative NF-κB, alone and in combination, in macrophages *in vivo*:

2a. Evaluate population distribution of nanoparticles associated with macrophages in vivo by flow cytometry. Use the mouse model of metastatic human breast cancer provided by the FVB mice, tail-vein-injected with PyVT mammary tumor cell lines. Macrophage phenotype (M1/M2) will be correlated with high and low particle delivery following flow cytometric cell sorting.

We have initiated studies to optimize delivery of nanoparticles to the lung microenvironment in the presence of metastatic mammary derived tumors. Mammary tumor cells derived from the polyoma model were injected via the tail vein (9). Eighteen days after injection of tumor cells, when lung metastasis had formed, mannosylated or untargeted nanoparticles containing fluorescent (FAM) labeled siRNA were injected via an i.v. retro-orbital route into mice. Control mice were injected with PBS. 24hrs post nanoparticle injection, mice were euthanized and lungs were harvested. The lungs were perfused with cold PBS, minced and incubated in RPMI media containing 0.7mg/ml collagenase XI (Sigma) and 30µg/ml DNAse I (Sigma) for 40 minutes at 37°C. Digests were strained through a 70 micron filter. Cells were pelleted and treated with 1ml ACK red cell lysis buffer, washed, and re-suspended in PBS. Cells were blocked with anti-mouse CD16/CD32 antibody (eBioscience, San Diego, CA) before staining with anti-mouse antibodies: CD45 (30-F11), CD11b (M1/70), and F4/80. Flow cytometry was performed to determine uptake of fluorescently labeled RNA related to nanoparticle treatment. Analysis was performed on an LSRII cytometer with DIVA software (BD Biosciences, Franklin Lakes, NJ). Cells were pre-gated on CD45 and data is shown as percentage of total CD11b+ leucocytes. The data plots shown indicate FITC (fluorescent RNA) versus F4/80 staining cell populations (**Figure 8).**

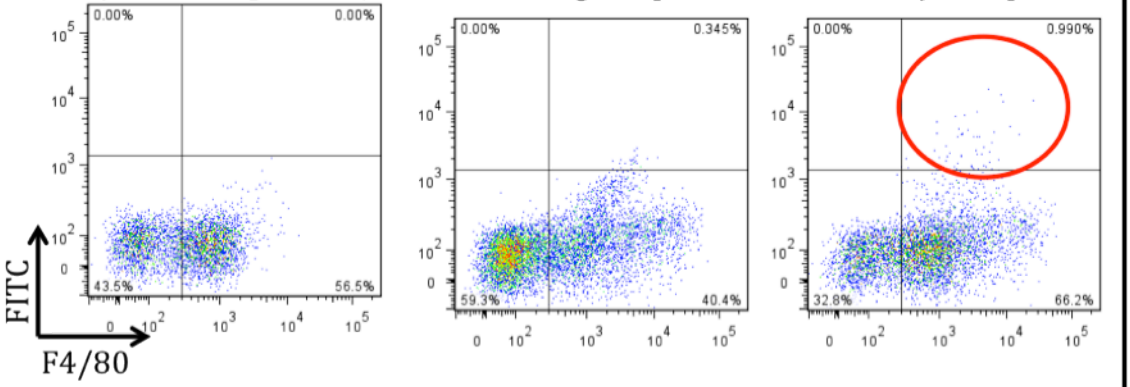

Figure 8. Mice were injected with PYL tumor cells via the tail vein. Two weeks post injection, when lung metastases had formed, mice were injected systemically with nano-particles which contained a FITC labeled siRNA (IV, 1 mg/kg). 24 hours after particle injection, mice were sacrificed, and lungs were prepared for FLOW cytometry analysis. Viable cells were pre-gated on CD45 and are shown here as percentage of total CD11b+ leukocytes. The percentage of FITC positive F4/80 positive cells was increased in the lungs of mice injected with the mannosylated vs. non-targeted particles (red circle), even in this small pilot (n=3 in each group, p = 0.0719).

Results show a significant population of labeled cells in the $CD45^+$:$CD11B^+$:$F4/80^+$ population in mice treated with the targeted, mannosylated form of nanoparticles relative to untargeted mice. Labeled cells are undetectable in untreated mice. While some FITC positive cells are detected in mice treated with untargeted particles, it should be noted that these have a relatively low level of fluorescence. The differences in percentage of FITC positive F4/80 cells in targeted versus untargeted nanoparticle subsets is approaching significance even in this study with only 3 mice per group. The overall pattern of cell populations in the mannosylated particle group is similar to that of control mice. However, there appears to be a shift towards a CD45:CD11B+:F4/80- population in the mice that receive untargeted nanoparticles. We suspect that these particles are eliciting a stronger host response than the targeted particles due to intrinsic differences in the structure of the particles and lack of a relatively innocuous mannose layer. This remains to be confirmed with further studies.

While the preliminary data with respect to targeting macrophages in the lungs *in vivo* is promising considerable improvements in targeting efficiency may be feasible. We intend to optimize dosing, timing, and frequency of injection in future studies.

<u>2b.</u> *Using optimized nanoparticle dosage from tasks 1c and 1d, in combination with in vivo delivery results from task 2a, evaluate pharmacokinetics of nanoparticles in NGL-reporter mice with overt lung metastases generated by tail vein injection of Polyoma-derived breast cancer cells using in vivo fluorescence imaging. This system enables detection of host response during tumor progression with respect to NF-κB activity. Use model to further optimize delivery strategy of nanoparticles in terms of dispersibility, accumulation in lung tissue, dose, and duration of treatment.*

These studies are imminent and will be performed using NGL reporter trangenics as soon as the initial optimization of dosage and timing for delivery has been optimized as described in 2a.

<u>2c.</u> *Functional amendments to the nanoparticle design will be carried out based on in vivo pharmacokinetic results of task 2b. The specific changes will be dictated by in vivo performance, but may include adjustment of the surface functionalizations for improved biodistribution and/or altered siRNA content per particle to optimize dosing based on achievable administration volumes and frequencies.*

This work will be informed by the initial optimization and dosage studies currently underway and partially completed as described in subaim 2a.

<u>2d.</u> *Using siRNA sequence from task 1d and optimized nanoparticle administration conditions (tasks 2a-2b), assess modulation of NF-κB activity by luciferase assay and western blots of nuclear extracts from lung tissue containing overt lung metastases to determine translocation of p65 or p52 to the nucleus. In addition, in vivo imaging of reporter mice will determine if impact is sufficient to be significant in intact live animals. Determine effects on local macrophage populations by RT-PCR of RNA to quantify expression of target genes correlated with M1 (iNOS, MIP1-α, IL-12) or M2 (IL-10, CCL17, mannose receptor) phenotype.*

These studies were scheduled for year 2 of this funding and have not yet commenced.

<u>2e.</u> *Isolate TAMs from lung tissue containing overt metastases using anti-CD11 antibody-mediated magnetic separation and assess NF-κB activity by luciferase assay and westerns, and macrophage phenotype (M1/M2) by RT-PCR.*

We have not yet commenced the studies in which nanoparticles carrying defined "behavior modifying" siRNAs are injected into mice bearing lung tumors. However, we have made initial efforts to establish methodologies that will be used to analyze effects of treatment with the targeted nanoparticles. Total lung tissue was dissociated into single cells, then, magnetic beads were used to purify CD11B+ cells. The resulting cells were used for cytospin preparations, H&E stained and the proportions of monocytes/macrophages, neutrophils and other lymphocytes were quantified (**Figure 9**). Slides were then stained for CD68 to identify myeloid cells and

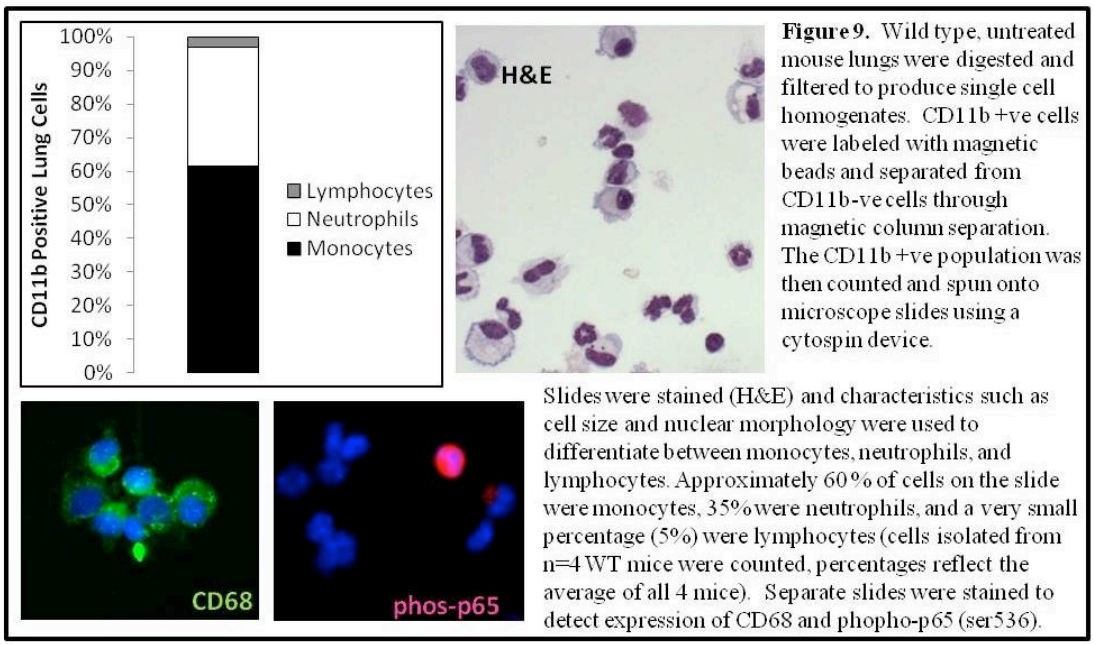

Figure 9. Wild type, untreated mouse lungs were digested and filtered to produce single cell homogenates. CD11b +ve cells were labeled with magnetic beads and separated from CD11b-ve cells through magnetic column separation. The CD11b +ve population was then counted and spun onto microscope slides using a cytospin device. Slides were stained (H&E) and characteristics such as cell size and nuclear morphology were used to differentiate between monocytes, neutrophils, and lymphocytes. Approximately 60% of cells on the slide were monocytes, 35% were neutrophils, and a very small percentage (5%) were lymphocytes (cells isolated from n=4 WT mice were counted, percentages reflect the average of all 4 mice). Separate slides were stained to detect expression of CD68 and phopho-p65 (ser536).

with phospho-p65 (ser-536) to identify cells containing significant NF-κB activity (**Figure 9**). We recently reported using Real-Time PCR analysis to demonstrate shifting patterns of M1 versus M2 macrophage markers in similar magnetic bead isolated CD11B+ cell preparations (9).

Milestone #2: The result of subtasks 2a-2d is *in vivo* testing of novel multifunctional nanomaterials capable of modulating NF-κB locally at tumor sites and location reporting by fluorescence imaging. These aims include sufficient controls to enable preparation of a manuscript for peer-reviewed publication in a nanomedicine or immunology journal.

Task 3. Utilize siRNA-delivering nanoparticles to inhibit classical or alternative NF-κB activity alone and in combination in macrophages and determine effects on tumor progression:

3a. Optimize generation of PyVT:NGL double transgenics. We currently have breeding colonies of PyVT and NGL transgenics. We have previously generated homozygous NGL transgenics demonstrating the feasibility of this approach. Due to the pathology of the PyVT model, only heterozygous males are competent for breeding. We will generate a breeding colony of PyVT heterozygous:NGL homozygous mice to improve the efficiency of generating experimental animals.

We have generated the necessary breeding colonies for the most efficient generation of experimental mice for the ongoing studies.

We have performed a preliminary study to provide evidence that the nanoparticle formulations can deliver siRNA to macrophages in the context of primary mammary tumors (appendix page 22 and page 25). PyVT mice rapidly produce multifocal mammary adenocarcinomas together with secondary metastatic tumors in the lung by 12 weeks (14,15). PyVT mice in which a significant load of primary mammary tumors had developed were injected i.v. (retro-orbital) with mannosylated and non-mannosylated nanoparticle versions containing fluorescently labeled (FAM) siRNA. 24 hours after injection, mammary and liver tissue was harvested. Immunostaining of frozen sections demonstrated co-localization of delivered siRNA with CD206 (mannose receptor)-expressing cells in tumor sections. In addition, flow cytometry analysis demonstrated co-localization of delivered siRNA with tumor-associated F4/80^{+} cells. This data supports the feasibility of targeted delivery of specific siRNAs into tumor-associated macrophages.

The studies listed under 3b-d were scheduled for year 2 of this funding and have not yet commenced.

3b. Evaluate primary tumor response to treatment by measurement of tumor latency, weight, and size in two dimensions. Evaluate tumor response to treatment by immunohistochemical analysis of sections, including

assessment of TAM populations (anti-F4/80 antibody), cell proliferation (Ki67 staining), and survival (TUNEL staining). Evaluate nanoparticle delivery by fluorescence microscopy of tumor sections. (Months 15-22)
3c. Evaluate tumor response to treatment by macrometastasis count on lung tissue. Evaluate micrometastases and tumor response to treatment by immunohistochemical analysis of lung tissue sections, including assessment of TAM populations (anti-F4/80 antibody), cell proliferation (Ki67), survival (TUNEL), matrix remodeling (MMP-9 and MMP-12 zymography) and angiogenesis (vWF, VEGF staining). Evaluate nanoparticle delivery by fluorescence microscopy of lung tissue sections. (Months 15-22)
3d. Establish correlations among nanoparticle delivery, NF-κB activity, TAM phenotype, and tumor response to treatment. (Months 23-24)

Milestone #3: The results from Specific Aim 3 include localized modulation of NF-κB activity and TAM phenotype *in vivo* and correlation of the modulated phenotype with primary and metastatic tumor characteristics. These results will be reported as a peer-reviewed paper in a high-impact breast cancer journal.

KEY RESEARCH ACCOMPLISHMENTS

During this reporting period;

1) We have established a new collaboration between the Giorgio and Yull laboratories. We have regular combined group meetings and Ryan Ortega (predoctoral student) represents a direct link between the two groups. This collaborative study is proving educational for members of both research teams and we have developed a shared interest in the progress and outcome of these studies.
2) We have generated siRNA-delivering nanoparticles and demonstrated optimized delivery of siRNA into BMDMs *ex vivo* utilizing a mannose receptor targeting approach (Specific Aim 1a-c and Yu et al manuscript).
3) We have obtained data that suggests that nanoparticle delivery is approaching the efficacy of commercial transfection agents with respect to macrophage transfection.
4) We have modified our selection of genes that will be targeted with siRNA based on our initial studies. We will now focus on p65 as the major target for inhibition of the canonical pathway.
5) We have performed initial in vivo studies in the context of both primary tumor and of lung metastases that are showing promise with respect to the feasibility of targeted delivery of siRNA to TAMS.

REPORTABLE OUTCOMES

Manuscripts, Abstracts, Presentations

1. Yu SS, Bloodworth NC, Barham WJ, Yull FE, Duvall CL, and Giorgio TD: 'Click' Glycoconjugate Nanoparticles for Dual-Mode Fluorescence/MRI Imaging of siRNA Delivery to Pathologically-Activated Inflammatory Cells In Vivo. Biomedical Engineering Society Annual Fall Meeting, Atlanta, GA, October 2012. {accepted abstract; poster to be presented in October 2012} **[abstract on appendix page21]**

2. Yu SS, Lau CM, Barham WJ, Nelson CE, Yull FE, Duvall CL, and Giorgio TD: Achieving Cancer Immunotherapy Through RNAi Interference in Tumor-Associated Macrophages via 'Click', Mannosylated Polymeric Nanoparticles. Biomedical Engineering Society Annual Fall Meeting, Atlanta, GA, October 2012. {accepted abstract; podium talk to be presented in October 2012; *winner of the 2012 Design and Research Awards from the Biomedical Engineering Society*} **[abstract on appendix page 22]**

3. Ortega RA, Kumar B, Yu SS, Yull FE, Giorgio TD: Targeted Knockdown of NF-kB in Tumor Associated Macrophages. Biomedical Engineering Society Annual Fall Meeting, Atlanta, GA, October 2012. {accepted abstract; poster to be presented in October 2012} **[abstract on appendix page 23]**

4. Yu SS, Lau CM, Barham WJ, Nelson CE, Yull FE, Duvall CL, and Giorgio TD: *In Vivo*, Cell- and Site-Specific RNAi Interference in Tumor-Associated Macrophages via 'Click', Mannosylated Polymeric Nanoparticles. NanoBio Seattle, Seattle, WA, July 2012. {accepted abstract and poster presentation} **[abstract on appendix page 24; poster on appendix page 25]**

5. Yu SS, Lau CM, Barham WJ, Onishko HM, Nelson CE, Li H, Yull FE, Duvall CL and Giorgio TD: Macrophage-Specific RNAi Targeting via 'Click', Mannosylated Polymeric Micelles. ACS Chemical Biology 2012. {scientific manuscript in peer review} **[manuscript in review on appendix pages 26-76]**

6. Yu SS, Lau CM, Barham WJ, Onishko HM, Nelson CE, Yull FE, Duvall CL and Giorgio TD: Cell- and Site-Specific RNAi Interference in Tumor-Associated Macrophages via 'Click', Mannosylated Polymeric Nanoparticles. American Society for Gene and Cell Therapy Annual Meeting, Philadelphia, PA, May 2012. {accepted abstract and poster presentation} **[abstract on appendix page 77; poster on appendix page 78]**

7. Yu SS, Lau CM, Barham WJ, Onishko HM, Nelson CE, Yull FE, Duvall CL and Giorgio TD: Environmentally-Responsive Nanoparticles for the Intracellular Delivery of RNAi Therapeutics into Tumor-Associated Macrophages. American Association for Cancer Research Annual Meeting, Chicago, IL, March 2012. {accepted abstract and poster presentation} **[abstract on appendix page 79; poster on appendix page 80]**

8. Yu SS, Lau CM, Barham WJ, Onishko HM, Nelson CE, Li H, Yull FE, Duvall CL, and Giorgio TD: In Vivo, Macrophage-Specific RNAi Targeting via "Click", Mannosylated Polymeric Micelles. Society for Biomaterials, Memphis, TN, February 2012. {accepted abstract and podium presentation} **[abstract on appendix page 81; presentation on appendix pages 82-90]**

9. Yu SS: Environmentally-Responsive Nano-Carriers for the Intracellular Delivery of RNAi Therapeutics into Tumor-Associated Macrophages. Cancer Biology Science Hour Seminar, Vanderbilt-Ingram Cancer Center, Nashville, TN, February 2012. **[no abstract (only a title required); presentation on appendix pages 91-99]**

10. Lau CM, Yu SS and Giorgio TD: Macrophage-Targeted siRNA Delivery for Cancer Therapy. 13th Annual Nanoscience and Nanotechnology Forum, Nashville, TN, October 2011. (3rd place poster award). {accepted abstract and poster presentation} **[no abstract (only a title required); poster on appendix page 100]**

Funding applied for based on work supported by this award

1. Yu SS: Biofunctional Materials for the Modulation of Macrophage Phenotype and Polarization. 2012 Vanderbilt University Dissertation Enhancement Grant, $2,000. This mechanism enables the best predoctoral students to explore an enhancement of their dissertation using funds distributed on a competitive basis informed by an application. Mr. Yu will use this award to explore new approaches for cell-specific drug delivery to macrophages located at pathologic sites. **[no appendix entry]**

Employment or research opportunities applied for and/or received based on experience/training supported by this award

1. Yu SS: Visiting Research Fellow, University of Washington Medical Center. Mr. Yu is using the award noted above to spend approximately two months in the laboratory of Dr. Nora Disis to enhance his dissertation work and strengthen collaborations between the Giorgio lab, the Disis lab and the NIH-supported Cancer Immunotherapy Trials Network, centered at the Washington Medical Center and led by Dr. Mac Cheever. **[no appendix entry]**

CONCLUSIONS

The ***hypothesis*** to be tested in these studies is that siRNA-mediated inhibition of NF-κB signaling in TAMs will decrease primary tumor growth and metastatic potential. Our ***objectives*** are (1) exploration of macrophage response to inhibition of NF-κB activation by the canonical and alternative pathways, separately and in combination using siRNA knockdown *in vitro* and (2) development of a nanobiotechnology delivery vehicle with the capacity for siRNA delivery TAMs for the purpose of pathway-specific NF-κB knockdown *in vivo*.

In order to reach our ultimate goal of testing the efficacy of this approach in *in vivo* tumor models three major milestones will need to be reached; 1) synthesis and development of the nanoparticles (manuscript prepared), 2) selection of appropriate siRNA (underway), 3) optimization of delivery of nanoparticles (initial *in vivo* treatment has proved not to be toxic via i.v. route and to deliver with some specificity to a population of macrophages in both primary tumor and lung metastases).

Overall, we believe that we are "on track" to achieving our stated goal of performing an initial set of tumor response studies.

REFERENCES

1. Mantovani, A., et al., *Macrophage polarization: tumor-associated macrophages as a paradigm for polarized M2 mononuclear phagocytes.* Trends Immunol, 2002. **23**:549-55.
2. Miselis, N.R., et al., *Targeting tumor-associated macrophages in an orthotopic murine model of diffuse malignant mesothelioma.* Mol Cancer Ther, 2008. **7**:788-99.
3. de Visser, K.E., A. Eichten, and L.M. Coussens, *Paradoxical roles of the immune system during cancer development.* Nat Rev Cancer, 2006. **6**:24-37.
4. Dirkx, A.E., et al., *Monocyte/macrophage infiltration in tumors: modulators of angiogenesis.* J Leukoc Biol, 2006. **80**:1183-96.
5. Murdoch, C., et al., *The role of myeloid cells in the promotion of tumour angiogenesis.* Nat Rev Cancer, 2008. **8**:618-31.
6. Pollard, J.W., *Macrophages define the invasive microenvironment in breast cancer.* J Leukoc Biol, 2008. **84**:623-30.
7. Stout, R.D., et al., *Macrophages sequentially change their functional phenotype in response to changes in microenvironmental influences.* J Immunol, 2005. **175**:342-9.
8. Watkins, S.K., et al., *IL-12 rapidly alters the functional profile of tumor-associated and tumor-infiltrating macrophages in vitro and in vivo.* J Immunol, 2007. **178**:1357-62.
9. Connelly L, Barham W, Onishko HM, Chen L, Sherrill T, Zabuwala T, Ostrowski MC, Blackwell TS, Yull FE. *NF-kappaB activation within macrophages leads to an anti-tumor phenotype in a mammary tumor lung metastasis model.* Breast Cancer Res. 2011; **13**:R83.
10. Cao, Y. and M. Karin, *NF-kappaB in mammary gland development and breast cancer.* J Mammary Gland Biol Neoplasia, 2003. **8**:215-23.
11. Eliopoulos, A.G., et al., *Epstein-Barr virus-encoded latent infection membrane protein 1 regulates the processing of p100 NF-kappaB2 to p52 via an IKKgamma/NEMO-independent signalling pathway.* Oncogene, 2003. **22**(48):7557-69.
12. Perkins, N.D., *Oncogenes, tumor suppressors and p52 NF-kappaB.* Oncogene, 2003. **22**:7553-6.
13. Romieu-Mourez, R., et al., *Roles of IKK kinases and protein kinase CK2 in activation of nuclear factor-kappaB in breast cancer.* Cancer Research, 2001. **61**:3810-8.

14. Guy, C.T., Cardiff, R.D., Muller, W.J. *Induction of mammary tumors by expression of polyomavirus middle T oncogene: a transgenic mouse model for metastatic disease.* Mol Cell Biol. 1992. **12**:954-61.
15. Lin, E.Y., Jones, J.G., Li, P., Zhu, L., Whitney, K.D., Muller, W.J., Pollard, J.W. *Progression to malignancy in the polyoma middle T oncoprotein mouse breast cancer model provides a reliable model for human diseases.* Am J Pathol. 2003. **163**:2113-26.

APPENDICES

Appendix materials start with Biographical Sketches for the PIs (Giorgio, Todd D. and Yull, Fiona E.) and the other major personnel contributing to this research effort during the award period (June 2011 – July 2012)

1. Giorgio, Todd D., Biographical Sketch **[appendix pages 1-5]**
2. Yull, Fiona E., Biographical Sketch **[appendix pages 6-9]**
3. Barham, Whitney J, Biographical Sketch **[appendix page 10]**
4. Chen, Lianyi, Biographical Sketch **[appendix page 11]**
5. Ortega. Ryan A., Biographical Sketch **[appendix pages 12-13]**
6. Tikhomirov, Oleg Y, Biographical Sketch **[appendix pages 14-16]**
7. Yu, Shann S., Biographical Sketch **[appendix pages 17-20]**

Following Biographical Sketches, each item identified as a 'reportable outcome' for this project is included in appendices. The appendix materials appear in inverse chronological order (newest first) in agreement with the order shown as 'reportable outcomes' and identified below.

8. Yu SS, Bloodworth NC, Barham WJ, Yull FE, Duvall CL, and Giorgio TD: 'Click' Glycoconjugate Nanoparticles for Dual-Mode Fluorescence/MRI Imaging of siRNA Delivery to Pathologically-Activated Inflammatory Cells In Vivo. Biomedical Engineering Society Annual Fall Meeting, Atlanta, GA, October 2012. {accepted abstract; poster to be presented in October 2012} **[abstract on appendix page21]**

9. Yu SS, Lau CM, Barham WJ, Nelson CE, Yull FE, Duvall CL, and Giorgio TD: Achieving Cancer Immunotherapy Through RNAi Interference in Tumor-Associated Macrophages via 'Click', Mannosylated Polymeric Nanoparticles. Biomedical Engineering Society Annual Fall Meeting, Atlanta, GA, October 2012. {accepted abstract; podium talk to be presented in October 2012; *winner of the 2012 Design and Research Awards from the Biomedical Engineering Society*} **[abstract on appendix page 22]**

10. Ortega RA, Kumar B, Yu SS, Yull FE, Giorgio TD: Targeted Knockdown of NF-κB in Tumor Associated Macrophages. Biomedical Engineering Society Annual Fall Meeting, Atlanta, GA, October 2012. {accepted abstract; poster to be presented in October 2012} **[abstract on appendix page 23**]

11. Yu SS, Lau CM, Barham WJ, Nelson CE, Yull FE, Duvall CL, and Giorgio TD: *In Vivo*, Cell- and Site-Specific RNAi Interference in Tumor-Associated Macrophages via 'Click', Mannosylated Polymeric Nanoparticles. NanoBio Seattle, Seattle, WA, July 2012. {accepted abstract and poster presentation} **[abstract on appendix page 24; poster on appendix page 25]**

12. Yu SS, Lau CM, Barham WJ, Onishko HM, Nelson CE, Li H, Yull FE, Duvall CL and Giorgio TD: Macrophage-Specific RNAi Targeting via 'Click', Mannosylated Polymeric Micelles. ACS Chemical Biology 2012. {scientific manuscript in peer review} **[manuscript in review on appendix pages 26-76]**

13. Yu SS, Lau CM, Barham WJ, Onishko HM, Nelson CE, Yull FE, Duvall CL and Giorgio TD: Cell- and Site-Specific RNAi Interference in Tumor-Associated Macrophages via 'Click', Mannosylated

Polymeric Nanoparticles. American Society for Gene and Cell Therapy Annual Meeting, Philadelphia, PA, May 2012. {accepted abstract and poster presentation} **[abstract on appendix page 77; poster on appendix page 78]**

14. Yu SS, Lau CM, Barham WJ, Onishko HM, Nelson CE, Yull FE, Duvall CL and Giorgio TD: Environmentally-Responsive Nanoparticles for the Intracellular Delivery of RNAi Therapeutics into Tumor-Associated Macrophages. American Association for Cancer Research Annual Meeting, Chicago, IL, March 2012. {accepted abstract and poster presentation} **[abstract on appendix page 79; poster on appendix page 80]**

15. Yu SS, Lau CM, Barham WJ, Onishko HM, Nelson CE, Li H, Yull FE, Duvall CL, and Giorgio TD: In Vivo, Macrophage-Specific RNAi Targeting via "Click", Mannosylated Polymeric Micelles. Society for Biomaterials, Memphis, TN, February 2012. {accepted abstract and podium presentation} **[abstract on appendix page 81; presentation on appendix pages 82-90]**

16. Yu SS: Environmentally-Responsive Nano-Carriers for the Intracellular Delivery of RNAi Therapeutics into Tumor-Associated Macrophages. Cancer Biology Science Hour Seminar, Vanderbilt-Ingram Cancer Center, Nashville, TN, February 2012. **[no abstract (only a title required); presentation on appendix pages 91-99]**

17. Lau CM, Yu SS and Giorgio TD: Macrophage-Targeted siRNA Delivery for Cancer Therapy. 13th Annual Nanoscience and Nanotechnology Forum, Nashville, TN, October 2011. (3rd place poster award). {accepted abstract and poster presentation} **[no abstract (only a title required); poster on appendix page 100]**

'Click' Glycoconjugate Nanoparticles for Dual-Mode Fluorescence/MRI Imaging of siRNA Delivery to Pathologically-Activated Inflammatory Cells In Vivo

S. S. Yu[1], N. C. Bloodworth[2], W. J. Barham[3], F. E. Yull[3], C. L. Duvall[1], and T. D. Giorgio[1]
[1]Vanderbilt University, Nashville, TN, [2]Vanderbilt University Medical Center, Nashville, [3]Vanderbilt-Ingram Cancer Center, Nashville, TN

Introduction: Aberrant inflammatory activation contributes to the pathogenesis of a range of debilitating diseases, including cancer, atherosclerosis, and autoimmune diseases. The advent of RNA interference (RNAi) therapeutics shows promise in enabling the silencing of entire genetic pathways responsible for these pathologic inflammatory processes, but off-target delivery of RNAi mediators (e.g., siRNA) may lead to significant side effects resulting from interference with normal genetic processes in healthy tissues. To specifically target RNAi therapeutics to immune cells, we have synthesized a range of polymeric nanoparticles surface-functionalized with sugars including mannose, fucose, and galactose via 'click' chemistry. In this work, we show that the incorporation of contrast agents into the nanoparticles enables the noninvasive tracking of siRNA delivery *in vivo* via fluorescence tomography/magnetic resonance imaging.

Materials and Methods: The glycoconjugates were tri-block co-polymers synthesized via reversible addition-fragmentation chain transfer (RAFT) polymerization, including the following blocks: (1) an azide-displaying block for the attachment of alkyne-functionalized mannose, fucose, or galactose via 'click' chemistry, (2) a cationic block for the condensation of polyanions such as siRNA, and (3) a pH-responsive terpolymer block that facilitates endosomal disruption.[1] The polymers were covalently labeled with a Cy7 dye before being used to encapsulate iron oxide nanoparticles (USPIOs) in order to form dual-model contrast agents (Figure 1). Following complexation with FAM-labeled anti-GAPDH siRNA, nanoparticles were delivered into tumor-bearing FVB mice via retro-orbital injection. To quantify biodistribution and knockdown, mice were imaged via FMT and MRI within 48 h post-injection. Animals were then sacrificed, and organs were collected for spectral imaging, flow cytometry, and confocal microscopy. Knockdown of GAPDH expression was assessed via real-time PCR.

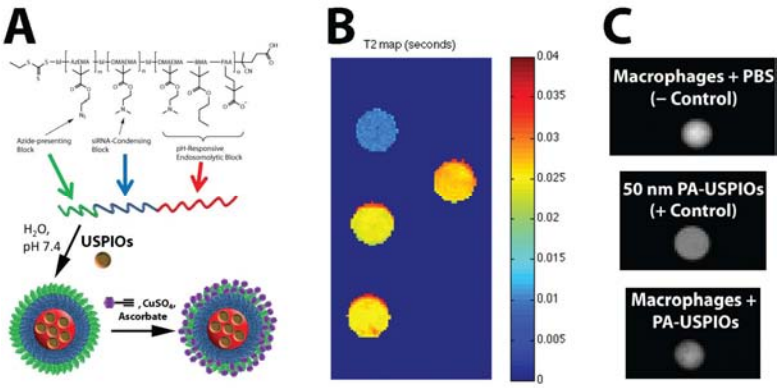

Figure 1. (A) Schematic of triblock copolymers used for encapsulation of iron oxides (USPIOs) and functionalization with sugars via 'click' chemistry. (B) MRI of polymeric nanoparticles without (top) or with (bottom three spots) encapsulated USPIOs. (C) MRI of human macrophages untreated (top) or treated with polymeric nanoparticles containing iron (bottom). (Middle) NPs were also imaged as a control.

Results and Discussion: Tri-block co-polymers formed micelles of 20-30 nm in diameter, and showcased the same size range following the encapsulation of USPIOs. The resulting contrast agents had R_2 constants in the range of 500-1000 s^{-1} μM^{-1}, suggesting that the presence of sub-μM scale concentrations of the agents are sufficient to enable clinically-relevant detection of nanoparticle localization *in vivo* (Figure 1). Administration of these polymer-USPIO nanoparticles to macrophages *in vitro* shows that while macrophages internalize < 50% of the administered dose (60 nM or less NPs), this small local concentration of USPIOs is enough to enable detection of nanoparticle internalization by these cells. The addition of the mannose targeting block to these nanoparticles enhances delivery of the payload to macrophages by 400% as evidenced by flow cytometry and confocal microscopy, and has been shown to selectively target tumor-associated macrophages in FVB mice bearing dispersed mammary tumors (as shown via immunohistochemistry). Biodistribution studies involving the fucose- and galactose-targeted nanoparticles are ongoing.

Conclusions: The materials developed here showcase glycobiology-inspired approaches to target immune cells *in vivo*. Further, the ability to incorporate multiple contrast agents into the same nanoparticle platform, including iron oxides and fluorophores, as well as fluorescent siRNA cargoes, enables the visualization of both the delivery system and the payload *in vivo*.

Acknowledgements: This work is supported by multiple grants through the Department of Defense CDMRP Breast Cancer Research Program (#W81XWH-10-1-0684, #W81XWH-11-1-0344 & #W81XWH-11-1-0242).

References: [1]AJ Convertine et al. *J Control Release* 2009, 133, 221-9.

Achieving Cancer Immunotherapy Through RNAi Interference in Tumor-Associated Macrophages via 'Click', Mannosylated Polymeric Nanoparticles

S. S. Yu[1], C. M. Lau[1], W. J. Barham[2], C. E. Nelson[1], F. E. Yull[2], C. L. Duvall[1], and T. D. Giorgio[1,2]
[1]Vanderbilt University, Nashville, TN, [2]Vanderbilt-Ingram Cancer Center, Nashville, TN

Introduction: Tumor-associated macrophages (TAMs) represent a promising therapeutic target in cancer because they have been shown to facilitate tumor growth and invasiveness. However, macrophage-specific drug delivery within tumor sites is a significant challenge, as systemic interference with macrophage behavior may lead to autoimmune manifestations. In this work, we designed and characterized mannosylated polymeric nanoparticles (ManNPs) in order to achieve CD206 (macrophage mannose receptor)-targeted siRNA delivery. CD206 is almost exclusively expressed on macrophages and dendritic cells, and upregulated in tumor-associated macrophages.

Materials and Methods: The ManNPs were tri-block co-polymers synthesized via reversible addition-fragmentation chain transfer (RAFT) polymerization, including the following blocks: (1) an azide-displaying block for the attachment of alkyne-functionalized mannose via 'click' chemistry, (2) a cationic block for the condensation of polyanions such as siRNA, and (3) a pH-responsive terpolymer block that facilitates endosomal disruption.[1] ManNPs were complexed with FAM-labeled anti-GAPDH siRNA, and delivery into primary murine bone marrow-derived macrophages (BMDMs) was measured via confocal microscopy and flow cytometry. Knockdown of GAPDH expression was assessed via real-time PCR. The same methods were used to quantify biodistribution and knockdown *in vivo* following 24 h after retro-orbital injection of nanoparticles into tumor-bearing "PyT" mice. The PyT mouse model overexpresses the polyoma middle T oncoprotein in the mammary epithelium, leading to the natural development of mammary tumors at 9-13 weeks after birth.

Results and Discussion: The glycoconjugates improved siRNA delivery into BMDMs by 4.5-fold, relative to a non-mannosylated version of the same carrier. Internalization of these constructs can be blocked by co-incubation with mannose or suppressed by downregulation of CD206 via LPS pre-treatment, showcasing the specificity of the construct for CD206. This is particularly important for cancer applications because CD206 is upregulated in tumor-suppressed and non-activated macrophages, enabling more specific targeting of TAMs versus healthy macrophages in other tissues. Finally, the delivered siRNA retains its activity following delivery, resulting in 40±10% knockdown of a model gene within 4 h of delivery, relative to non-transfected macrophages. Further, within 24 h of administration into tumor-bearing PyT mice, the ManNPs facilitated improved delivery of siRNA into CD206-expressing cells in tumors, as shown by immunostaining of tumor frozen sections (Figure 1). Flow cytometry analysis also shows significant co-localization of the delivered siRNA with tumor-associated F4/80+ cells. This correlated with enhanced knockdown of GAPDH gene expression in $CD11b^+$ cells in the tumor.

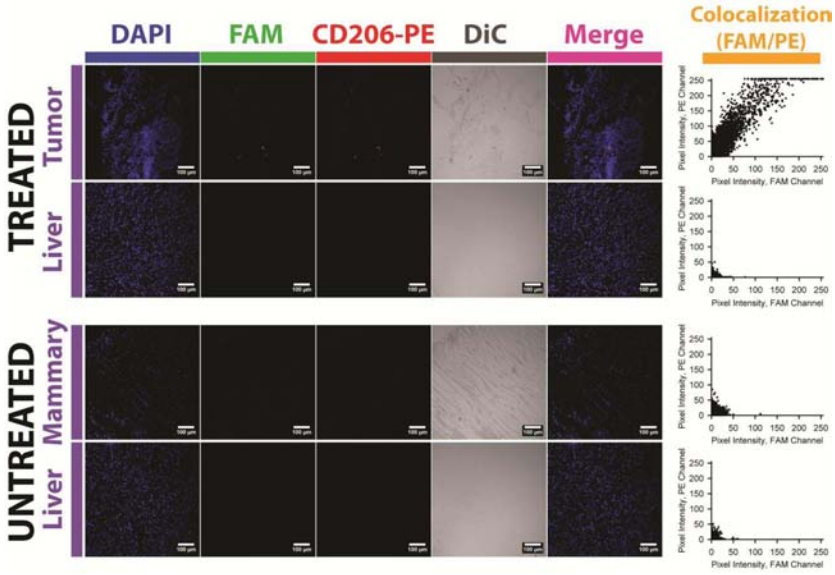

Figure 1. ManNPs deliver FAM-siRNA to CD206+ cells, as shown in frozen sections of mammary tumors of PyT mice treated with nanoparticles for 24h. Moreover, TAMs usually make up <5% of the cells in the tumor, and this is reflected by the limited amount of overall FAM signal in the tumor sections.

Conclusions: The ManNPs described here present new opportunities to target TAMs, providing an enabling technology for the modification of the immunosuppressive tumor environment by targeting TAM activity.

Acknowledgements: This work is supported by multiple grants through the Department of Defense CDMRP Breast Cancer Research Program (#W81XWH-10-1-0684, #W81XWH-11-1-0344 & #W81XWH-11-1-0242).

References: [1]AJ Convertine et al. *J Control Release* 2009, 133, 221-9.

Ortega RA, Kumar B, Yu SS, Yull FE, Giorgio TD: Targeted Knockdown of NF-kB in Tumor Associated Macrophages. Biomedical Engineering Society Annual Fall Meeting, Atlanta, GA, October 2012.

Introduction: Macrophages have been proposed as a drug target in breast cancer because they are potent effectors of the immune system, demonstrating the ability to secrete a wide range of pro-inflammatory cytokines and growth factors. The NF-κB pathways are major controlling factors of macrophage phenotype, consisting of multiple nuclear transcription factor protein dimmers. Aberrant NF-κB signaling in tumor associated macrophages (TAMs) has been implicated in tumorigenesis. We have developed a polymeric nanoparticle to act as a targeted therapeutic delivery device to treat TAMs by knocking down the production of key proteins in the NF-κB pathways using small interfering RNA (siRNA). Current delivery of siRNA therapeutics to macrophages generally entails purchasing a commercially available transfection agent and developing an optimized protocol for transfection. The cells of interest for this work, macrophages, are traditionally difficult to transfect effectively. Therefore, the specific objectives of this work is to validate our chosen therapeutic targets, show that the nanoparticle platform developed by our group and our collaborators to deliver siRNA is effective, and show that it is capable of altering macrophage phenotype by knocking down activation of the NF-κB pathways.

Materials and Methods: Bone marrow cells were isolated from NGL reporter mice on an FVB background. NGL reporter mice have been genetically modified to produce luciferase and green fluorescent protein upon NF-κB pathway activation. The bone marrow, harvested from the murine femurs, was transformed into bone marrow derived macrophages (BMDMs) using a source of colony stimulating factor-1. BMDMs have been shown to phenotypically mimic TAMs with regards to morphology and cellular products. The cells were transfected with siRNA targeting key proteins in the NF-κB pathways using a commercial transfection agent (HiPerFect), untargeted nanoparticles, and the targeted nanoparticles. The nanoparticles used consisted of a pH-responsive, endosomolytic core, an siRNA condensing region, and an optional targeting moiety consisting of a mannose chain targeted to the mannose receptor, unique to macrophages. The BMDMs were stimulated with tumor necrotic factor-α (TNF-α) to create model of tumoral presence near the stromal macrophages. After stimulation, the cells were frozen in a luciferase assay lysis buffer and analyzed for NF-κB pathway activation via luciferase assay. Real time PCR was also performed to analyze levels of cellular RNA as descriptors of macrophage phenotype.

Results and Discussion: Our nanoparticle transfection agent is comparable to commercial agents for transfection efficiency with the added effect of macrophage specific targeting. Initial transfections with commercial agents proved largely ineffective at knocking down NF-kB activation, showing only a 5-10 % decrease, on average, in pathway activation when a key regulatory protein in the pathways, IKKβ, was targeted. PCR revealed that this protein, predicted by literature and our group to be an efficacious target, was in fact a poor target due to an unforeseen lack of upregulation during pathway activation. Other proteins in the pathway, for example the p100/p52 protein (aka: NF-κB2), are upregulated and are a more efficacious target (Figure 1).

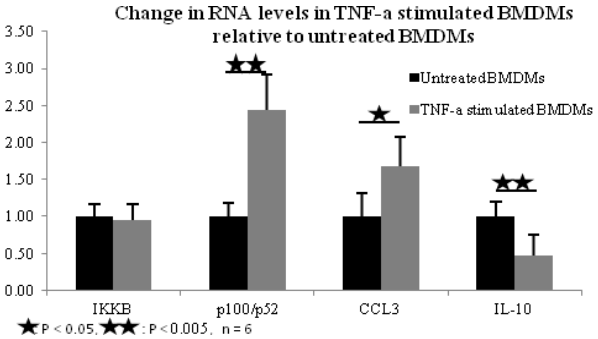

Figure 1: Activation of the NF-κB pathways using TNF-α showed an increase in p100/p52 but not IKKβ. This is corroborated by transfection experiments showing ineffective pathway knockdown with IKK protein targeting and more effective knockdown with NF-κB protein targeting Activation was confirmed by the increased presence of inflammatory cytokines such as CCL3 and the decrease in inhibitory cytokine IL-10.

Conclusion: The transcription factors NF-κB1 and NF-κB2 are better therapeutic targets for TAM phenotype modulation than initial targets, IKK family proteins, using siRNA. Our targeted nanoparticle transfection agent performed comparably to commercial agents with the added effect of specific targeting.

In Vivo, Cell- and Site-Specific RNAi in Tumor-Associated Macrophages via 'Click', Mannosylated Polymeric Nanoparticles

Shann S. Yu, Cheryl M. Lau, Whitney J. Barham, Christopher E. Nelson, Fiona E. Yull, Craig L. Duvall, & Todd D. Giorgio

Vanderbilt University, Nashville, TN

Macrophages represent an important therapeutic target, because their activity has been implicated in the progression of common, debilitating diseases such as cancer and atherosclerosis. However, macrophage-specific drug delivery within pathologic sites is a significant challenge, as non-specific drug delivery may lead to side effects and undesired interference with molecular mechanisms in healthy tissues. Because CD206 (mannose receptor) is almost exclusively expressed on macrophages and dendritic cells, and upregulated in tumor-associated macrophages, we designed and characterized pH-responsive, mannosylated polymeric micelles in order to achieve CD206-targeted drug delivery. The glycoconjugates improved siRNA delivery into primary murine macrophages by fivefold relative to a non-targeted carrier. Internalization of these constructs can be blocked by co-incubation with mannose or suppressed by downregulation of CD206 via LPS. The delivered siRNA retained its activity following delivery, resulting in 40±10% knockdown of a model gene within 4h of delivery. Additionally, the glycoconjugates were avidly recognized and internalized by human macrophages, and facilitated the delivery of 13-fold more siRNA into these cells relative to model cancer cell lines. Preliminary results also show that the glycoconjugates co-localize with CD206 in murine breast tumors in vivo, suggesting that these vehicles may become an enabling technology to target macrophage activity in tumors.

In Vivo, Cell- and Site-Specific RNA Interference in Tumor-Associated Macrophages via Click-Mannosylated Polymeric Nanoparticles

Shann S. Yu[1], Cheryl M. Lau[1], Whitney J. Barham[2], Christopher E. Nelson[1], Fiona E. Yull[2], Craig L. Duvall[1], & Todd D. Giorgio[1-3]

[1]Dept. of Biomedical Engineering, [2]Dept. of Cancer Biology, & [3]Dept. of Chemical & Biomolecular Engineering, Vanderbilt University, Nashville, TN

Tumor-Associated Macrophages (TAMs) are an Important Drug Target in Cancer

- Problem: Macrophages resident in tumors have been 'hijacked' into promoting tumor growth and invasiveness.
  - Tumor-elicited activation of genetic pathways leading to immunosuppression and release of growth factors.

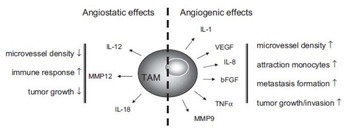

AE Dirkx et al. (2006) *J Leukocyte Biol.* 80:1183-1196.

- Challenge: Development of drug delivery system that targets macrophages specifically in a tumor microenvironment.
  - Ability to deliver siRNA to knock down the expression of genetic pathways responsible for tumor-promoting effects.

- **DESIGN GOALS: Synthesize polymeric nanoparticles that target TAMs, and mediate intracellular delivery of siRNA.**
  - Immobilization of mannose to nanoparticle surface enables targeting of CD206 (macrophage mannose receptor), which is expressed almost exclusively on macrophages.
  - Build in modules that are responsible for mediating escape of the polymers and their cargo from the endosomal pathway.

Mimicking the Endosomal Escape of HIV via Synthetic Block Co-polymers

- Common viruses interact with endocytotic receptors to enter target cells, and eventually escape the endosomal pathway.
  - pH-mediated change in conformation of a viral protein enables the virus to disrupt phospholipid membranes at late endosomal pH (< 6.2)

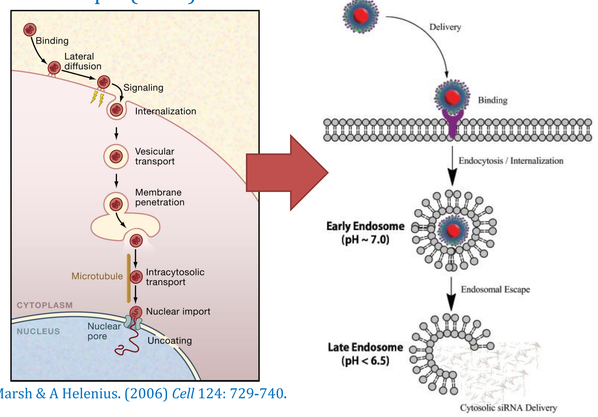

- M Marsh & A Helenius. (2006) *Cell* 124: 729-740.

Objectives

- Physicochemical characterization of the nanoparticles.
- Evaluate nanoparticle-mediated siRNA delivery to CD206-expressing macrophages *in vitro* and *in vivo*.

Mannosylated Polymeric Nanoparticles (ManNPs)

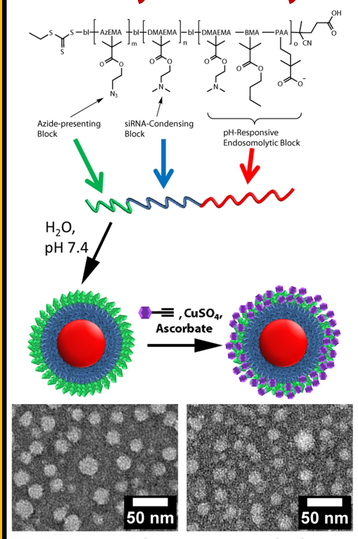

FIGURE 1. Smart Polymeric Nanoparticles for Macrophage-Specific Cytosolic Delivery of siRNA. Schematic representation of the triblock copolymers developed in this work, and resulting, multi-functional nanoscale siRNA delivery vehicles. The blocks include (red) a pH-responsive block that is capable of disrupting endosomes at low pH, (blue) a cationic block for condensation of nucleic acids, and (green) an azide-displaying block for conjugation of targeting motifs (purple) via 'click' chemistry. The pH-responsive block is hydrophobic at pH 7.4, enabling the formation of micelles. At pH < 6.2, protonation of this block produces a net cationic charge, resulting in disassembly of the micelles. (Bottom) Transmission electron micrographs of (bottom left) micelles of non-targeted diblock copolymers, and (bottom right) ManNPs. Scale bars = 50 nm.

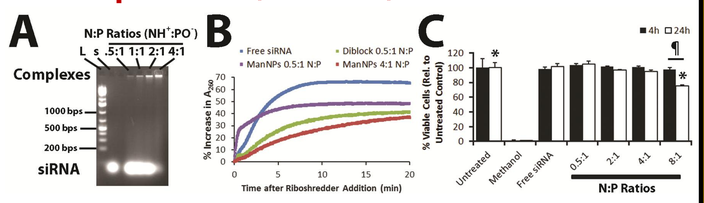

FIGURE 2. ManNPs Effectively Complex and Protect siRNA from Local Nuclease Activity, and Exhibit Negligible Cytotoxicity to THP-1 Macrophages. (A) Gel retardation assay of siRNA-loaded ManNPs at various N:P ratios. Control samples included the DNA ladder (L; numbers indicate # base pairs) and free, Cy3-labeled siRNA (s). (B) Micelle/ siRNA complexes were incubated with RNAse cocktails. RNAse-mediated degradation of siRNA was characterized by a hyperchromic effect at 260 nm. (C) Cell viability assay of human THP-1 leukemic macrophages treated with ManNPs/siRNA at varying N:P ratios for 4-24 h show minimal cytotoxicity for N:P < 8:1, relative to untreated cells.

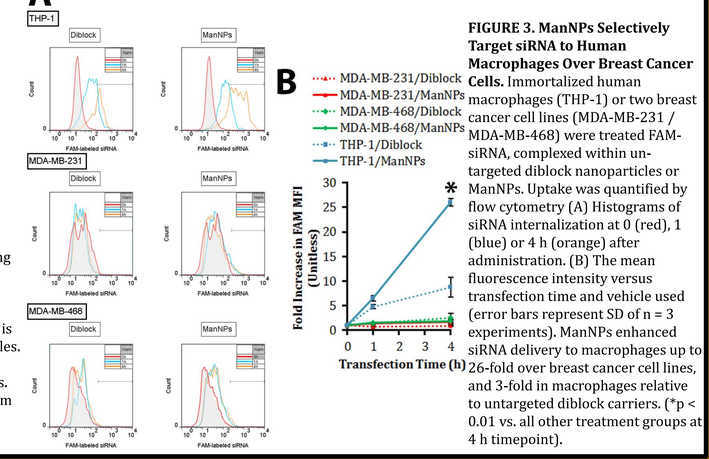

FIGURE 3. ManNPs Selectively Target siRNA to Human Macrophages Over Breast Cancer Cells. Immortalized human macrophages (THP-1) or two breast cancer cell lines (MDA-MB-231 / MDA-MB-468) were treated FAM-siRNA, complexed within un-targeted diblock nanoparticles or ManNPs. Uptake was quantified by flow cytometry (A) Histograms of siRNA internalization at 0 (red), 1 (blue) or 4 h (orange) after administration. (B) The mean fluorescence intensity versus transfection time and vehicle used (error bars represent SD of n = 3 experiments). ManNPs enhanced siRNA delivery to macrophages up to 26-fold over breast cancer cell lines, and 3-fold in macrophages relative to untargeted diblock carriers. (*p < 0.01 vs. all other treatment groups at 4 h timepoint).

ManNPs Enhance siRNA Delivery and Gene Knockdown in Primary Murine Macrophages

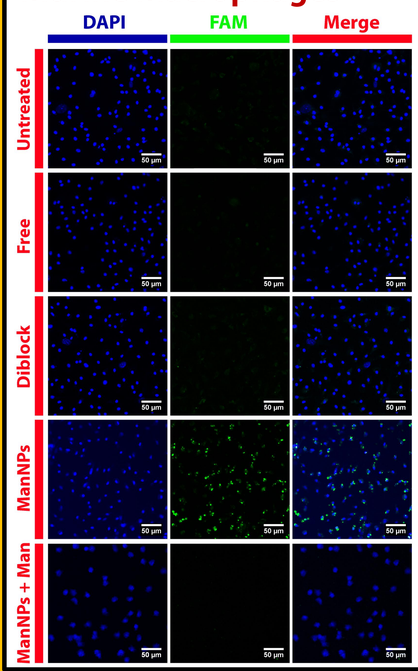

FIGURE 4. Improved Targeting of Primary Macrophages via ManNPs and Specificity for Mannose Receptor (CD206). Following 4h of transfection with FAM-siRNA (green; free or complexed into nanoparticles), BMDMs were fixed and imaged via confocal microscopy. Co-administration of the ManNPs with free D-mannose blocks uptake of siRNA.

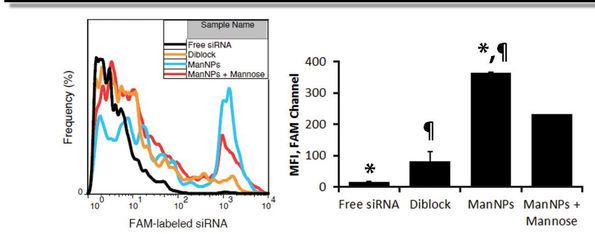

FIGURE 5. Improved Targeting of BMDMs via ManNPs. Flow cytometry confirms enhanced delivery of FAM-siRNA into BMDMs via ManNPs (blue) relative to untargeted nanoparticles (orange) or free siRNA without vehicle (black) within 4 h of administration. Co-administration of free mannose with the ManNPs reduces delivery of siRNA into BMDMs (red). (Left) FAM histograms for gated BMDMs, and (right) corresponding mean fluorescence intensity versus treatment. Error bars represent SD from 2 independent experiments (*,¶ p < 0.01).

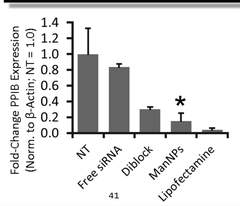

FIGURE 6. ManNPs Enhance siRNA-Mediated Knockdown of PPIB Expression in BMDMs within 24 h of Administration. qRT-PCR confirmed ManNPs carrying anti-PPIB siRNA mediated 85 ± 10% decrease in expression of the target gene, relative to non-transfected (NT) cells. Error bars represent standard deviation of 3 independent experiments (*p < 0.05 vs. all other treatment groups by Student's t-test).

ManNPs Selectively Target CD206-Expressing Cells in Murine Tumors *In Vivo*

Mouse Model

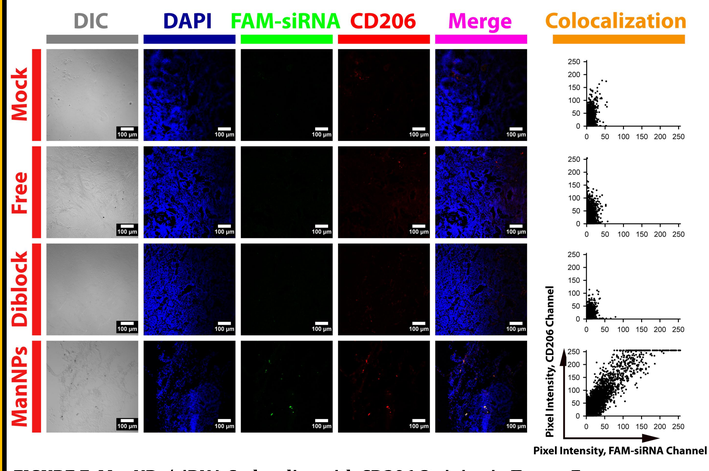

FIGURE 7. ManNPs/siRNA Co-localize with CD206 Staining in Tumor Frozen Sections. (Above) The expression of the PyMT oncogene in FVB mice results in the natural development of mammary epithelial tumors in these mice at 7-12 weeks after birth. We treated tumor-bearing PyMT mice with nanoparticles for 24 h prior to the collection and preservation of various organs. (Below) ManNPs facilitate the delivery FAM-labeled siRNA to CD206-positive cells in the tumors of PyMT mice. Co-localization is not seen for siRNA delivered via the other vehicles investigated. CD206 brightness and contrast have been enhanced equally for all panels (Scale bar = 100 μm)

Conclusions

- ManNPs form micelles that electrostatically complex siRNA and protect the siRNA from nuclease-mediated degradation.
- ManNPs deliver siRNA to BMDMs in a CD206-dependent manner, and enhance siRNA-mediated knockdown of the expression of a model gene.
- ManNPs selectively deliver siRNA to CD206-expressing cells in tumors of PyMT mice.

Acknowledgments

This work is supported through a Concept Award through the Department of Defense CDMRP Breast Cancer Research Program (#W81XWH-10-1-0684). Bone marrow-derived macrophages and in vivo work was supported through a multi-investigator, collaborative IDEA Award through the Department of Defense CDMRP Breast Cancer Research Program (#W81XWH-11-1-0344 & #W81XWH-11-1-0242). CML acknowledges partial support through a fellowship from the Vanderbilt Undergraduate Summer Research Program (VUSRP). Portions of this work were performed at the Vanderbilt Institute of Nanoscale Science and Engineering, using facilities renovated under NSF ARI-R2 DMR-0963361. Confocal microscopy (Zeiss LSM 710) was supported in part by the NCI Cancer Center Support Grant #P30 CA068485, utilizing the Vanderbilt University Medical Center Cell Imaging Shared Resource. The Vanderbilt University Medical Center Cell Imaging Shared Resource is also supported by NIH grants CA68485, DK20593, DK58404, HD15052, DK59637 and EY08126. qRT-PCR was performed in the laboratory of Prof. David G. Harrison (Division of Clinical Pharmacology, Vanderbilt University Medical Center).

References

1. A.E. Dirkx, M.G. Oude Egbrink, J. Wagstaff, A.W. Griffioen. (2006) *Monocyte/macrophage infiltration in tumors: modulators of angiogenesis*. J Leukoc Biol **80** (6), 1183-96.
2. M. Marsh & A. Helenius. (2006) *Virus entry: open sesame*. Cell **124** (4): 729-40.
3. S.S. Yu, C.M. Lau, W.J. Barham, H.M. Onishko, C.E. Nelson, H. Li, F.E. Yull, C.L. Duvall, & T.D. Giorgio. (2012) *Macrophage-Specific RNAi Targeting via 'Click', Mannosylated Polymeric Micelles*. (Submitted).

Macrophage-Specific RNAi Targeting via 'Click', Mannosylated Polymeric Micelles

Journal:	*ACS Chemical Biology*
Manuscript ID:	cb-2012-003682
Manuscript Type:	Article
Date Submitted by the Author:	17-Jul-2012
Complete List of Authors:	Yu, Shann; Vanderbilt University, Biomedical Engineering Lau, Cheryl; Vanderbilt University, Biomedical Engineering Barham, Whitney; Vanderbilt-Ingram Cancer Center, Cancer Biology Onishko, Halina; Vanderbilt-Ingram Cancer Center, Cancer Biology Nelson, Christopher; Vanderbilt University, Biomedical Engineering Li, Hongmei; Vanderbilt University, Biomedical Engineering Yull, Fiona; Vanderbilt-Ingram Cancer Center, Cancer Biology Duvall, Craig L.; Vanderbilt University, Biomedical Engineering Giorgio, Todd; Vanderbilt University, Dept. of Biomedical Engineering

Macrophage-Specific RNAi Targeting via 'Click', Mannosylated Polymeric Micelles

Shann S. Yu[†,‡], Cheryl M. Lau[†], Whitney J. Barham[§], Halina M. Onishko[§], Christopher E. Nelson[†,‡], Hongmei Li[†,‡], Fiona E. Yull[§], Craig L. Duvall[†,‡], & Todd D. Giorgio[†,‡,§,⊥,*].

[†]Department of Biomedical Engineering, Vanderbilt University, Nashville, TN 37235

[‡]Vanderbilt Institute for Nanoscale Science & Engineering, Vanderbilt University, Nashville, TN 37235

[§]Department of Cancer Biology, Vanderbilt-Ingram Cancer Center, Nashville, TN 37232

[⊥]Department of Chemical & Biomolecular Engineering, Vanderbilt University, Nashville, TN 37235

*Correspondence should be addressed to Todd D. Giorgio, Ph.D., Department of Biomedical Engineering, Vanderbilt University, 5824 Stevenson Center, Nashville, TN 37235, United States. E-mail: todd.d.giorgio@vanderbilt.edu . Phone: 615.322.3521. Fax: 615.343.7919.

Abbreviations: AzEMA: 2-azidoethyl methacrylate, BMA: butyl methacrylate, BMDM: bone marrow-derived macrophage, CD206: macrophage mannose receptor, DLS: dynamic light scattering, DMAEMA: 2-dimethylaminoethyl methacrylate, FAM-siRNA: FAM-labeled anti-GAPDH siRNA, ManNPs: mannosylated triblock copolymer nanoparticles, MFI: mean fluorescence intensity, N:P: NH^+:PO^-, PAA: 2-propylacrylic acid, PPIB: Peptidyl-prolyl cis-trans-isomerase B (cyclophilin B), qRT-PCR: quantitative real time PCR, RAFT: reverse addition-fragmentation chain transfer, TAM: tumor-associated macrophage, THP-1: immortalized human leukemic monocytes/macrophages.

ABSTRACT

Macrophages represent an important therapeutic target, because their activity has been implicated in the progression of debilitating diseases such as cancer and atherosclerosis. However, macrophage-specific drug delivery within pathologic sites is a significant challenge, as non-specific drug delivery may lead to off-target side effects and undesired interference with molecular mechanisms in healthy tissues. In this work, we designed and characterized pH-responsive polymeric micelles that were mannosylated using 'click' chemistry. Mannose was chosen in order to achieve CD206 (mannose receptor)-targeted drug delivery, though this 'clickable' platform could be generally used to attach other targeting ligands to this efficient siRNA carrier. CD206 is almost exclusively expressed on macrophages and dendritic cells, and upregulated in tumor-associated macrophages, a potentially useful target for cancer therapy. The glycosylated nanoparticles improved siRNA delivery into primary macrophages relative to a non-mannosylated version of the same carrier. Further, the mannose-targeted siRNA carriers achieved 85±10% knockdown of a model gene within 24h of delivery, relative to non-transfected macrophages. Finally, these nanoparticles were also avidly recognized and internalized by human macrophages, and facilitated the delivery of 13-fold more siRNA into these cells relative to model breast cancer cell lines. We anticipate these glycoconjugates to become an enabling technology to target macrophage activity in various diseases, especially those where CD206 is up-regulated in macrophages present within the pathologic site.

Keywords: mannose | nanoparticles | macrophages | siRNA | drug delivery | immunotherapy

Macrophages perform a spectrum of functions, some of which have cytotoxic effects (i.e., when fighting infection) and others which promote cell growth, matrix remodeling, and wound healing.[1] However, the dysregulation of these multifaceted activities can initiate pathogenesis and promote disease progression. For example, in various cancers, significant levels of macrophage infiltration have been observed, and this has been correlated with poor prognoses. This is hypothesized to occur because tumor-associated macrophages (TAMs) overexpress growth factors, VEGF, and matrix metalloproteinases, promoting tumor growth and invasiveness.[2] Therefore, macrophages are believed to represent an important therapeutic target in order to address a major underlying cause of cancer progression. Based on this hypothesis, technologies that enable cell-specific phenotypic modulation of aberrant macrophage activity would potentially be of high impact on human health.

A promising strategy to address aberrant macrophage behavior is through the use of RNA interference (RNAi) therapy. One approach to therapeutically harnessing RNAi involves the delivery of duplex RNA sequences called small interfering RNA (siRNA). siRNA is processed by the target cell's inherent machinery, with the ultimate effect of gene silencing through cleavage and degradation of mRNA complementary to the antisense strand of the delivered siRNA duplex.[3] By silencing master genes that regulate aberrant macrophage activity, RNAi therapy has the potential to directly block macrophage functions that lead to disease progression. However, due to their highly degradative phagocytic, endosomal, and lysosomal compartments, delivery and cytoplasmic release of siRNA in macrophages is particularly challenging, especially in primary cells.[4] Conventional transfection methods have led to limited success, because they

involve chemically-mediated transfection, based on strongly cationic materials which are cytotoxic and have been largely restricted to the laboratory bench.[5]

While strategies exist for targeting macrophages at pathologic sites, some of these strategies require prior knowledge of the locations of these sites, in order to design injection routes for local delivery directly into the site of the macrophages.[6, 7] Such strategies include, for example, intratumoral or peritumoral injections of biologics, which may be useful when treating a primary tumor site but are poorly translatable to the treatment of dispersed, metastatic cancers. Alternative strategies require expensive technologies with uncertain practical clinical applicability, such as macrophage extraction, *ex vivo* modification, and adoptive transfer;[8] antibody-nanoparticle conjugates;[9, 10] or custom phospholipids.[11] Very few of these proposed approaches can be practically scaled for pharmaceutical purposes. Some of these methods deliver drugs to all cells non-specifically, and systemic interference with macrophage behavior may lead to autoimmune manifestations. Therefore, the clinical translation of macrophage-targeted drug delivery is hampered by barriers spanning multiple disciplines, including targeting method, synthesis, and cost.

Therefore, we designed and evaluated a polymeric glycoconjugate that can be assembled into nanocarriers for macrophage-specific siRNA delivery (Figure 1A). These agents represent a targeted version of construct reported by Convertine et al.,[12] which is capable of mediating the escape of its cargo from the endosomal pathway, due to their ability to disrupt phospholipid membranes at pH < 6.5. The original version of this efficient siRNA carrier lacked any molecular targeting functionality and has the ability to enter a range of cell types via non-specific mechanisms.

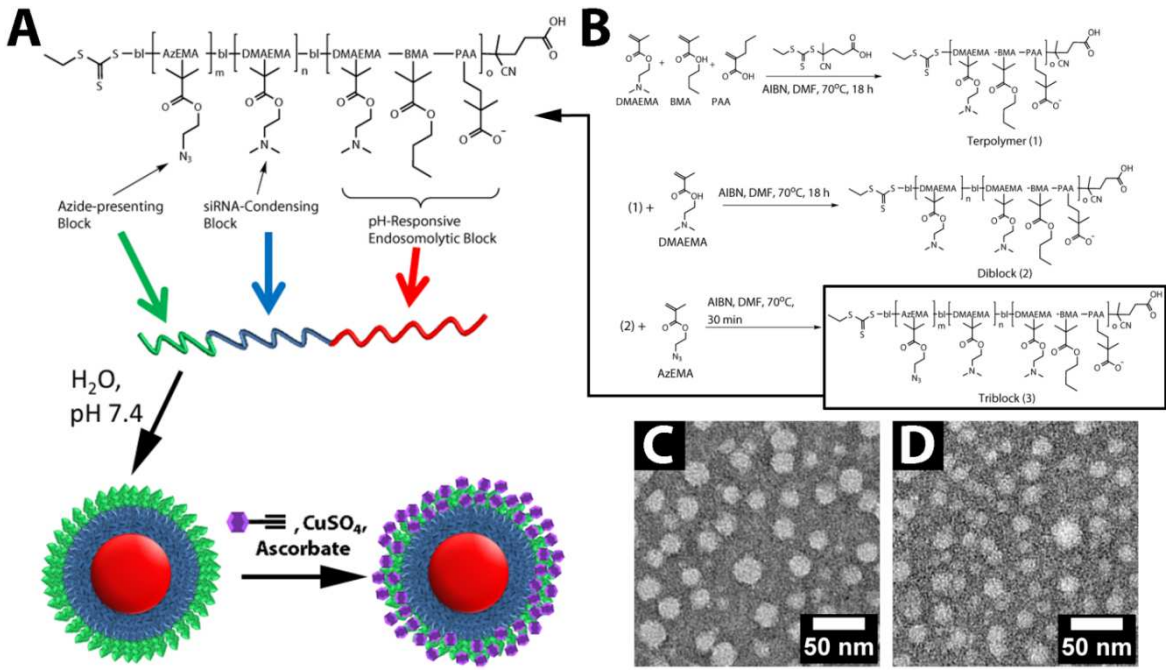

FIGURE 1. Smart Polymeric Nanoparticles for Macrophage-Specific Cytosolic Delivery of siRNA. (A) Schematic representation of the triblock copolymers developed in the manuscript, and resulting, multi-functional nanoscale siRNA delivery vehicles. The blocks include (red) a pH-responsive block that is capable of disrupting endosomes at low pH, (blue) a cationic block for condensation of nucleic acids, and (green) an azide-displaying block for conjugation of targeting motifs (purple) via 'click' chemistry. (B) Synthetic scheme for RAFT polymerization of triblock copolymers composed of blocks of AzEMA, DMAEMA, and the DMAEMA-*co*-BMA-*co*-PAA terpolymer. (C-D) Uranyl acetate-counterstained transmission electron micrographs of (C) micelles of diblock copolymers **(2)**, which had an average diameter of 13.0 ± 6.1 nm (n = 367). (D) ManNPs had an average diameter of 9.7 ± 6.2 nm (n = 415). Scale bars = 50 nm.

The molecular structure includes a hydrophobic, pH-responsive component, a cationic, siRNA-condensing component, and a terminal segment with reactive sites for 'click'

bioconjugation. These multifunctional polymers were synthesized via reverse addition-fragmentation chain transfer (RAFT) polymerization, which has the advantage of enabling the orthogonal polymerization of acrylate monomers displaying a wide range of chemical functionalities.[13] Additionally, it is a controlled radical polymerization method that leads to highly monodisperse products in an industrially-scaleable fashion, making it appropriate for pharmaceutical applications. Therefore, it is ideal for the proposed block copolymers, which feature carboxylic acids, azides, and tertiary amines among their functional groups (Figure 1). In aqueous media at pH 7.4, the polymers self-assemble into micelles and can be surface-functionalized with a wide range of possible molecular structures through the azide-alkyne 'click' reaction. 'Click' reactions have been widely employed to perform covalent conjugations for biological applications, due to their orthogonality, specificity, speed, and efficiency.[14]

Mannose was chosen as the targeting motif, since mannose receptor (CD206) is primarily expressed by macrophages and some dendritic cells.[15] In these cells, CD206 mediates the recognition and endocytosis of mannosylated, fucosylated, or N-acetylglucosaminated substrates, which occurs via clathrin-coated vesicles.[16] Further, CD206 is upregulated in TAMs, and the potential to directly target these macrophages via mannose has not been explored.[17] Mannose is also readily available at significantly lower costs than most alternative targeting motifs, improving the practicality of the approach. In this study, the capabilities of the mannose-targeted nanocarrier for cytosolic siRNA delivery and gene knockdown were evaluated in primary, murine bone marrow-derived macrophages (BMDMs). Specificity of the carriers was examined based on the ability of the glycoconjugate to deliver siRNA into immortalized human macrophages in competition with cancer cell lines. Results indicate that the described carrier offers significant opportunities for drug and siRNA targeting to TAMs.

RESULTS

Modular Design, Synthesis, and Characterization of Mannosylated siRNA Delivery Vehicles. The synthesis of the mannosylated delivery vehicles could be summarized into three parts: (1) the polymeric components were synthesized in three sequential iterations of RAFT polymerization and purification (Figure 1A-B), (2) alkyne-functionalized mannose was separately synthesized (Supplementary Figure S2), and (3) the polymers from (1) are formed into micelles and reacted with the alkyne-functionalized mannose from (2). These steps result in immobilization of mannose onto the micelle corona through reaction with the distal azide groups via 'click' chemistry (Figure 1A).

The polymers that make up the mannosylated siRNA carriers were synthesized via RAFT polymerization. These modules include a pH-responsive block (Figure 1A, red), a cationic block for condensing nucleic acids (blue) and an azide-presenting block (green) for the attachment of alkyne-functionalized ligands. First, a ~14 kDa random terpolymer block composed of 47% butyl methacrylate (BMA), 25% 2-propylacrylic acid (PAA), and 28% 2-dimethylaminoethyl methacrylate (DMAEMA) was synthesized (Figure 1B; Table 1). The percentages represent molar composition of each monomer in the copolymer structure, as determined by proton nuclear magnetic resonance spectroscopy (^{1}H-NMR).

To form a hydrophilic, corona-forming segment, a cationic DMAEMA block (8.9 kDa by ^{1}H-NMR) was block-polymerized from the terpolymer, yielding a diblock copolymer (22.8 kDa; Figure 1, red and blue; Table 1). This diblock copolymer forms micellar nanoparticles (Figure 1C), consistent with previous work by others.[12, 18-20]

Finally, an azide-presenting block composed of 2-azidoethyl methacrylate (AzEMA) was extended from the DMAEMA terminus of these polymers (Supplementary Figure S3). The

synthetic route for AzEMA (Supplementary Figure S1) was significantly modified from published schemes for the synthesis of 3-azidopropyl methacrylate, a similar monomer, in order to remove the need for chromatographic purification of the desired product.[21, 22] The polymerization kinetics of AzEMA have also been shown here (Supplementary Figure S4).

Morphologically, the triblock copolymers are expected to form assemblies as depicted in Figure 1, where the azide-presenting block effectively shields the pDMAEMA block in the final micellar structures. However, the addition of the final, AzEMA block to the base diblock leads to a 6 nm decrease in the hydrodynamic diameter of the resulting micelles, and a corresponding +10 mV increase in ζ-potential (Table 1). NMR spectra of the micelles were also obtained in D_2O. The base diblock micelles featured peaks in chemical shift regions characteristic of DMAEMA, while the micelles composed of the triblock produced none of these peaks (Supplementary Figure S5). Furthermore, the latter micelles featured a strong peak at 3.6 ppm, a region that is consistent with the expected chemical shift of alkyl protons adjacent to an azide group. Therefore, the triblock copolymers form micelles that present azide groups at their corona, enabling the facile immobilization of alkyne-functionalized ligands onto the micelles.

The synthesis of alkyne-functionalized mannose (Supplementary Figure S2) was adapted from a synthetic scheme for derivatized sugars presented by Plotz and Rifai.[23] The resulting NMR spectra of the product indicated the successful alkyne-functionalization of the monosaccharide. HPLC showed that the product is 70-80% pure following synthesis. No further purification was done because during micelle functionalization, any non-functionalized mannose that was present would be unable to ‘click’ onto the polymers and was easily removed via dialysis from the final, mannosylated nanoparticles (ManNPs).

Following the 'click' reaction to functionalize the polymers with mannose, the polymers retained the ability to form micellar nanoparticles, similar to those formed by the diblock copolymers lacking the azide block and mannose (Figure 1C-D). The ManNPs also exhibited a distinct NMR signature compared to that of the micelles made of triblock copolymer before the 'click' mannosylation reaction (Supplementary Figure S5). This is particularly evident in the 3.0-3.5 ppm region, where the appearance of a broad peak, corresponding to mannose, is consistent with the success of the 'click' reaction.

ManNPs Form Complexes with siRNA and Protect Cargo from Degradation. The completed ManNPs are able to complex siRNA in an N:P ratio-dependent fashion as evidenced by a gel retardation assay (Figure 2A). The slow-moving band corresponding to siRNA/ManNP complexes increased in brightness with increasing N:P ratios, while the fast-moving band corresponding to free siRNA decreased in brightness. The ManNPs are also able to protect their cargo from degradation by RNAses, and this ability is elevated at higher N:P ratios (Figure 2B). In this study, the degradation of siRNA results in a hyperchromic effect, which is characterized by increased sample absorbance at 260 nm.[24] The 65% increase in Abs_{260} of free siRNA within 10 min of RNAse treatment is a demonstration of this effect and is used as a positive control. At a 1:2 N:P ratio, diblock copolymers were more effective than the ManNPs in protecting siRNA from degradation. At an 4:1 N:P ratio, the ManNPs were most effective at protecting their cargo from RNAse degradation, which was in agreement with the siRNA complexation seen in the gel retardation assay.

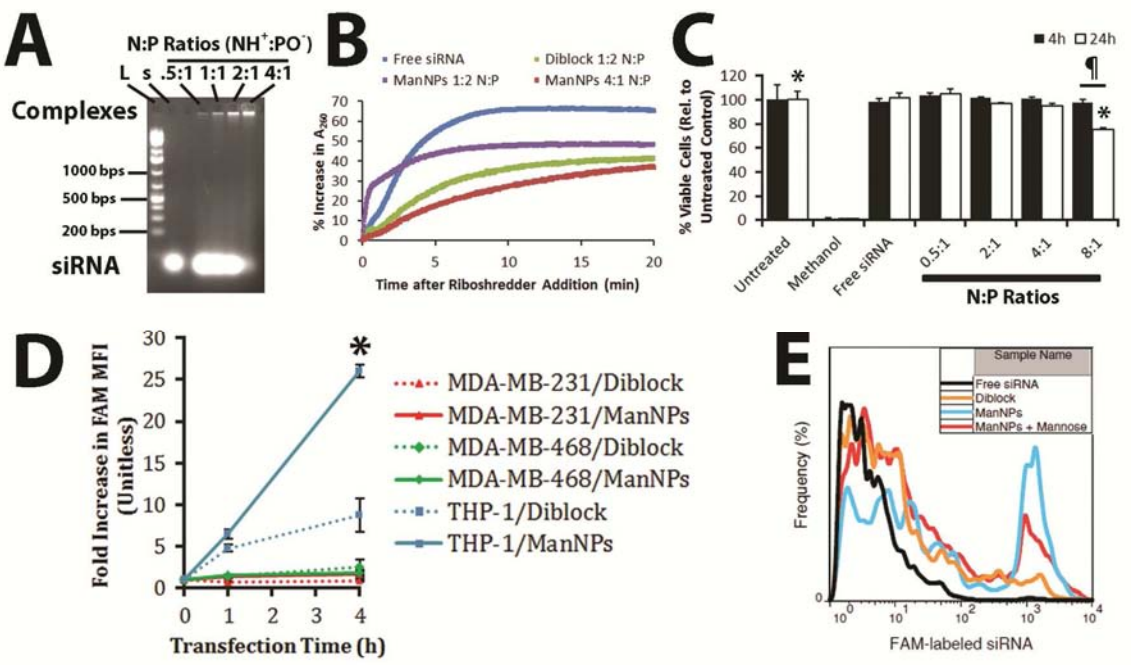

FIGURE 2. ManNP siRNA Complexation, Nuclease Protection, and Enhanced siRNA Delivery into Macrophages. (A) Gel retardation assay of siRNA-loaded ManNPs at various N:P ratios. Control samples included the DNA ladder (L; numbers indicate # base pairs corresponding to band) and free, Cy3-labeled siRNA (s). (B) Protection of siRNA from degradation by RNAses. Micelle/siRNA complexes were incubated with RNAse cocktails. RNAse-mediated degradation of siRNA was characterized by a hyperchromic effect at 260 nm, which is less pronounced for samples containing the polymeric nanoparticles. (C) Cytotoxicity assay of immortalized THP-1 macrophages, treated with ManNPs complexed with siRNA at various N:P ratios. Error bars represent standard deviation from 3 independent experiments (*,¶ $p < 0.01$). (D) ManNPs enhanced siRNA delivery to macrophages up to 26-fold over two model breast cancer cell lines, and 3-fold in macrophages relative to untargeted diblock carriers, as measured via flow cytometry. (*$p < 0.01$ vs. all other treatment groups at 4 h timepoint; n = 3). (E) Flow cytometry confirms improved delivery of FAM-siRNA into BMDMs via ManNPs (blue) relative to untargeted nanoparticles (orange) or free siRNA without vehicle (black) within

4 h of administration. Co-administration of 100 mg/mL free mannose with the ManNPs reduces delivery of siRNA into BMDMs (red). Quantification of mean fluorescence intensity in each treatment group is in Supplementary Figure S7.

ManNPs Are Cytocompatible at N:P < 8:1. Immortalized human THP-1 macrophages were incubated with siRNA-loaded ManNPs at various N:P ratios, with siRNA concentration kept at 50 nM for all conditions. Cell viability was assessed via calcein AM/ethidium homodimer incorporation at 4 or 24 h after ManNP delivery, and experimental groups were quantified via flow cytometry relative to untreated cells (100%) or methanol-killed cells (set to 0%; Figure 2C). For all N:P ratios investigated, negligible cytotoxicity was observed at 4 h of treatment. However, at 24 h, only 76 ± 1% of the cells treated at the 8:1 N:P ratio remained viable, indicating that prolonged treatment of BMDMs with ManNPs/siRNA at this charge ratio results in significant cytotoxicity (¶ $p < 0.01$, vs. 4 h treatment; *$p < 0.01$ relative to 24 h untreated cells). The 4:1 N:P ratio was selected for further experiments because it did not result in significant cytotoxicity at 24 h.

ManNPs are Avidly Internalized by Human Macrophages, but not Cancer Cells. To examine the potential of using the ManNPs to selectively target TAMs, ManNPs loaded with FAM-siRNA were incubated with immortalized human macrophages (THP-1) or human breast cancer cell lines (MDA-MB-231 & MDA-MB-468) for up to 4 h. Cellular internalization of the siRNA was assessed via flow cytometry (Supplementary Figure S6, Figure 2D). As controls, untreated cells were measured, as well as cells treated with complexes made with the non-targeted diblock copolymers. For both breast cancer cell lines, internalization of FAM-

siRNA/ManNPs was relatively minimal, and both cell types experienced less than a two-fold increase in FAM mean fluorescence intensity (MFI) over the 4 h study period. With the macrophages, the same study period led to a 26-fold increase in the FAM MFI of the cells, showing that these cells preferentially internalize the constructs relative to the model cancer cell lines (Figure 2D; *$p < 0.01$ vs. all other treatment groups at 4 h). Further, ManNPs facilitated a 3-fold increase in siRNA delivery to the macrophages, relative to the non-targeted diblock micelles.

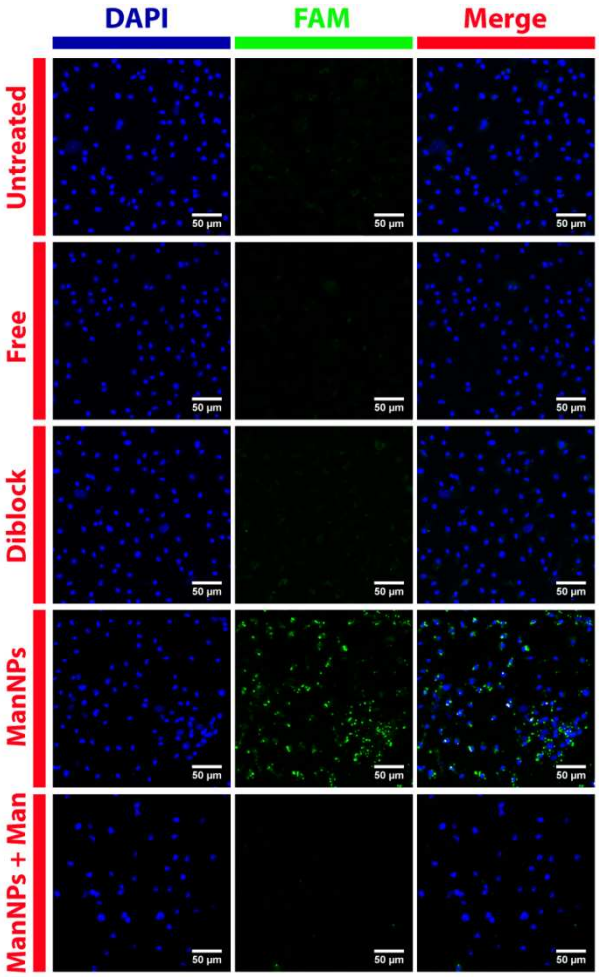

FIGURE 3. Improved Delivery to Primary Macrophages using ManNPs with Specificity for Mannose Receptor (CD206). Following 4h of transfection with FAM-siRNA (green; free or complexed into nanoparticles), BMDMs were fixed, nuclei stained with DAPI (blue), and

imaged via confocal microscopy. (Scale bars = 50 μm). Mannosylation of the polymeric vehicles enhanced their internalization by BMDMs. This could be competed away by co-administration of the ManNPs with 100 mg/mL of free D-mannose. Brightness & contrast were enhanced in the DAPI channel to account for small differences in staining between samples. FAM channels were left unaltered.

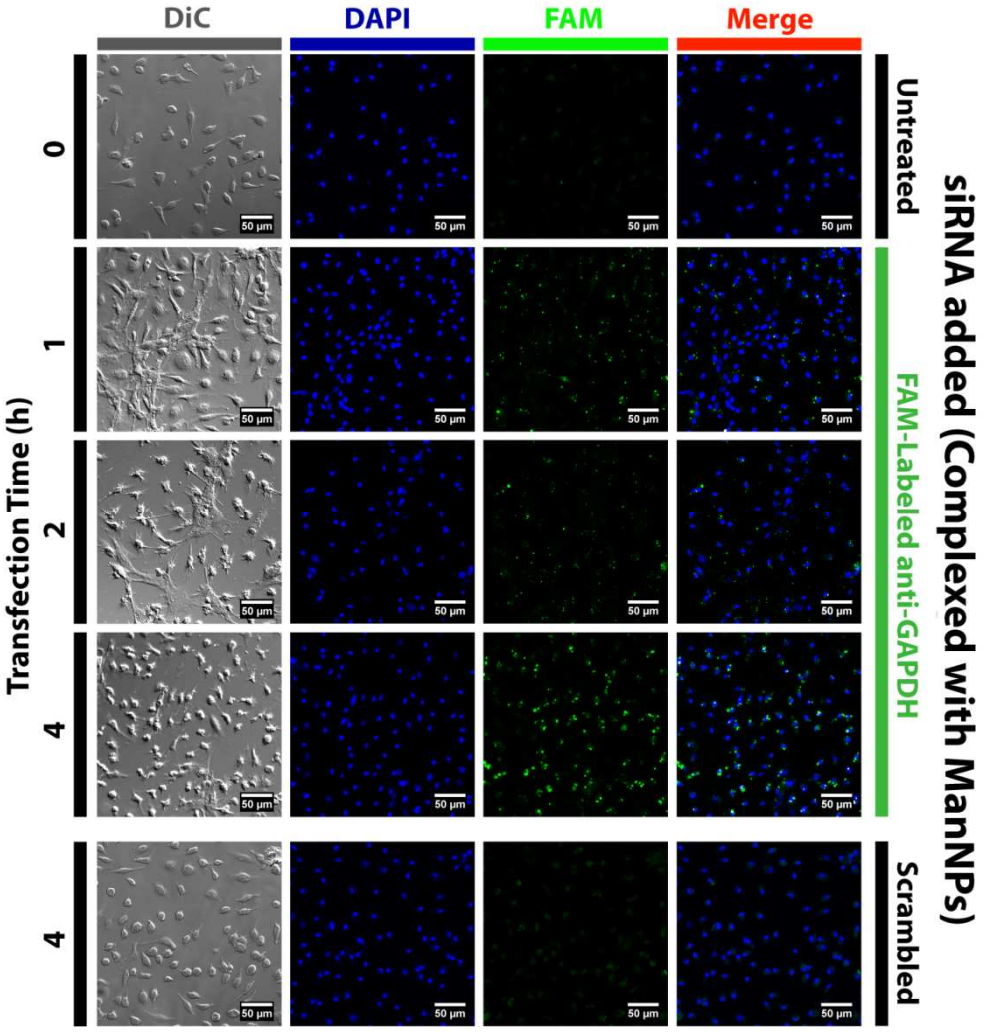

FIGURE 4. Kinetics of ManNP-Mediated siRNA Delivery into Primary Macrophages. BMDMs were transfected with FAM-siRNA (green; complexed into ManNPs) for 1-4 h prior to being fixed, stained with DAPI (blue), and imaged via confocal microscopy. (Scale bars = 50

μm). As a comparison, BMDMs treated with non-fluorescent, scrambled siRNA (complexed into ManNPs) have been shown. Brightness & contrast were enhanced in the DAPI channel to account for small differences in staining between samples. FAM channels were unaltered. Punctate green signal is observed within 1-2 h of administration, suggesting internalization of siRNA into vesicles. At 4h, the green fluorescence is more diffuse, consistent with endosomal escape of the siRNA into the cytosol.

ManNPs Enhance CD206-Dependent Intracellular siRNA Delivery and Target Gene Knockdown in Primary Murine Macrophages. siRNA delivery and gene knockdown were next examined in primary murine bone marrow-derived macrophages (BMDMs). Within 4 h of siRNA administration, ManNPs improved delivery of FAM-siRNA into macrophages by more than 40-fold relative to free siRNA or fourfold relative to the untargeted, diblock copolymers (Figure 2E, Supplementary Figure S7; $p < 0.01$). Notably, the uptake of ManNPs can be partially blocked via co-administration with D-mannose, indicating that internalization of the ManNPs is mediated by the mannose receptor.

In support of these observations, imaging of the uptake of fluorescently-labeled siRNA into BMDMs was accomplished by confocal microscopy (Figures 3-4, Supplementary Figure S8). Consistent with the flow cytometry results, mannose targeting significantly increased siRNA delivery into macrophages, and co-administration of D-mannose with the ManNPs reduced FAM-siRNA signal in the BMDMs. Significant levels of FAM-siRNA can be visualized in the BMDMs within 1-2 h of administration. The punctate staining (Figure 4) is consistent with the sequestration of the siRNA into intracellular vesicles. Within 4 h, the FAM staining becomes

more diffuse, suggesting that the FAM-siRNA has escaped the endosomal compartment and accessed the cytosol.

The enhanced delivery of siRNA via the ManNPs also corresponded with significantly improved knockdown of target gene expression in BMDMs relative to non-transfected cells and cells treated with free siRNA (PPIB; Figure 5; *$p < 0.05$). The commercially-available Lipofectamine RNAiMAX® transfection reagent was even more effective at facilitating the knockdown of PPIB expression, but was also cytotoxic at the 24 h time point used in this study. In spite of lower levels of siRNA delivery into the BMDMs relative to ManNPs (Figure 3), the diblock nanoparticles also facilitated a significant level of PPIB knockdown ($p = 0.06$ relative to ManNPs, via one-way ANOVA). This is likely due to the higher hemolytic activity of the diblock nanoparticles at endosomal pH ranges, relative to the ManNPs (Supplementary Figure S9).

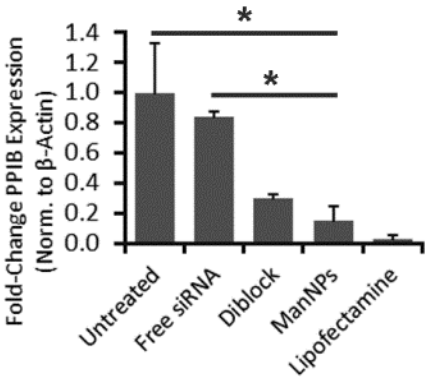

FIGURE 5. ManNPs Enhance Knockdown of PPIB Expression in BMDMs. siRNA-mediated knockdown of PPIB expression by transfection vehicle. qRT-PCR confirmed ManNPs carrying anti-PPIB siRNA mediated 85 ± 10% decrease in target gene expression following 24 h of treatment, relative to non-transfected (NT) cells. Error bars represent standard deviation of 3 independent experiments (*$p < 0.05$ by one-way ANOVA).

DISCUSSION

Recently, polymers for siRNA delivery applications were described by Convertine et al., but these polymers lack cell specificity, due to their cationic corona.[12] Other variants of these carriers have been recently developed that target folate receptor and CD22.[19, 20] In spite of the improved cell specificity of these constructs, their production required the use of more tedious, multi-step synthetic schemes[19, 25] or expensive targeting motifs such as antibodies.[20] Furthermore, unlike the approach described herein, these approaches did not generate a generalized platform that can be utilized for "clicking" on alternative targeting agents. Because macrophage-specific siRNA delivery is the central goal of the current work, CD206 was evaluated as the target receptor, motivated by its expression primarily on macrophages and some dendritic cells.[15]

Therefore, the first objective of this work was to develop a simple and rapid method for the immobilization of mannose onto micelle-forming polymeric siRNA carriers. Due to the presence of a number of reactive functional groups in the structure of the polymers, an orthogonal synthetic scheme was necessary to enable the synthesis of the desired block co-polymers, followed by site-selective functionalization with mannose in a final step. To accomplish this goal, we opted for a strategy involving the rapid and highly-efficient Huisgen 1,3-dipolar cycloaddition reaction, otherwise known as azide-alkyne 'click' chemistry (Figure 1). Compared with other variants of the mannosylated carriers, our synthetic scheme yields the modular, molecularly-targeted siRNA delivery vehicles from less costly starting materials, and requires fewer reaction steps.

The terpolymer block confers pH-responsiveness to the final polymers because at pH 7.4, approximately 50% of the carboxylic groups on PAA and approximately 50% of the amine

groups on DMAEMA are protonated, resulting in approximate charge neutrality of this block. Electrostatic and hydrophobic interactions enable this block to form a micelle core at pH 7.4, when it is covalently attached to a hydrophilic polymeric block. With decreasing pH, the PAA and DMAEMA become increasingly protonated, leading to a net cationic charge on this block that triggers micelle disassembly.[12] The exposed terpolymer is hypothesized to disrupt endosomal and lysosomal membranes and ferry siRNA into the cytoplasm.

Diblock copolymers composed of a cationic DMAEMA component bound to this terpolymer were next synthesized (Figure 1B-C). Such polymers have been shown to facilitate the cytosolic delivery of siRNA and peptides into immortalized cell lines *in vitro.*[12, 18-20] These 'base', diblock nanoparticles can enter many cell types because of their cationic surface charge, arising from the DMAEMA corona, which promotes interactions with the anionic cell membrane, triggering internalization.[26]

The ManNPs retain the functional properties of the cationic DMAEMA component, endowing the micelles with the ability to complex siRNA and protect it from nucleases that may be present in the *in vivo* environment (Figure 2). These properties are somewhat attenuated from those of the diblock copolymers, and is likely due to the morphology of the ManNPs, as the mannosylated corona may partially alter the properties of the underlying DMAEMA layer, including access of siRNA to binding through its cationic charge (Supplementary Figure S5). Therefore, the ManNPs are likely to be slightly less amenable to complexation with siRNA than is the base diblock copolymer, which displays an outermost corona of DMAEMA. Nevertheless, the resulting ManNPs form multifunctional nanoparticles that display mannose on the surface, while veiling underlying structures designed to carry nucleic acids and other biologics into the cytosol of targeted cells.

The ManNPs show cell selectivity, and the data suggest that in a tumor environment where cancer cells coexist with a significantly smaller population of macrophages, the ManNPs will enter macrophages markedly faster than the cancer cells (Figure 2D). While this increased internalization rate was also observed for the non-targeted diblock copolymers, the effect was more enhanced for the mannosylated constructs. Despite significant levels of cytotoxicity at N:P ratios of > 4:1, these results were not surprising, as cationic transfection agents have been shown to exhibit charge-dependent cytotoxicity.[5] To counter this, all polyplexes for subsequent experiments were prepared at N:P ratios for which negligible cytotoxicity was observed at 24 h treatment time (Figure 2C). It is anticipated that the presented strategy for preferential macrophage targeting can be leveraged in diseases where infiltrating macrophages at pathologic sites exhibit upregulated CD206 expression, including cancer.[27] Therefore, ManNPs provide a promising platform for macrophage-specific delivery of RNAi therapeutics in pathologic sites.

The ManNPs also facilitated improved siRNA delivery into primary murine macrophages and generated robust knockdown of a model gene (Figures 2-5. The untargeted, diblock polymers also achieved potent gene knockdown despite delivering significantly lower amounts of siRNA into the macrophages. However, these effects were likely due to the significantly higher ability of the diblock polymers to disrupt phospholipid bilayers as measured via the hemolysis assay (Supplementary Figure S9). The decreased hemolytic activity displayed by the ManNPs is possibly due to the addition of the AzEMA/mannose layer, which may ‘shield’ the endosomolytic components of the nanoparticles. While the mechanisms of this ‘shielding’ effect are as yet unknown, other groups have observed the same attenuation in polymer-mediated hemolysis following the PEGylation of polyethyleneimine-based gene delivery vehicles.[28, 29]

Nevertheless, these results are significant because primary macrophages possess highly degradative phagocytic, endosomal and lysosomal compartments, providing a formidable barrier to the cytosolic delivery of siRNA.[4] Moreover, these data suggest that the ManNPs and their cargo are interacting with an endocytotic receptor, leading to internalization of the complexes. The cargo is then able to escape the endosomal pathway, through a mechanism that is likely mediated by the pH-responsive, endosomolytic behavior of the terpolymer block within the ManNPs.[12] Moreover, the data implies that the targeted receptor is likely CD206, as it is known to effectively bind mannosylated substrates, resulting in internalization of the bound substrates via receptor-mediated endocytosis or phagocytosis.[30]

CONCLUSIONS

The data presented here showcase a novel strategy to selectively target TAMs. The capacity of this system for endosomal disruption enables biologics to be delivered into the cytosol, promoting their access to intracellular drug targets and processes. In a broader sense, this work is the first demonstration of a 'clickable' siRNA delivery platform that will enable the attachment of other targeting ligands to the azide-functionalized corona of pH-responsive, endosomolytic micelles. These strategies will potentially open up new areas in cancer immunotherapy, enabling selective intervention with the activities of TAMs while leaving surrounding cells relatively undisturbed.

METHODS

Materials. All reagents and materials were purchased from Sigma-Aldrich (St. Louis, MO) and used as described unless described otherwise. Monomers for radical polymerization, including BMA, DMAEMA, PAA, and AzEMA, were all purified by vacuum distillation and stored at 4°C

in clean, inhibitor-free containers. Riboshredder RNAse blend was purchased from Epicentre (Madison, WI). Immortalized cell lines were acquired from American Type Culture Collection (Manassas, VA). Cell culture supplies, including media, fetal bovine serum, antibiotics, and non-essential amino acids were obtained from Life Technologies (Carlsbad, CA). The siRNA sequences purchased for transfections were: FAM-labeled anti-GAPDH siRNA (FAM-siRNA) and Cy3-labeled siRNA. The anti-PPIB siRNA used in knockdown experiments was purchased from Integrated DNA Technologies (Coralville, IA). Horse serum was purchased from Atlanta Biologicals (Norcross, GA).

Synthesis of 2-azidoethanol. In a 500 mL round-bottom flask, 15.6 g of sodium azide (0.24 mol) was dissolved in 100 mL of nanopure water, followed by the addition of 5.67 mL of 2-bromoethanol (10 g, 0.08 mol; Supplementary Figure S1). After capping the system with a septum, the reaction was heated to 80°C and allowed to stir overnight, during which the reaction changes darkens from yellow to orange. After allowing the reaction to cool to room temperature, the product was extracted 4x with 75 mL diethyl ether. Following two extractions, the aqueous phase changed colors from orange to clear. The pooled organic fractions were concentrated by rotary evaporation to yield a clear, colorless oil (95% yield; 6.66 g : 27.6137g – 20.9532g). ^{1}H NMR (400 MHz, $(CD_3)_2SO$): δ (ppm) 3.20 – 3.27 (t, 2H, C**H**$_2$N$_3$), 3.44 (s, 1H, O**H**), 3.54 – 3.60 (q, 2H, C**H**$_2$O). FT-IR (KBr pellet): 3380 cm^{-1} (broad, O-H), 2100 cm^{-1} (N_3), 1295 cm^{-1} (C-N), 1050 cm^{-1} (C-O).

Synthesis of 2-Azidoethyl methacrylate (AzEMA). In a round-bottom flask, 10 g of 2-azidoethanol (0.11 mol) was mixed with 30.6 mL of Et_3N (22.3 g, 0.22 mol) in 50 mL of CH_2Cl_2

in a dry ice-acetone bath (-78°C; Supplementary Figure S1). The reaction vessel was capped with a septum and degassed by alternating evacuation of the vessel and equilibration with nitrogen gas, 6x. Next, 8.6 mL of methacryloyl chloride (9.2 g, 0.088 mol) was injected into the system dropwise, and the reaction proceeded overnight (Caution: azide compounds may become shock-sensitive above 75-80°C, and this step is highly exothermic). The dry ice-acetone bath was allowed to warm to room temperature during this reaction. The crude product was extracted 3x with 1N hydrochloric acid to remove excess Et_3N, extracted 2x with 1N aqueous NaOH, and precipitated in nanopure water. After drying the organic fraction over $MgSO_4$, the product was concentrated under rotary evaporation to yield a dark red-orange liquid, which was further distilled under high vacuum to produce pure 2-azidoethyl methacrylate. ^{1}H NMR (400 MHz, $CDCl_3$): δ (ppm) 1.97 (s, 3H, C**H$_3$**), 3.5 (t, 2H, C**H$_2$**N_3), 4.33 (t, 2H, C**H$_2$**O), 5.62 (s, 1H), 6.18 (s, 1H).

Synthesis of alkyne-functionalized mannose. The reaction diagram and characterization have been shown in Supplementary Figure S2. In a round-bottom flask, 11 g of D-mannose (60 mmol) were dissolved into 30 mL dimethylsulfoxide (DMSO). To activate the sugar into a nucleophile, 10 mL Et_3N (triethylamine; 72 mmol) was added to the reaction, prior to the addition of 5 g propargyl chloride (67 mmol). After flushing the reaction with argon, the reaction proceeded for 24 h at 40°C. Excess reagents were removed by 5X extraction into diethyl ether. The remaining ether-insoluble phase was dissolved into nanopure water and further extracted 5X with dichloromethane to remove other byproducts and DMSO. The product was flash-frozen in liquid N_2 and lyophilized. ^{1}H- and ^{13}C-NMR and HPLC characterization data are presented in Supplementary Figure S2.

RAFT Polymerizations. Synthesis of the RAFT chain transfer agent (CTA) 4-cyano-4-(ethylsulfanylthiocarbonyl) sulfanylpentanoic acid (ECT) and 2-propylacrylic acid monomer have been described in detail in our previous work.[12, 31] Polymerization of the 47%BMA-25%PAA-28%DMAEMA terpolymer was conducted at 70°C under N_2 for 18 h with DMF as the solvent (90 wt% in feed), an initial monomer-to-CTA molar ratio of 100, and a CTA to initiator molar ratio of 10. After rapidly cooling the reaction in an ice bath, the organic mixture was mixed 1:1 (by volume) with aqueous HCl at pH 2, which initially results in a turbid mixture but quickly turns clear-yellowish as the monomers and polymers equilibrate with the acidic environment. Next, the polymer was precipitated 7x in hexanes and 2x in diethyl ether to remove residual monomers. Finally, the polymers, which were at this point still soluble in the acidic aqueous medium, were dialyzed across 10kDa molecular weight cutoff membrane (Pierce, Rockford, IL) against nanopure water (pH ~ 5, so no change in polymer solubility was observed) overnight. Lyophilization yielded pure terpolymer, which was a yellowish powder (Table 1).

The same monomer:macroCTA:I molar ratios, and 90 wt% DMF conditions were used to polymerize the DMAEMA block onto the terpolymer macroCTA. To purify the diblock, the completed reaction was precipitated in ether at -20°C for 1h, and then pelleted by centrifugation at 800 x g for 5 min. After discarding the supernatant, the pellet was resuspended in deionized water, forming a slightly turbid suspension. Dialysis against deionized water for 48 h, across 10kDa-MWCO membrane, and lyophilization yielded pure diblock, which was a yellow-white powder.

The polymerization of the AzEMA block onto the diblock was done to form triblock copolymers according to the same protocol. This mixture was then extensively dialyzed across

10kDa MWCO membranes overnight, against nanopure water, to yield the completed triblocks. Triblocks were dissolved in deionized water at 1 mg/mL and stored at -20°C until ready for use in 'click' reactions.

^{1}H-NMR spectra for all polymers are shown in Supplementary Figure S3.

'Click' Chemistry. In a scintillation vial, 1 mL of triblock co-polymer (1 mg/mL in nanopure H_2O) was mixed with 6 mg alkyne-functionalized mannose (27.5 mmol). After the addition of $CuSO_4$ and sodium ascorbate to final concentrations of 1 mM and 5 mM, respectively, the reaction was allowed to proceed at 37°C on an orbital shaker in the dark for 48 h. Excess copper was removed by treating the crude product with Chelex 100 Resin (Bio-Rad Laboratories, Hercules, CA) according to manufacturer's instructions. The product was filtered through a 0.45 μm Teflon filter to remove the resin, and then dialyzed through a 2 kDa-MWCO membrane against deionized water to remove excess reactants. ^{1}H-NMR characterization of the micelles before and after 'click' chemistry is shown in Supplementary Figure S5.

siRNA Protection Experiments. 50 pmol Cy3-labeled siRNA was complexed with mannosylated nanoparticles at N:P ratios of: 1:2, 1:1, 2:1, and 4:1. Ratios were calculated by using the concentration of NH^+ (based on the degree of polymerization of the DMAEMA homopolymer block of the polymers, and the concentration of the polymers in μM) and PO_4^- (based off the number of siRNA base pairs and the concentration of siRNA in μM). Because the pK_a of the DMAEMA occurs at around pH 7.2, we assumed that the DMAEMA block was 50% charged for the calculation of N:P ratios. The complexes were loaded onto a 2% agarose gel containing 1.5 μM ethidium bromide.

The RNAse protection experiment was performed on siRNA complexes with either diblock copolymers (0.5:1 N:P ratio) or mannosylated nanoparticles (0.5:1 or 4:1 N:P ratios), as described elsewhere.[24]

Animals and Cell Lines. Animal work was approved by the Vanderbilt University Institutional Animal Care and Use Committee. All mice were on an FVB background strain. Bone marrow-derived macrophages were isolated from tibiae and femurs immediately after sacrificing the mice and cultured as described elsewhere.[32] Cells were seeded at 300,000 cells/cm^2 for all experiments. Detailed information on culturing of immortalized cell lines can be found in the Supplementary Information.

Transfections. Complexes were prepared by as described above. For some transfections, Lipofectamine RNAiMAX® (Life Technologies, Carlsbad, CA) was used to complex siRNA, and was used according to manufacturer's instructions (Except for knockdown experiment, which was conducted for 24 h in order to compare all vehicles in head-to-head fashion). Cells were prepared for transfection by rinsing wells twice with PBS to remove growth medium. This was replaced with serum-free medium, which is composed of DMEM with 4.5 g/L glucose, 1 U/mL penicillin, 1 μg/mL streptomycin, and 2 mM L-glutamine. Complexes were then added to the wells such that the final concentration of siRNA in the wells was 50 nM (ten-fold dilution from stock). At set time points, wells were rinsed thrice with PBS to remove unbound complexes. Cells were then processed according to the desired experiment as described below.

Transfected cells were analyzed for cell viability using a Live-Dead kit (Life Technologies) according to the manufacturer's instructions. Quantification of live and dead cells was done by flow cytometry.

Quantitative real-time PCR. Total RNA was isolated from cell samples using the RNeasy Kit and QIAShredder columns (Qiagen). After the removal of genomic contamination through DNAse treatment (DNA-free kit, Life Technologies), cDNA libraries were constructed using a reverse transcriptase kit (Life Technologies).

For qRT-PCR, Primers were purchased from Integrated DNA Technologies (Coralville, IA). PPIB sense: 5'- TTCCATCGTGTCATCAAG-3' and antisense: 5'-GAAGAACTGTGAGCCATT-3'. β-actin sense: 5' – CACACCTTCTACAATGAG – 3' and antisense: 5' – GGTCTCAAACATGATCTG – 3'. CD206 sense: 5'-CAAGGAAGGTTGGCATTTGT - 3' and antisense: 5'– CCTTTCAGTCCTTTGCAAGC - 3'. Samples were treated with a SYBR Green PCR Master Mix in MicroAmp Fast optical 96-well plates (both from Life Technologies), according to the manufacturer's instructions. Details on data analysis for relative GAPDH expression can be found in the Supplementary Information.

Flow Cytometry. Flow cytometry was performed on a BD FACSCalibur system (Franklin Lakes, NJ), operated via a BD Cellquest Pro (version 5.2) software. The FL1 channel was used for the quantification of FAM emission of each cell. Data analysis and reporting were performed on FlowJo (version 7.6.4).

Confocal Microscopy. Transfections were performed as described above for 1,2, or 4 h. To prepare cells for confocal microscopy, they were washed with PBS, fixed for 15 min with 10%

buffered formalin, rinsed 3x with PBS, and then stained with DAPI (Invitrogen, Carlsbad, CA) for 10 min. After rinsing cells 3x with PBS, slides were mounted with the Invitrogen ProLong Antifade kit. Imaging was performed on a Zeiss LSM 710 system (Oberkochen, Germany). Image processing is described in the Supplementary Information.

Statistical Significance. For all experiments, statistical significance was assessed using the unpaired Student's t-test or one-way ANOVA as indicated in the text.

REFERENCES

1. Kindt, T. J., Goldsby, R. A., Osborne, B. A., and Kuby, J. (2007) *Kuby immunology*, 6th ed., W.H. Freeman, New York.
2. Dirkx, A. E., Oude Egbrink, M. G., Wagstaff, J., and Griffioen, A. W. (2006) Monocyte/macrophage infiltration in tumors: modulators of angiogenesis, *J Leukoc Biol 80*, 1183-1196.
3. Fire, A., Xu, S., Montgomery, M. K., Kostas, S. A., Driver, S. E., and Mello, C. C. (1998) Potent and specific genetic interference by double-stranded RNA in Caenorhabditis elegans, *Nature 391*, 806-811.
4. Stacey, K. J., Ross, I. L., and Hume, D. A. (1993) Electroporation and DNA-dependent cell death in murine macrophages, *Immunol Cell Biol 71*, 75-85.
5. Lv, H., Zhang, S., Wang, B., Cui, S., and Yan, J. (2006) Toxicity of cationic lipids and cationic polymers in gene delivery, *Journal of Controlled Release 114*, 100-109.
6. Kortylewski, M., Swiderski, P., Herrmann, A., Wang, L., Kowolik, C., Kujawski, M., Lee, H., Scuto, A., Liu, Y., Yang, C., Deng, J., Soifer, H. S., Raubitschek, A., Forman, S., Rossi, J. J., Pardoll, D. M., Jove, R., and Yu, H. (2009) In vivo delivery of siRNA to

immune cells by conjugation to a TLR9 agonist enhances antitumor immune responses, *Nat Biotechnol 27*, 925-932.

7. Watkins, S. K., Egilmez, N. K., Suttles, J., and Stout, R. D. (2007) IL-12 rapidly alters the functional profile of tumor-associated and tumor-infiltrating macrophages in vitro and in vivo, *J Immunol 178*, 1357-1362.

8. Hagemann, T., Lawrence, T., McNeish, I., Charles, K. A., Kulbe, H., Thompson, R. G., Robinson, S. C., and Balkwill, F. R. (2008) "Re-educating" tumor-associated macrophages by targeting NF-kappaB, *J Exp Med 205*, 1261-1268.

9. Briley-Saebo, K. C., Cho, Y. S., Shaw, P. X., Ryu, S. K., Mani, V., Dickson, S., Izadmehr, E., Green, S., Fayad, Z. A., and Tsimikas, S. (2011) Targeted Iron Oxide Particles for In Vivo Magnetic Resonance Detection of Atherosclerotic Lesions With Antibodies Directed to Oxidation-Specific Epitopes, *J Am Coll Cardiol 57*, 337-347.

10. Lipinski, M. J., Amirbekian, V., Frias, J. C., Aguinaldo, J. G., Mani, V., Briley-Saebo, K. C., Fuster, V., Fallon, J. T., Fisher, E. A., and Fayad, Z. A. (2006) MRI to detect atherosclerosis with gadolinium-containing immunomicelles targeting the macrophage scavenger receptor, *Magn Reson Med 56*, 601-610.

11. Cormode, D. P., Skajaa, T., van Schooneveld, M. M., Koole, R., Jarzyna, P., Lobatto, M. E., Calcagno, C., Barazza, A., Gordon, R. E., Zanzonico, P., Fisher, E. A., Fayad, Z. A., and Mulder, W. J. (2008) Nanocrystal core high-density lipoproteins: a multimodality contrast agent platform, *Nano Lett 8*, 3715-3723.

12. Convertine, A. J., Benoit, D. S., Duvall, C. L., Hoffman, A. S., and Stayton, P. S. (2009) Development of a novel endosomolytic diblock copolymer for siRNA delivery, *J Control Release 133*, 221-229.

13. Boyer, C., Bulmus, V., Davis, T. P., Ladmiral, V., Liu, J., and Perrier, S. (2009) Bioapplications of RAFT polymerization, *Chem Rev 109*, 5402-5436.

14. Kolb, H. C., and Sharpless, K. B. (2003) The growing impact of click chemistry on drug discovery, *Drug Discovery Today 8*, 1128-1137.

15. Taylor, P. R., Gordon, S., and Martinez-Pomares, L. (2005) The mannose receptor: linking homeostasis and immunity through sugar recognition, *Trends in Immunology 26*, 104-110.

16. East, L., and Isacke, C. M. (2002) The mannose receptor family, *Biochimica et Biophysica Acta (BBA) - General Subjects 1572*, 364-386.

17. Vasievich, E. A., and Huang, L. (2011) The Suppressive Tumor Microenvironment: A Challenge in Cancer Immunotherapy, *Molecular Pharmaceutics 8*, 635-641.

18. Duvall, C. L., Convertine, A. J., Benoit, D. S., Hoffman, A. S., and Stayton, P. S. (2010) Intracellular Delivery of a Proapoptotic Peptide via Conjugation to a RAFT Synthesized Endosomolytic Polymer, *Mol Pharm*.

19. Benoit, D. S. W., Srinivasan, S., Shubin, A. D., and Stayton, P. S. (2011) Synthesis of Folate-Functionalized RAFT Polymers for Targeted siRNA Delivery, *Biomacromolecules 12*, 2708-2714.

20. Palanca-Wessels, M. C., Convertine, A. J., Cutler-Strom, R., Booth, G. C., Lee, F., Berguig, G. Y., Stayton, P. S., and Press, O. W. (2011) Anti-CD22 antibody targeting of pH-responsive micelles enhances small interfering RNA delivery and gene silencing in lymphoma cells, *Molecular therapy : the journal of the American Society of Gene Therapy 19*, 1529-1537.

21. Crownover, E., Duvall, C. L., Convertine, A., Hoffman, A. S., and Stayton, P. S. (2011) RAFT-synthesized graft copolymers that enhance pH-dependent membrane destabilization and protein circulation times, *Journal of controlled release : official journal of the Controlled Release Society 155*, 167-174.

22. Sumerlin, B. S., Tsarevsky, N. V., Louche, G., Lee, R. Y., and Matyjaszewski, K. (2005) Highly Efficient "Click" Functionalization of Poly(3-azidopropyl methacrylate) Prepared by ATRP, *Macromolecules 38*, 7540-7545.

23. Plotz, P. H., and Rifai, A. (1982) Stable, Soluble, Model Immune-Complexes Made with a Versatile Multivalent Affinity-Labeling Antigen, *Biochemistry 21*, 301-308.

24. Kirkland-York, S., Zhang, Y., Smith, A. E., York, A. W., Huang, F., and McCormick, C. L. (2010) Tailored design of Au nanoparticle-siRNA carriers utilizing reversible addition-fragmentation chain transfer polymers, *Biomacromolecules 11*, 1052-1059.

25. Henry, S. M., Convertine, A. J., Benoit, D. S., Hoffman, A. S., and Stayton, P. S. (2009) End-functionalized polymers and junction-functionalized diblock copolymers via RAFT chain extension with maleimido monomers, *Bioconjug Chem 20*, 1122-1128.

26. Kumari, A., Yadav, S. K., and Yadav, S. C. (2010) Biodegradable polymeric nanoparticles based drug delivery systems, *Colloids and Surfaces B: Biointerfaces 75*, 1-18.

27. Luo, Y., Zhou, H., Krueger, J., Kaplan, C., Lee, S.-H., Dolman, C., Markowitz, D., Wu, W., Liu, C., Reisfeld, R. A., and Xiang, R. (2006) Targeting tumor-associated macrophages as a novel strategy against breast cancer, *The Journal of Clinical Investigation 116*, 2132-2141.

28. Neu, M., Germershaus, O., Behe, M., and Kissel, T. (2007) Bioreversibly crosslinked polyplexes of PEI and high molecular weight PEG show extended circulation times in vivo, *Journal of Controlled Release 124*, 69-80.

29. Petersen, H., Fechner, P. M., Martin, A. L., Kunath, K., Stolnik, S., Roberts, C. J., Fischer, D., Davies, M. C., and Kissel, T. (2002) Polyethylenimine-graft-Poly(ethylene glycol) Copolymers: Influence of Copolymer Block Structure on DNA Complexation and Biological Activities as Gene Delivery System, *Bioconjugate Chemistry 13*, 845-854.

30. Stahl, P. D., and Ezekowitz, R. A. B. (1998) The mannose receptor is a pattern recognition receptor involved in host defense, *Current Opinion in Immunology 10*, 50-55.

31. Nelson, C. E., Gupta, M. K., Adolph, E. J., Shannon, J. M., Guelcher, S. A., and Duvall, C. L. (2012) Sustained local delivery of siRNA from an injectable scaffold, *Biomaterials 33*, 1154-1161.

32. Connelly, L., Jacobs, A. T., Palacios-Callender, M., Moncada, S., and Hobbs, A. J. (2003) Macrophage endothelial nitric-oxide synthase autoregulates cellular activation and pro-inflammatory protein expression, *J Biol Chem 278*, 26480-26487.

Supporting Information. This material is available free of charge via the Internet at http://pubs.acs.org.

ACKNOWLEDGMENTS

This work is supported through a Concept Award through the Department of Defense CDMRP Breast Cancer Research Program (#W81XWH-10-1-0684). Bone marrow-derived macrophages and *in vivo* work was supported through a multi-investigator, collaborative IDEA Award through

the Department of Defense CDMRP Breast Cancer Research Program (#W81XWH-11-1-0344 & #W81XWH-11-1-0242). CML acknowledges partial support through a fellowship from the Vanderbilt Undergraduate Summer Research Program (VUSRP). Portions of this work were performed at the Vanderbilt Institute of Nanoscale Science and Engineering, using facilities renovated under NSF ARI-R2 DMR-0963361. Confocal microscopy (Zeiss LSM 710) was supported in part by the NCI Cancer Center Support Grant #P30 CA068485, utilizing the Vanderbilt University Medical Center Cell Imaging Shared Resource. The Vanderbilt University Medical Center Cell Imaging Shared Resource is also supported by NIH grants DK020593, DK058404, HD015052, DK059637 and EY08126. qRT-PCR was performed in the laboratory of Prof. David G. Harrison (Division of Clinical Pharmacology, Vanderbilt University Medical Center).

Author Contributions S.S.Y. oversaw all materials design and synthesis, experimental design, and data collection, analysis and interpretation, with extensive input from F.E.Y., C.L.D., and T.D.G. C.M.L. collected, analyzed, and interpreted data. W.J.B. and H.M.O. designed and selected the biological models used in this study, and assisted in biological experiments with S.S.Y. and C.M.L., under the oversight of F.E.Y. C.E.N. and H.L. helped design protocols for the synthesis and purification of polymeric products, and contributed new reagents and analytic tools crucial to the experiments shown. S.S.Y. wrote the manuscript. All authors discussed the results and commented on the manuscript.

Competing Financial Interests. The authors have no conflicts of interest to disclose.

TABLES

TABLE 1. Characterization of Polymers Synthesized via RAFT Polymerization

Polymer	dn/dc (mL/g) [a]	Target M_n (Da)	M_n (Da) [b]	M_w (Da) [b]	PDI	D_h (nm)	ζ-Potential (mV)
Terpolymer	0.081	14000	11400	13900	1.22		
Diblock	0.049	21000	16800	20700	1.23	34.2 ± 2.2	10.8 ± 11.2
Triblock (Before 'click')	---	22000	22300	28900	1.29	28.0 ± 1.5	19.6 ± 11.7

[a]Measured in off-line batch mode in a Shimadzu RID-10A differential refractive index (dRI) detector, with DMF + 0.1M LiBr as the solvent.
[b]Measured via gel-permeation chromatography with MALS and dRI in-line with columns.

Graphical Table of Contents Entry

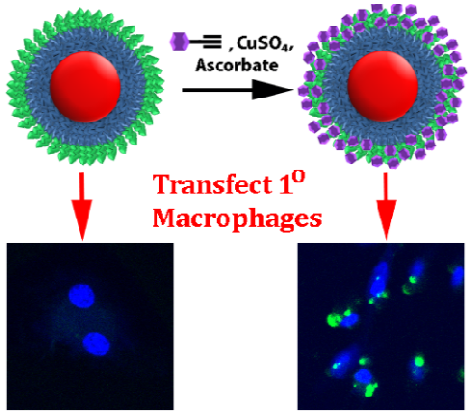

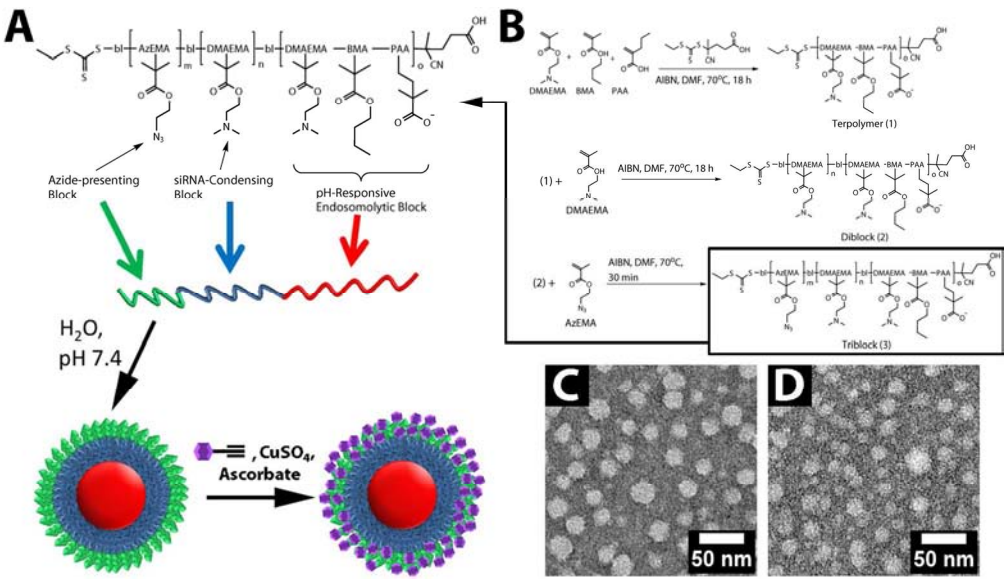

177x101mm (300 x 300 DPI)

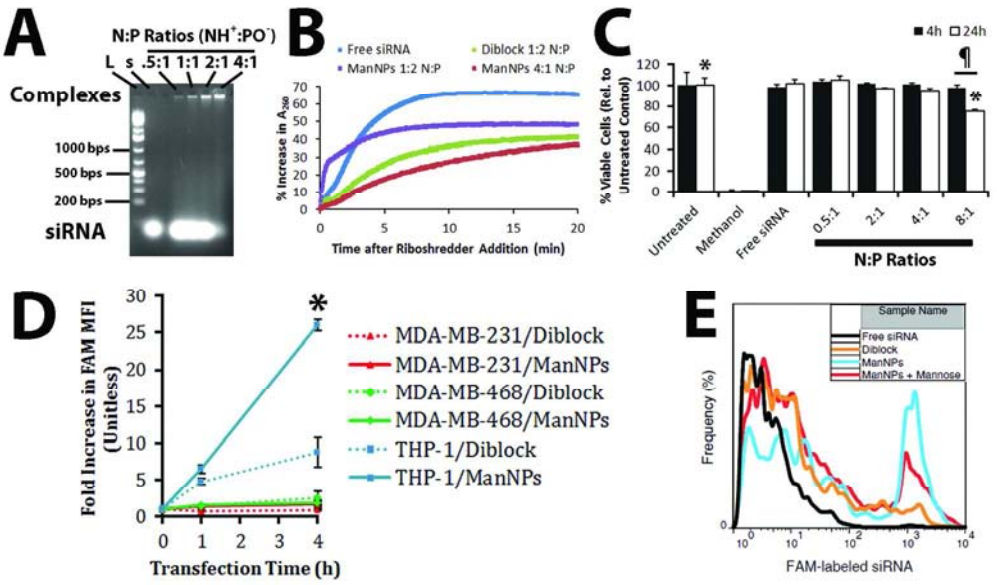

153x90mm (300 x 300 DPI)

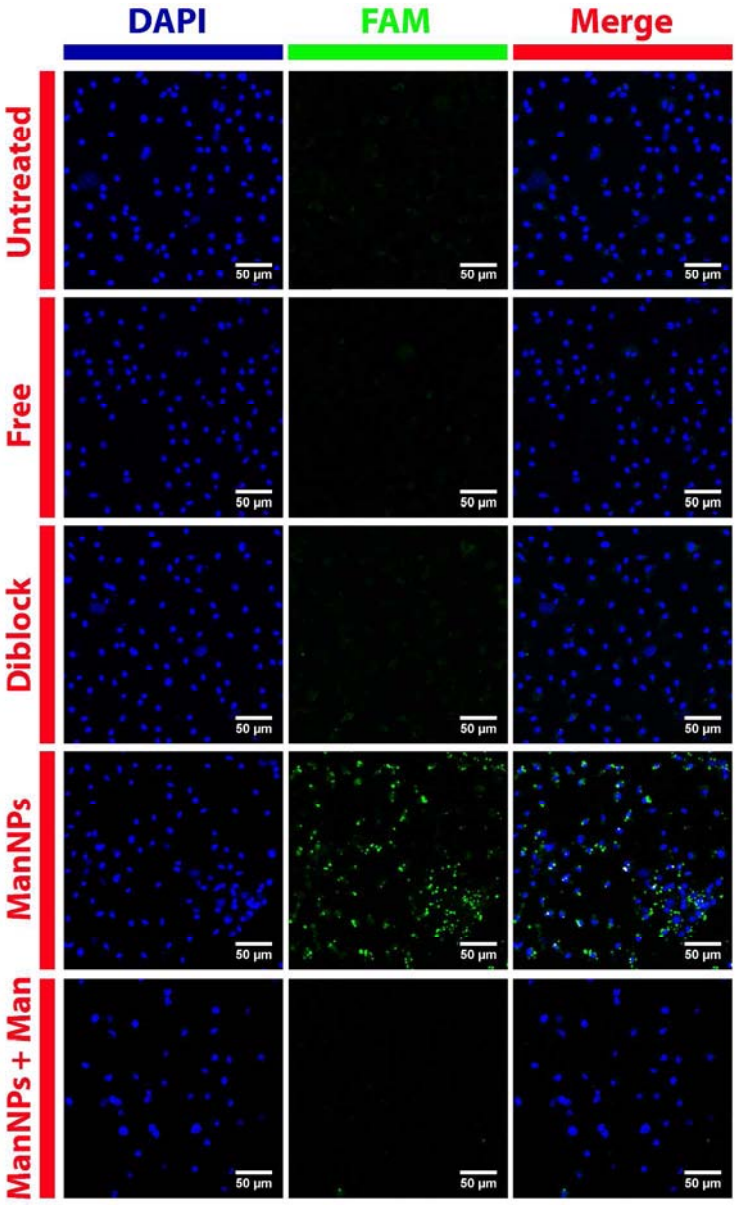

246x398mm (300 x 300 DPI)

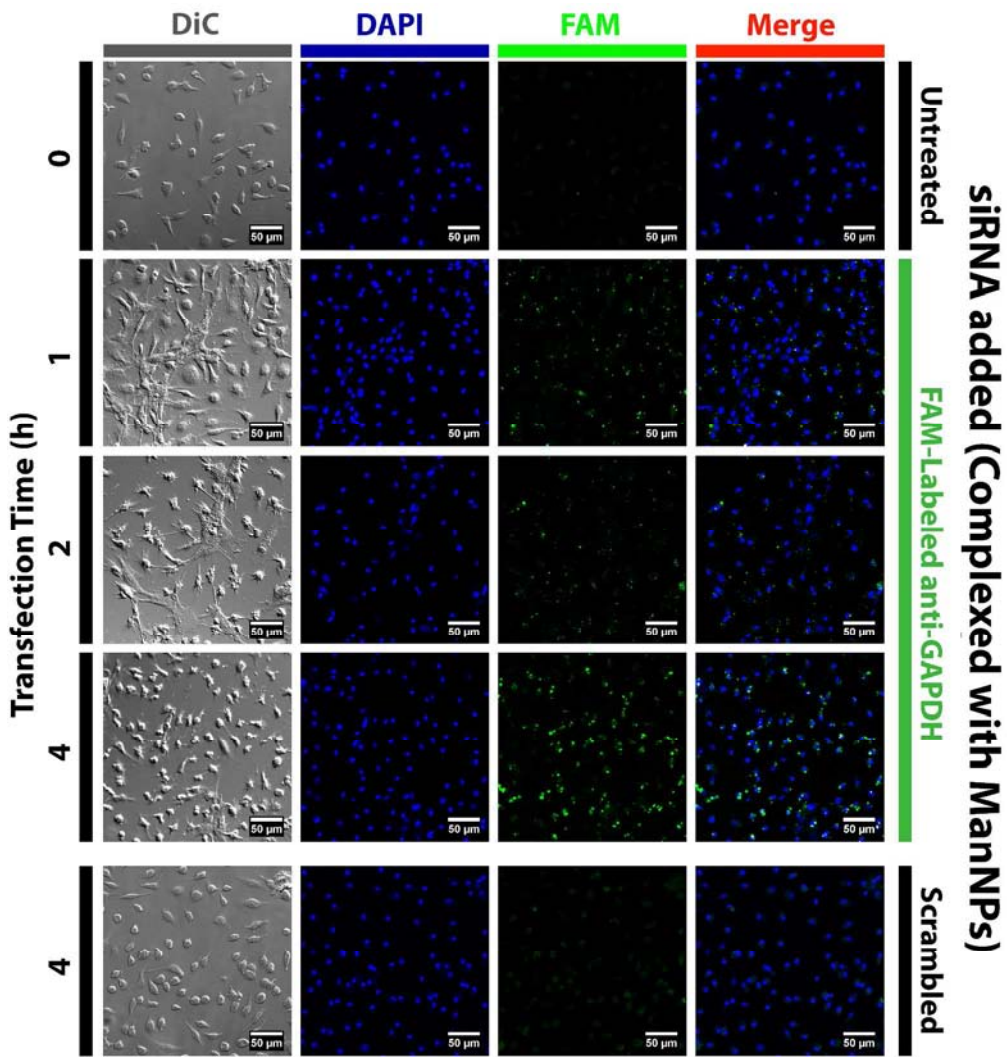

386x406mm (300 x 300 DPI)

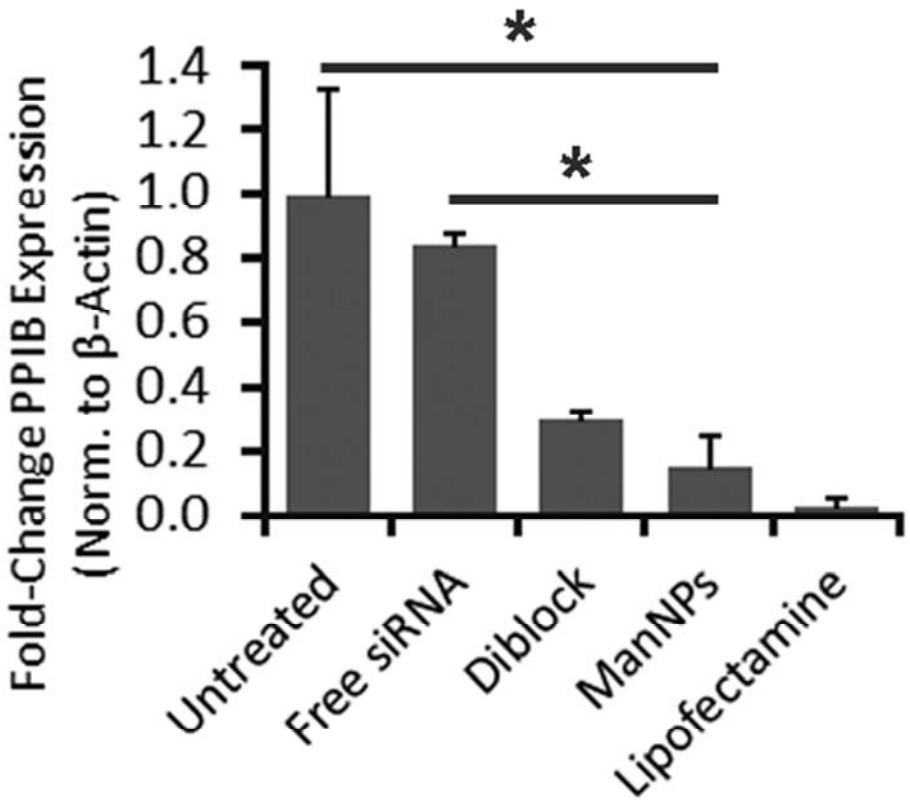

39x35mm (300 x 300 DPI)

SUPPLEMENTARY INFORMATION FOR:

Macrophage-Specific RNAi Targeting via 'Click', Mannosylated Polymeric Micelles

Shann S. Yu[†,‡], Cheryl M. Lau[†], Whitney J. Barham[§], Halina M. Onishko[§], Christopher E. Nelson[†,‡], Hongmei Li[†,‡], Fiona E. Yull[§], Craig L. Duvall[†,‡], & Todd D. Giorgio[†,‡,§,⊥,*].

[†]Department of Biomedical Engineering, Vanderbilt University, Nashville, TN 37235
[‡]Vanderbilt Institute for Nanoscale Science & Engineering, Vanderbilt University, Nashville, TN 37235
[§]Department of Cancer Biology, Vanderbilt-Ingram Cancer Center, Nashville, TN 37232
[⊥]Department of Chemical & Biomolecular Engineering, Vanderbilt University, Nashville, TN 37235

*Correspondence should be addressed to Todd D. Giorgio, Ph.D., Department of Biomedical Engineering, Vanderbilt University, 5824 Stevenson Center, Nashville, TN 37235, United States. E-mail: todd.d.giorgio@vanderbilt.edu . Phone: 615.322.3521. Fax: 615.343.7919.

SUPPLEMENTARY FIGURES

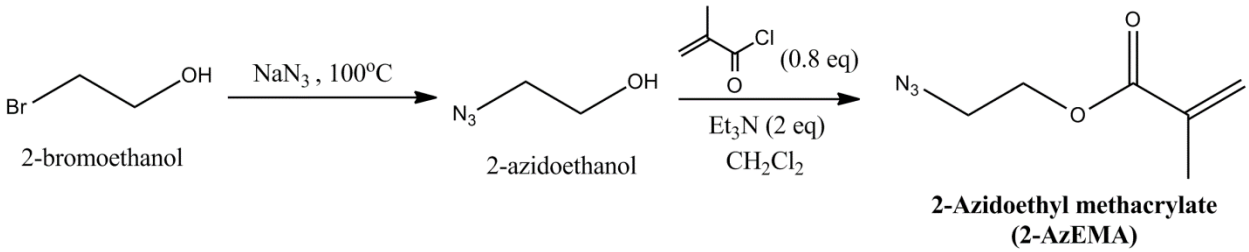

SUPPLEMENTARY FIGURE S1. Synthetic scheme for 2-Azidoethyl methacrylate (AzEMA).

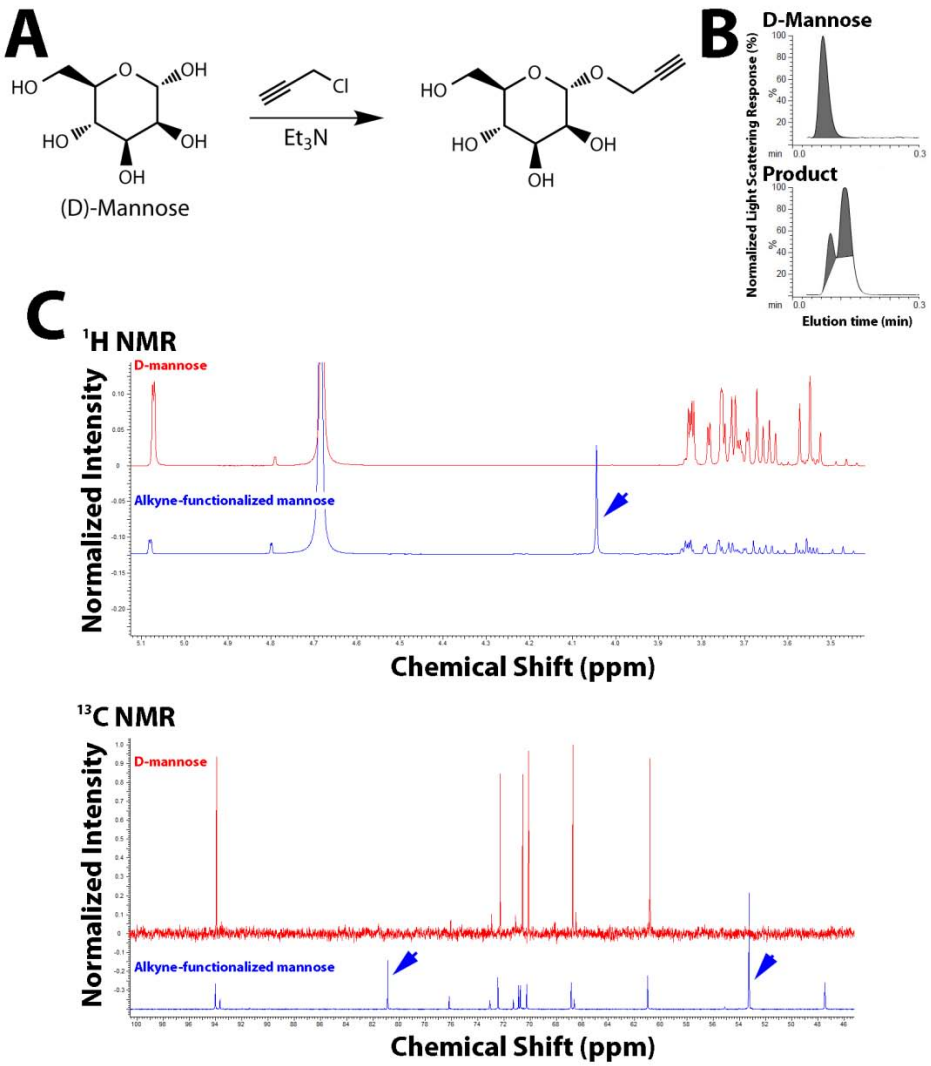

SUPPLEMENTARY FIGURE S2. Synthesis and characterization of alkyne-functionalized mannose. (A) Reaction diagram for the synthesis of alkyne-functionalized

mannose. The ideal product is shown on the right, but the scheme was not designed to be specific for the substitution of a particular hydroxyl group with a propargyl group. (B) Characterization of the precursor and product by HPLC. Evaporative light scattering chromatograms have been shown. The appearance of a large, later-eluting peak at ~0.1 min is due to the addition of a propargyl group onto the monosaccharide, which makes the molecule less polar than its precursor. The presence of excess precursor is not a concern, since the next reaction involving this mixture results in the 'clicking' of the modified sugar onto macromolecular assemblies (ManNPs), and purification by dialysis simply removes the excess precursor. (C) NMR spectroscopy of the precursor and product, with D_2O as the solvent. Because the propargyl chloride reagent is immiscible with water, the purification protocol used ensures the lack of this reagent in the final product. Blue arrowheads indicate peaks unique to the product, and are consistent with the attachment of alkyne groups onto the monosaccharide.

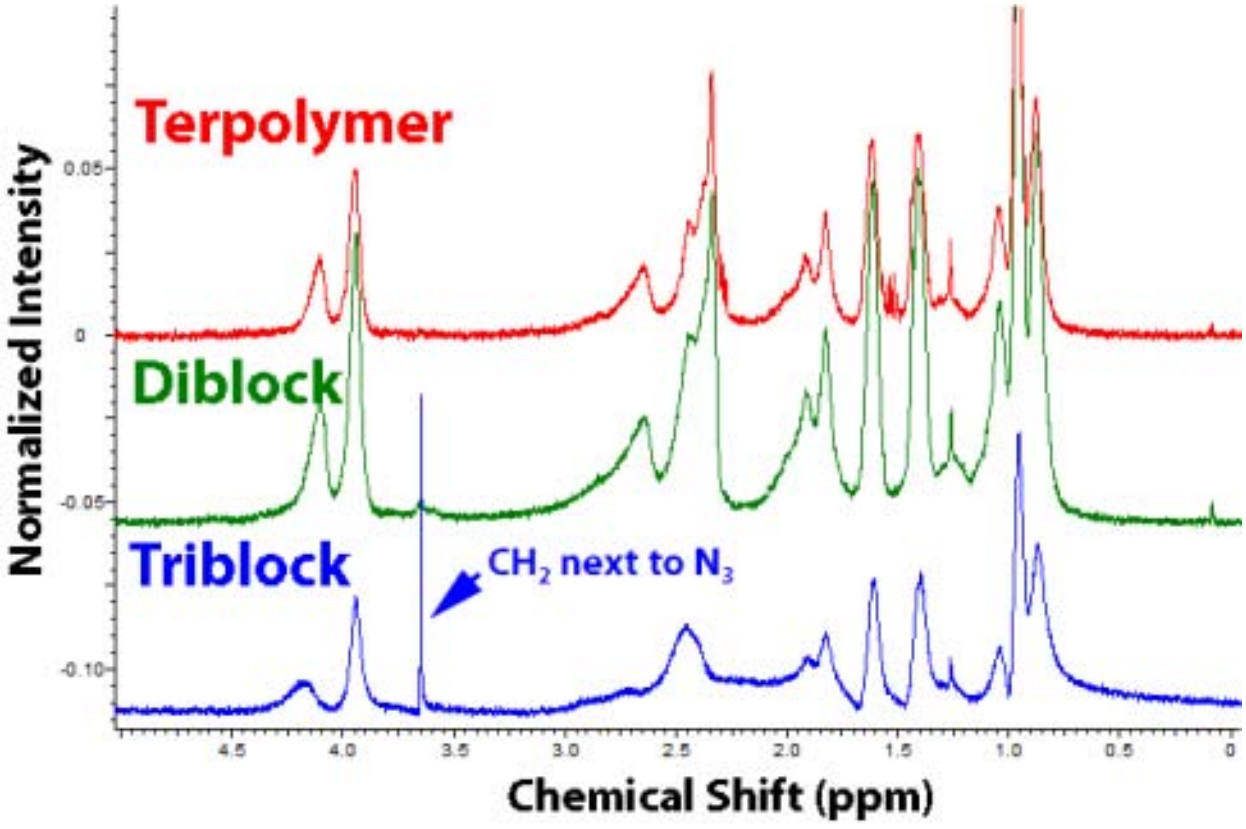

SUPPLEMENTARY FIGURE S3. Characterization of Block Copolymers Synthesized via RAFT Polymerization. NMR spectra of the purified copolymers were collected following

each round of synthesis and dialysis. Polymers were dissolved in $CDCl_3$ prior to spectral acquisition. The key difference between the terpolymer and the diblock is a quantifiable increase in DMAEMA composition (for diblock, relative to terpolymer). The triblock exhibits an additional peak at ~3.7 ppm, which is characteristic of the alkyl protons next to the free N_3 group presented on the AzEMA block.

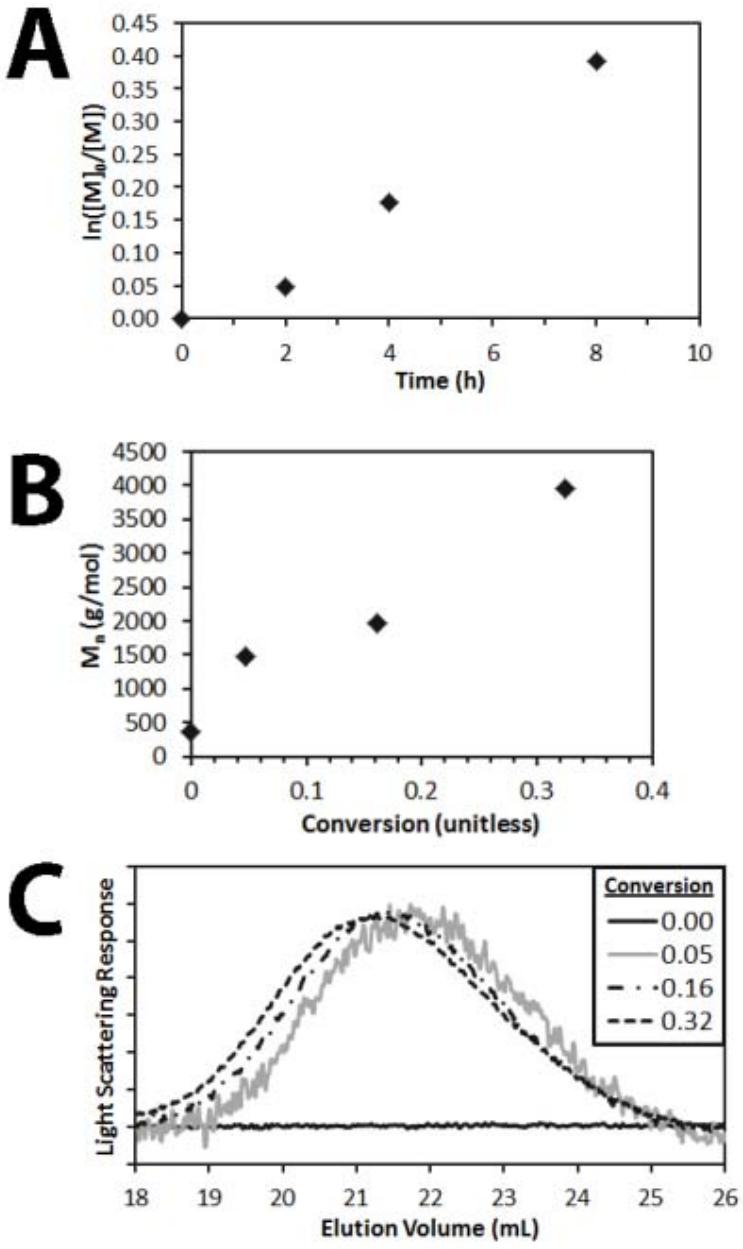

SUPPLEMENTARY FIGURE S4. RAFT Polymerization Kinetics of AzEMA. (A) Semilogarithmic kinetic plot of monomer conversion. (B) M_n vs. monomer conversion. (C)

Gel permeation chromatograms of light scattering response (signal normalized to tallest peak in chromatogram, therefore scale is not the same across samples) vs. elution volume, as a function of monomer conversion (see legend). Reaction conditions: [AzEMA]:[DCT]:[AIBN] 1000:10:1, 85 vol % DMF, T = 70°C.

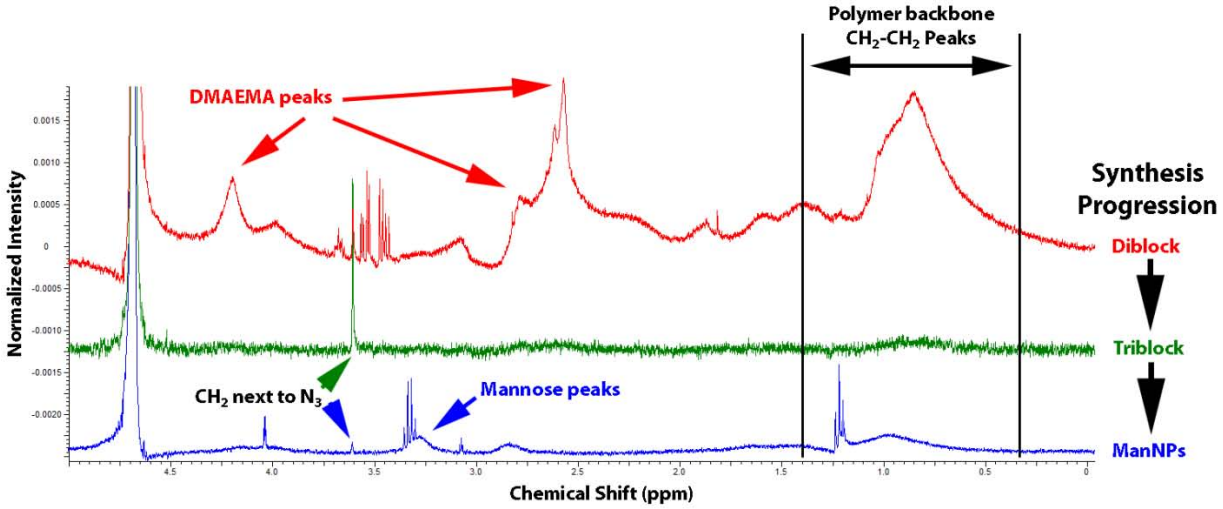

SUPPLEMENTARY FIGURE S5. NMR Spectroscopy of Micelles of Block Copolymers in D_2O. The surface moieties displayed by the various micelles are plotted at different steps of synthesis. All polymers were extensively dialyzed across 10 kDa-MWCO membranes and lyophilized, prior to reconstitution in D_2O for NMR measurements. The diblock co-polymer forms micelles that display DMAEMA, as evidenced by the broad peaks in its characteristic regions (red). This layer is effectively shielded following the polymerization of AzEMA, which yields strong azide peaks and a small hump in the polymer backbone region (characteristic of the alkyl backbone that composes all poly-acrylates). The mannosylation of the triblock by 'click' chemistry results in the appearance of new peaks in the 3.0-3.5 ppm region, which is slightly lower than where mannose peaks have been shown to appear (Supplementary Figure S1), but is consistent with the immobilization of these polar molecules onto a hydrophobic polymeric backbone.

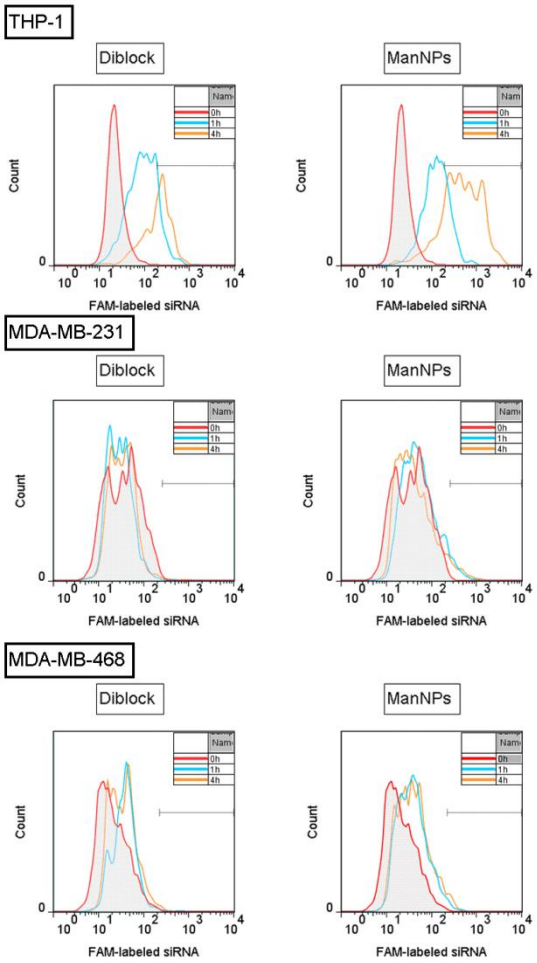

SUPPLEMENTARY FIGURE S6. ManNPs Selectively Target siRNA to Human Macrophages Over Breast Cancer Cells. Immortalized human macrophages (THP-1) or two breast cancer cell lines (MDA-MB-231 / MDA-MB-468) were treated with 50 nM FAM-siRNA, complexed within un-targeted diblock nanoparticles or ManNPs. Complexes were formed at an 4:1 N:P ratio. Flow cytometry was used to quantify internalization of siRNA at 0 (red), 1 (blue) or 4 h (orange) after administration. FAM histograms have been grouped by vehicle type (columns) or cell line (rows). Both breast cancer cell lines internalized little siRNA via either carrier, as indicated by the very slight shift in the fluorescence histogram of these cells over the incubation period. However, uptake was significantly greater for the macrophages.

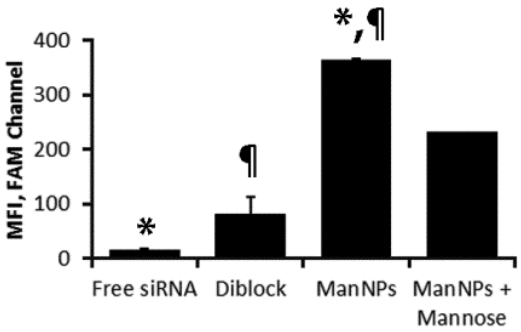

SUPPLEMENTARY FIGURE S7. Improved Delivery of siRNA into Primary Macrophages using ManNPs. Flow cytometry confirms improved delivery of FAM-siRNA into BMDMs via ManNPs within 4 h of administration. FAM mean fluorescence intensity for BMDMs versus vehicle type (corresponding to Figure 2E). Co-administration of 100 mg/mL free mannose with the ManNPs reduces delivery of siRNA into BMDMs. Error bars represent standard deviation from 2 independent experiments (*,¶ $p < 0.01$).

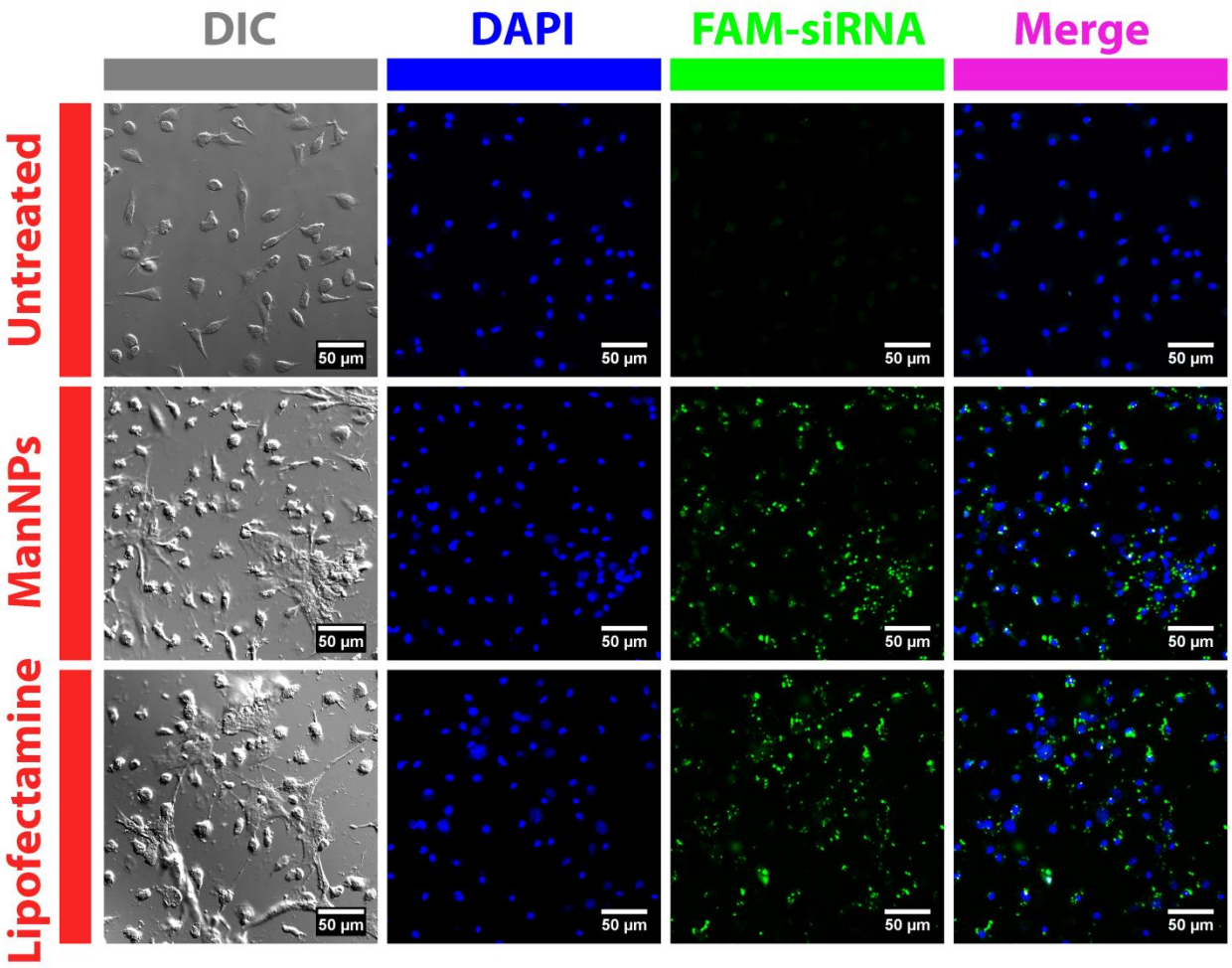

SUPPLEMENTARY FIGURE S8. siRNA Delivery into Primary Macrophages via ManNPs vs. Commercially Available Standard. Following 4h of transfection with FAM-siRNA (green; complexed into ManNPs or Lipofectamine RNAiMAX®), BMDMs were fixed, nuclei stained with DAPI (blue), and imaged via confocal microscopy. (Scale bars = 50 µm). Brightness & contrast were enhanced in the DAPI channel to account for small differences in staining between samples. FAM channels were left unaltered. Non-transfected BMDMs are shown for comparison.

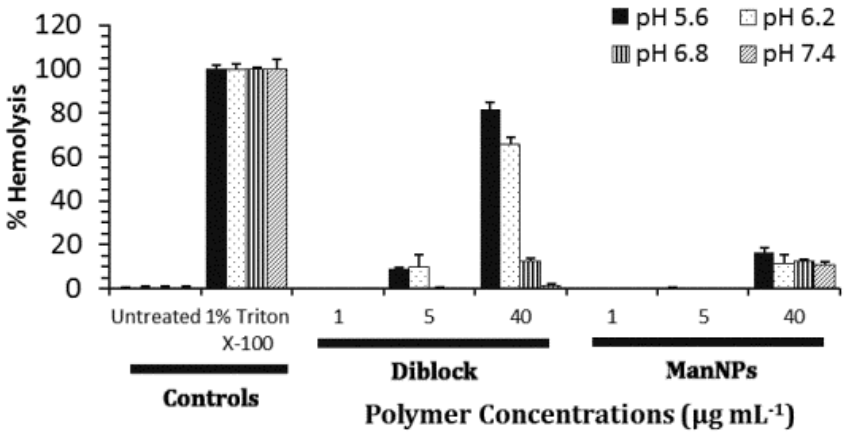

SUPPLEMENTARY FIGURE S9. Erythrocyte Hemolysis Assay Showcases pH-Responsive Behavior of Diblock Nanoparticles and ManNPs. The block copolymers exhibit pH-dependent disruption of phospholipid membranes, and better facilitate erythrocyte lysis at pH < 6.8 .

Supplementary Materials and Methods

NMR and Chromatography. Proton and carbon nuclear magnetic resonance (^{1}H and ^{13}C NMR) spectra were obtained at 400 MHz using a 9.4 Tesla Oxford magnet operated by a Bruker AV-400 console.

Gel permeation chromatography (GPC) was performed with dimethylformamide (DMF) + 0.1 M LiBr as the mobile phase, by running samples through three resolving columns in series (1 × TSKGel Alpha4000, 2 × TSKGel Alpha3000; Tosoh Bioscience, King of Prussia, PA). Columns were maintained at 60°C, and chromatograms were collected via a Shimadzu RID-10A refractive index detector (Shimadzu Scientific Instruments, Columbia, MD) and a Wyatt miniDAWN Treos multi-angle light scattering detector (MALS; Wyatt Technology, Santa Barbara, CA). Data collection and analysis was achieved through the Wyatt ASTRA software (v 5.3.4). Determination of absolute molecular weights was done by preparing known concentrations of purified polymer samples, and measuring their dn/dc in offline batch mode.

Analytical high performance liquid chromatography–mass spectrometry (HPLC-MS) was performed on an Agilent 1200 series system (Palo Alto, CA) as described elsewhere.[1]

Nanoparticle Characterization. To prepare polymeric nanoparticles for transmission electron microscope (TEM) imaging, carbon film-backed copper grids (Electron Microscopy Sciences, Hatfield, PA) were inverted onto droplets containing aqueous nanoparticle suspensions (1 mg/mL) and blotted dry. Next, all samples were inverted onto a droplet of 3% uranyl acetate and allowed to counterstain for 2 min. After blotting the sample dry, samples were further desiccated *in vacuo* for 2 h prior to imaging on a Philips CM20 system operating at 200 kV. Images were collected using a CCD camera with AMT Image Capture Engine software (v 600.335h; Advanced Microscopy Techniques, Danvers, MA).

Hydrodynamic diameter and ζ-potential of NPs were investigated by dynamic light scattering (DLS) in a Malvern Zetasizer Nano-ZS (Malvern Instruments Ltd., Worcestershire, U.K.).

Immortalized Cell Lines. L929 murine areolar fibroblasts were cultured in DMEM (purchased containing 4.5 g/L glucose, 110 mg/L sodium pyruvate, and 3.7 g/L $NaHCO_3$), supplemented with 10% FBS, 1 U/mL penicillin, 1 μg/mL streptomycin, and 1% MEM non-essential amino acids. To create the macrophage colony-stimulating factor (M-CSF) source for differentiating bone marrow into BMDMs, 1.16×10^7 L929 cells were seeded into T-225 flasks, in 77 mL of media. After 10 d of culture without any media changes, the supernatant was filtered through a 0.2 μm nylon membrane, and stored at -80°C until further use.[2]

THP-1 human leukemic monocytes were cultured in RPMI-1640 media containing 10% FBS, 1 U/mL penicillin, 1 μg/mL streptomycin, 1 X MEM vitamins (Mediatech, Manassas, VA), 120 μM β-mercaptoethanol, and 10 mM HEPES. For experiments, these non-adherent cells were plated at 300,000 cells/cm^2 in growth media containing 1 μg/mL lipopolysaccharide for 3 d, which activates the monocytes into macrophages and induces adherence of the cells to the substrate. For one experiment (shown in Figure 4), cells were seeded at 25,000 cells/cm^2, in order to keep cell number constant across the three independent variables that were tested (cell type).

MDA-MB-231 and MDA-MB-468 cells were cultured in DMEM (purchased containing 4.5 g/L glucose, 110 mg/L sodium pyruvate, and 2 mM L-glutamine), supplemented with 10% fetal bovine serum, 1 U/mL penicillin, 1 μg/mL streptomycin, and

1% MEM non-essential amino acids. For experiments, the cells were trypsinized and then re-seeded into 24-well plates at a density of 25,000 cells/cm^2.

All cells were maintained in a 5% CO_2 incubator at 37°C.

Calculation of Relative PPIB Expression. Data was analyzed for C_T values using the Applied Biosystems 7500 Fast Software (version 1.4.0). All plots of SYBR Green fluorescence versus cycle were set to the same baseline (usually within cycles 3-10; all of the sigmoidal amplification curves did not appear until after cycle ~15), thresholded evenly (same within samples analyzed for the same gene), and the intersection of the amplification curve and the threshold was reported as the C_T value. Relative expression (RE) of a gene of interest (goi) was calculated against a control gene (cont; GAPDH or β-actin), according to the formula: $RE_{goi} = 2^{(C_{T,cont} - C_{T,goi})}$.. Fold-change in goi expression was calculated by dividing RE_{goi} of experimental samples over RE_{goi} of control samples (usually untreated cells).

Hemolysis Assays. Whole, unfractionated human blood samples were obtained from consenting anonymous, healthy adults under Vanderbilt University Institutional Review Board (IRB) approval (Protocol #111251). Whole blood (in K_2EDTA-coated Vacutainer tubes) was centrifuged at 1500 rpm for 5 min (400 x g), and plasma was replaced with an equivalent volume of 150 mM NaCl. After inverting the tubes a few times to resuspend the pellet, and centrifuging the tubes at 1500 rpm for 5 min, the buffer was replaced with PBS at pH 7.4. The cell suspension was split into four tubes, corresponding to each pH to be assayed, and centrifuged at 1500 rpm for 5 min again. The supernatants were discarded, and replaced with PBS pre-adjusted to pH 5.6, 6.2, 6.8, or 7.4. 1 mL of each stock suspension was further diluted 1:50 into PBS at the corresponding pH, prior to further use.

In black, round-bottom 96-well plates, 10 μL of each test polymer, at three concentrations (20, 100, 800 μg/mL), were loaded. After the addition of 190 μL of purified red blood cells, the final concentrations of these polymer samples were adjusted to 1, 5, and 40 μg/mL, respectively. As controls, plain PBS (negative control) or 20% Triton X-100 (positive control) were added to some wells. These mixtures were allowed to incubate at

37°C in a 5% CO2 incubator for 1 h, following which they were centrifuged at 1500 rpm for 5 min. 100 µL of the supernatant in each well was transferred to clear, flat-bottom 96-well assay plates. This protocol enables the quantification of the release of hemoglobin as erythrocytes are lysed. Absorbance was plate-read at 450 nm using a Tecan Infinite F500 system (Männedorf, Switzerland), operated by Tecan i-Control software (version 1.7.1.12). The absorbance of the negative control sample was set to 0% hemolysis, and the absorbance of the positive control sample was set to 100% hemolysis. After setting up a linear regression based on these two data points, the resulting formula was applied on all other wells to calculate % hemolysis.

Confocal Microscopy: Image Processing. Images were processed via ImageJ software (version 1.43u; National Institute of Health, Bethesda, MD). 8-bit LSM images were converted to RGB images in order to make them compatible with the built-in "Merge Channels" function on the software, which creates the merged fluorescence overlay images used for some of the figures. Due to the low DAPI signal in some raw image files, the brightness/contrast of the DAPI channels for all images reported here were enhanced to varying levels.

REFERENCES

1 Yu, S. S. *et al.* Physiologically relevant oxidative degradation of oligo(proline) cross-linked polymeric scaffolds. *Biomacromolecules* **12**, 4357-4366 (2011).

2 Weischenfeldt, J. & Porse, B. Bone Marrow-Derived Macrophages (BMM): Isolation and Applications. *Cold Spring Harb Protoc* **2008**, pdb.prot5080- (2008).

Cell- and Site-Specific RNAi Interference in Tumor-Associated Macrophages via 'Click', Mannosylated Polymeric Nanoparticles

Shann S. Yu[1], Cheryl Lau[1], Whitney Barham[2], Halina M. Onishko[2], Christopher E. Nelson[1], Fiona E. Yull[2], Craig L. Duvall[1], & Todd D. Giorgio[1].

[1]Department of Biomedical Engineering, Vanderbilt University, Nashville, TN 37235
[2]Department of Cancer Biology, Vanderbilt-Ingram Cancer Center, Nashville, TN 37232

Tumor-associated macrophages (TAMs) represent a promising therapeutic target in cancer because they have been shown to facilitate tumor growth, invasiveness, and metastasis. However, macrophage-specific drug delivery within tumor sites is a significant challenge, as systemic interference with macrophage behavior may lead to autoimmune manifestations. In this work, we designed and characterized mannosylated polymeric nanoparticles (ManNPs) in order to achieve CD206 (macrophage mannose receptor)-targeted siRNA delivery. CD206 is almost exclusively expressed on macrophages and dendritic cells, and upregulated in tumor-associated macrophages.

The ManNPs are composed of tri-block co-polymers, including the following blocks: (1) an azide-displaying block for the attachment of alkyne-functionalized mannose via 'click' chemistry, (2) a cationic block for the condensation of polyanions such as siRNA, and (3) a pH-responsive terpolymer block that facilitates endosomal disruption. This terpolymer is hydrophobic at pH 7.4, allowing these polymers to self-assemble into 25 nm micelles under physiologic conditions, as shown by transmission electron microscopy. However, they become protonated at lower pH ranges representative of endosomal compartments (5.8–6.2), leading to disassembly of the nanoparticles, and increased ability to disrupt endosomal membranes. Therefore, this pH-dependent behavior facilitates improved cytoplasmic delivery of siRNA, access to the intracellular silencing machinery, and consequently, knockdown of target gene expression.

The glycoconjugates improved siRNA delivery into primary murine bone marrow-derived macrophages by 4.5-fold, relative to a non-mannosylated version of the same carrier. Internalization of these constructs can be blocked by co-incubation with mannose or suppressed by downregulation of CD206 via LPS pre-treatment, showcasing the specificity of the construct for CD206. This is particularly important for cancer applications because CD206 is upregulated in tumor-suppressed and non-activated macrophages, enabling more specific targeting of TAMs versus healthy macrophages in other tissues. Finally, the delivered siRNA retains its activity following delivery, resulting in 40±10% knockdown of a model gene within four hours of delivery, relative to non-transfected macrophages.

We have also examined the behavior of the ManNPs *in vivo* by delivering them retro-orbitally into mouse models of breast cancer, caused by the expression of the polyoma middle T oncoprotein in the mammary epithelium. Within 24 h, the ManNPs facilitated improved delivery of siRNA into CD206-expressing cells in tumors, as shown by immunostaining of tumor frozen sections. Flow cytometry analysis also shows significant co-localization of the delivered siRNA with tumor-associated $F4/80^+$ cells. The ManNPs described here present new opportunities to target TAMs in various cancers, providing an enabling technology for the modification of the immunosuppressive tumor environment by targeting TAM activity.

Cell- and Site-Specific RNA Interference in Tumor-Associated Macrophages via Click-Mannosylated Polymeric Nanoparticles

Shann S. Yu[1], Cheryl M. Lau[1], Whitney J. Barham[2], Halina M. Onishko[2], Christopher E. Nelson[1], Fiona E. Yull[2], Craig L. Duvall[1], & Todd D. Giorgio[1-3]

[1]Dept. of Biomedical Engineering, [2]Dept. of Cancer Biology, & [3]Dept. of Chemical & Biomolecular Engineering, Vanderbilt University, Nashville, TN

Tumor-Associated Macrophages (TAMs) are an Important Drug Target in Cancer

- Problem: Macrophages resident in tumors have been 'hijacked' into promoting tumor growth and invasiveness.
  - Tumor-elicited activation of genetic pathways leading to immunosuppression and release of growth factors.

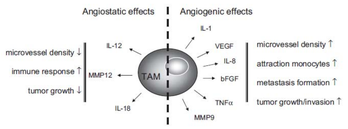

AE Dirkx et al. (2006) *J Leukocyte Biol.* 80:1183-1196.

- Challenge: Development of drug delivery system that targets macrophages specifically in a tumor microenvironment.
  - Ability to deliver siRNA to knock down the expression of genetic pathways responsible for tumor-promoting effects.

- **DESIGN GOALS: Synthesize polymeric nanoparticles that target TAMs, and mediate intracellular delivery of siRNA.**
  - Immobilization of mannose to nanoparticle surface enables targeting of CD206 (macrophage mannose receptor), which is expressed almost exclusively on macrophages.
  - Build in modules that are responsible for mediating escape of the polymers and their cargo from the endosomal pathway.

Mimicking the Endosomal Escape of HIV via Synthetic Block Co-polymers

- Common viruses interact with endocytotic receptors to enter target cells, and eventually escape the endosomal pathway.
  - pH-mediated change in conformation of a viral protein enables the virus to disrupt phospholipid membranes at late endosomal pH (< 6.2)

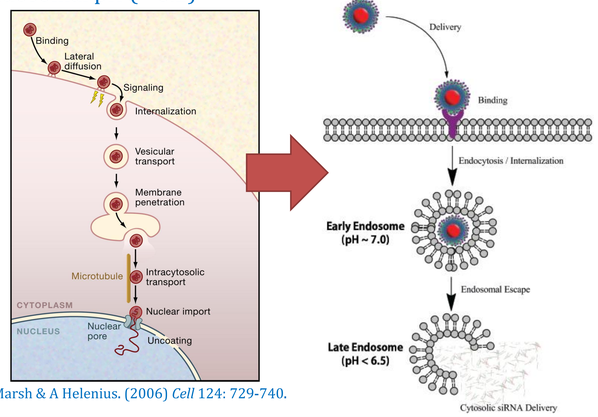

- M Marsh & A Helenius. (2006) *Cell* 124: 729-740.

Objectives

- Physicochemical characterization of the nanoparticles.
- Evaluate nanoparticle-mediated siRNA delivery to CD206-expressing macrophages *in vitro* and *in vivo*.

Mannosylated Polymeric Nanoparticles (ManNPs)

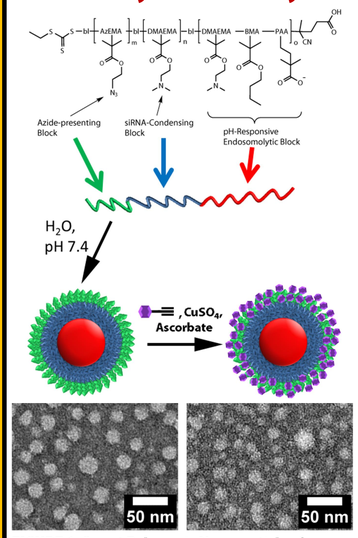

FIGURE 1. Smart Polymeric Nanoparticles for Macrophage-Specific Cytosolic Delivery of siRNA. Schematic representation of the triblock copolymers developed in this work, and resulting, multi-functional nanoscale siRNA delivery vehicles. The blocks include (red) a pH-responsive block that is capable of disrupting endosomes at low pH, (blue) a cationic block for condensation of nucleic acids, and (green) an azide-displaying block for conjugation of targeting motifs (purple) via 'click' chemistry. The pH-responsive block is hydrophobic at pH 7.4, enabling the formation of micelles. At pH < 6.2, protonation of this block produces a net cationic charge, resulting in disassembly of the micelles. (Bottom) Transmission electron micrographs of (bottom left) micelles of non-targeted diblock copolymers, and (bottom right) ManNPs. Scale bars = 50 nm.

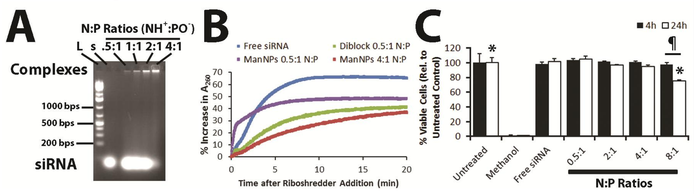

FIGURE 2. ManNPs Effectively Complex and Protect siRNA from Local Nuclease Activity, and Exhibit Negligible Cytotoxicity to THP-1 Macrophages. (A) Gel retardation assay of siRNA-loaded ManNPs at various N:P ratios. Control samples included the DNA ladder (L; numbers indicate # base pairs) and free, Cy3-labeled siRNA (s). (B) Micelle/ siRNA complexes were incubated with RNAse cocktails. RNAse-mediated degradation of siRNA was characterized by a hyperchromic effect at 260 nm. (C) Cell viability assay of human THP-1 leukemic macrophages treated with ManNPs/siRNA at varying N:P ratios for 4-24 h show minimal cytotoxicity for N:P < 8:1, relative to untreated cells.

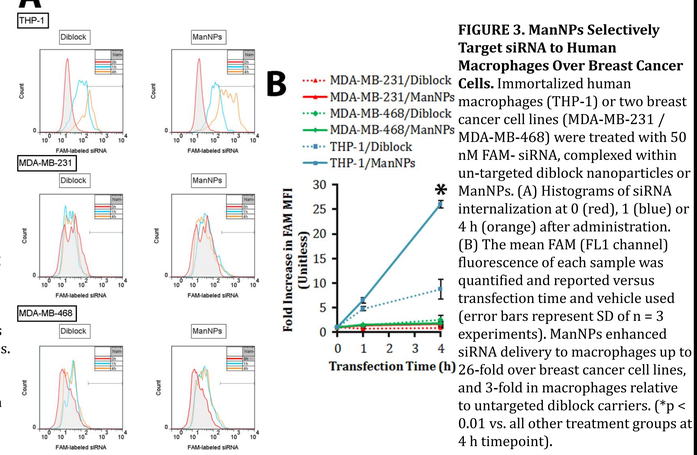

FIGURE 3. ManNPs Selectively Target siRNA to Human Macrophages Over Breast Cancer Cells. Immortalized human macrophages (THP-1) or two breast cancer cell lines (MDA-MB-231 / MDA-MB-468) were treated with 50 nM FAM- siRNA, complexed within un-targeted diblock nanoparticles or ManNPs. (A) Histograms of siRNA internalization at 0 (red), 1 (blue) or 4 h (orange) after administration. (B) The mean FAM (FL1 channel) fluorescence of each sample was quantified and reported versus transfection time and vehicle used (error bars represent SD of n = 3 experiments). ManNPs enhanced siRNA delivery to macrophages up to 26-fold over breast cancer cell lines, and 3-fold in macrophages relative to untargeted diblock carriers. (*p < 0.01 vs. all other treatment groups at 4 h timepoint).

ManNPs Enhance siRNA Delivery and Gene Knockdown in Primary Murine Macrophages

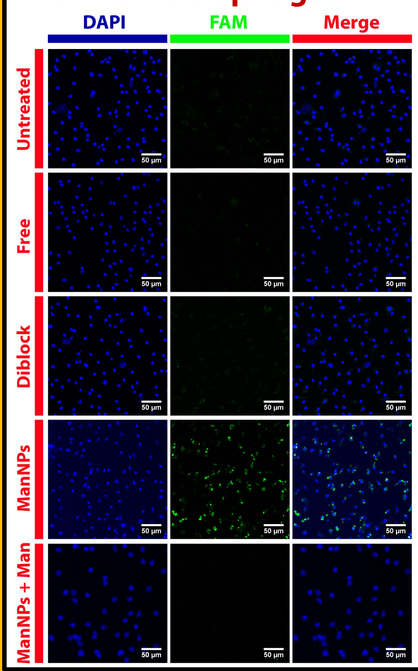

FIGURE 4. Improved Targeting of Primary Macrophages via ManNPs and Specificity for Mannose Receptor (CD206). Following 4h of transfection with FAM-siRNA (green; free or complexed into nanoparticles), BMDMs were fixed and imaged via confocal microscopy. Co-administration of the ManNPs with free D-mannose blocks uptake of siRNA.

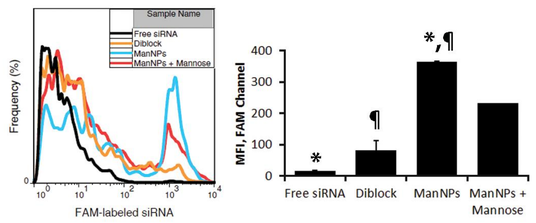

FIGURE 5. Improved Targeting of BMDMs via ManNPs. Flow cytometry confirms enhanced delivery of FAM-siRNA into BMDMs via ManNPs (blue) relative to untargeted nanoparticles (orange) or free siRNA without vehicle (black) within 4 h of administration. Co-administration of free mannose with the ManNPs reduces delivery of siRNA into BMDMs (red). (Left) FAM histograms for gated BMDMs, and (right) corresponding mean fluorescence intensity versus treatment. Error bars represent SD from 2 independent experiments (*,¶ p < 0.01).

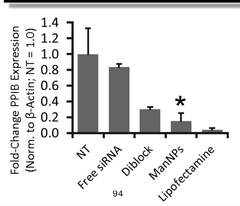

FIGURE 6. ManNPs Enhance siRNA-Mediated Knockdown of PPIB Expression in BMDMs within 24 h of Administration. qRT-PCR confirmed ManNPs carrying anti-PPIB siRNA mediated 85 ± 10% decrease in expression of the target gene, relative to non-transfected (NT) cells. Error bars represent standard deviation of 3 independent experiments (*p < 0.05 vs. all other treatment groups by Student's t-test).

ManNPs Selectively Target CD206-Expressing Cells in Murine Tumors *In Vivo*

Mouse Model

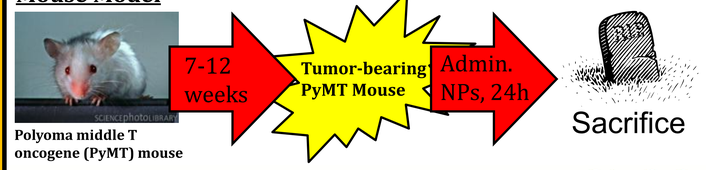

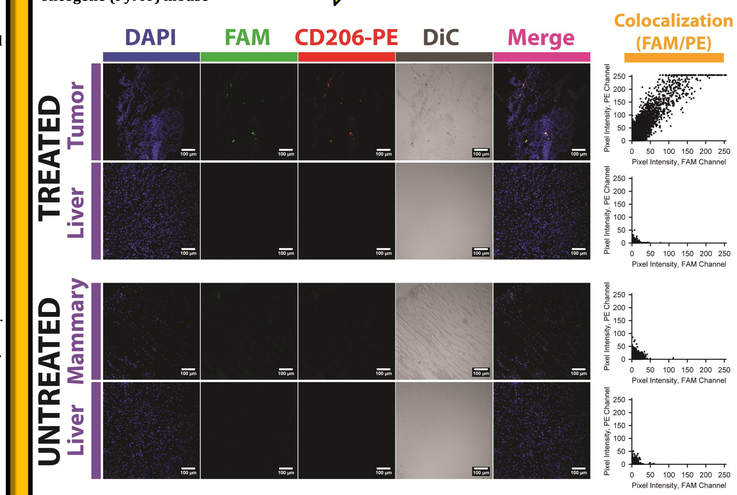

FIGURE 7. ManNPs/siRNA Co-localize with CD206 Staining in Tumor Frozen Sections. (Above) The expression of the PyMT oncogene in FVB mice results in the natural development of mammary epithelial tumors in these mice at 7-12 weeks after birth. We treated tumor-bearing PyMT mice with nanoparticles for 24 h prior to the collection and preservation of various organs. (Below) ManNPs deliver FAM-labeled siRNA to a select number of cells in the tumors of the treated mice, while showing low levels of clearance through the liver. Further, FAM-labeled siRNA colocalizes with CD206 staining in tumor sections of the treated mice, suggesting that siRNA delivery is specific for cells expressing CD206 in the tumor. (Scale bar = 100 µm)

Conclusions

- ManNPs form micelles that electrostatically complex siRNA and protect the siRNA from nuclease-mediated degradation.
- ManNPs deliver siRNA to BMDMs in a CD206-dependent manner, and enhance siRNA-mediated knockdown of the expression of a model gene.
- ManNPs selectively deliver siRNA to CD206-expressing cells in tumors of PyMT mice.

Acknowledgments

This work is supported through a Concept Award through the Department of Defense CDMRP Breast Cancer Research Program (#W81XWH-10-1-0684). Bone marrow-derived macrophages and in vivo work was supported through a multi-investigator, collaborative IDEA Award through the Department of Defense CDMRP Breast Cancer Research Program (#W81XWH-11-1-0344 & #W81XWH-11-1-0242). CML acknowledges partial support through a fellowship from the Vanderbilt Undergraduate Summer Research Program (VUSRP). Portions of this work were performed at the Vanderbilt Institute of Nanoscale Science and Engineering, using facilities renovated under NSF ARI-R2 DMR-0963361. Confocal microscopy (Zeiss LSM 710) was supported in part by the NCI Cancer Center Support Grant #P30 CA068485, utilizing the Vanderbilt University Medical Center Cell Imaging Shared Resource. The Vanderbilt University Medical Center Cell Imaging Shared Resource is also supported by NIH grants CA68485, DK20593, DK58404, HD15052, DK59637 and EY08126. qRT-PCR was performed in the laboratory of Prof. David G. Harrison (Division of Clinical Pharmacology, Vanderbilt University Medical Center).

References

1. A.E. Dirkx, M.G. Oude Egbrink, J. Wagstaff, A.W. Griffioen. (2006) *Monocyte/macrophage infiltration in tumors: modulators of angiogenesis*. J Leukoc Biol **80** (6), 1183-96.
2. M. Marsh & A. Helenius. (2006) *Virus entry: open sesame*. Cell **124** (4): 729-40.
3. S.S. Yu, C.M. Lau, W.J. Barham, H.M. Onishko, C.E. Nelson, H. Li, F.E. Yull, C.L. Duvall, & T.D. Giorgio. (2012) *Macrophage-Specific RNAi Targeting via 'Click', Mannosylated Polymeric Micelles*. (Submitted).

Environmentally-Responsive Nanoparticles for the Intracellular Delivery of RNAi Therapeutics into Tumor-Associated Macrophages

Shann S. Yu[1], Cheryl Lau[1], Whitney Barham[2], Halina M. Onishko[2], Christopher E. Nelson[1], Fiona E. Yull[2], Craig L. Duvall[1], & Todd D. Giorgio[1].

[1]Department of Biomedical Engineering, Vanderbilt University, Nashville, TN 37235
[2]Department of Cancer Biology, Vanderbilt-Ingram Cancer Center, Nashville, TN 37232

Tumor-associated macrophages (TAMs) represent a potentially promising therapeutic target in cancer because they have been shown to facilitate tumor growth, invasiveness, and metastasis. However, macrophage-specific drug delivery within pathologic sites is a significant challenge, as systemic interference with macrophage behavior may lead to autoimmune manifestations. In this work, we designed and characterized pH-responsive, mannosylated polymeric nanoparticles (ManNPs) in order to achieve CD206 (macrophage mannose receptor)-targeted drug delivery. CD206 is almost exclusively expressed on macrophages and dendritic cells, and upregulated in tumor-associated macrophages.

The ManNPs are composed of tri-block co-polymers, including the following blocks: (1) an azido-displaying block for the attachment of alkyne-functionalized mannose via 'click' chemistry, (2) a cationic block for the condensation of polyanions such as siRNA, and (3) a pH-responsive terpolymer block that facilitates endosomal disruption. This terpolymer is hydrophobic at pH 7.4, allowing these polymers to self-assemble into 25 nm micelles under physiologic conditions, as shown by transmission electron microscopy. However, they become protonated at lower pH ranges representative of endosomal compartments (5.8 – 6.2), leading to disassembly of the nanoparticles, and increased ability to disrupt endosomal membranes. This pH-dependent behavior was validated using a red blood cell hemolysis assay, and facilitated improved cytoplasmic delivery of siRNA, access to the intracellular silencing machinery, and consequently, knockdown of target gene expression.

The glycoconjugates improved siRNA delivery into primary murine bone marrow-derived macrophages by 4.5-fold, relative to a non-mannosylated version of the same carrier. Internalization of these constructs can be blocked by co-incubation with free mannose or suppressed by downregulation of CD206 via LPS pre-treatment, showcasing the specificity of the construct for CD206. This is particularly important for cancer applications because CD206 is upregulated in tumor-suppressed and non-activated macrophages, enabling more specific targeting of TAMs versus healthy macrophages in other tissues. Finally, the delivered siRNA retains its activity following delivery, resulting in 40 ± 10% knockdown of a model gene within four hours of delivery, relative to non-transfected macrophages.

We have also examined the behavior of the ManNPs *in vivo* by delivering them retro-orbitally into mouse models of breast cancer, caused by the expression of the polyoma middle T oncoprotein in the mammary epithelium. Within 24 h, the ManNPs facilitated improved delivery of siRNA into CD206-expressing cells in tumors, as shown by immunostaining of tumor frozen sections. Flow cytometry analysis also shows significant co-localization of the delivered siRNA with tumor-associated $F4/80^+$ cells. The ManNPs described here present new opportunities to target TAMs in various cancers, providing an enabling technology for the modification of the immunosuppressive tumor environment by targeting TAM activity.

Environmentally-Responsive Nanoparticles for the Intracellular Delivery of RNAi Therapeutics into Tumor-Associated Macrophages

Shann S. Yu[1], Cheryl M. Lau[1], Whitney J. Barham[2], Halina M. Onishko[2], Christopher E. Nelson[1], Hongmei Li[1], Fiona E. Yull[2], Craig L. Duvall[1], & Todd D. Giorgio[1-3]

[1]Dept. of Biomedical Engineering, [2]Dept. of Cancer Biology, & [3]Dept. of Chemical & Biomolecular Engineering, Vanderbilt University, Nashville, TN

Tumor-Associated Macrophages (TAMs) are an Important Drug Target in Cancer

- Problem: Macrophages resident in tumors have been 'hijacked' into promoting tumor growth and invasiveness.
  - Tumor-elicited activation of genetic pathways leading to immunosuppression and release of growth factors.

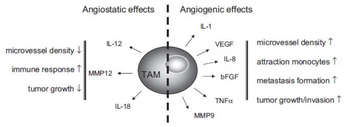

AE Dirkx et al. (2006) *J Leukocyte Biol.* 80:1183-1196.

- Challenge: Development of drug delivery system that targets macrophages specifically in a tumor microenvironment.
  - Ability to deliver siRNA to knock down the expression of genetic pathways responsible for tumor-promoting effects.

- **DESIGN GOALS: Synthesize polymeric nanoparticles that target TAMs, and mediate intracellular delivery of siRNA.**
  - Immobilization of mannose to nanoparticle surface enables targeting of CD206 (macrophage mannose receptor), which is expressed almost exclusively on macrophages.
  - Build in modules that are responsible for mediating escape of the polymers and their cargo from the endosomal pathway.

Mimicking the Endosomal Escape of HIV via Synthetic Block Co-polymers

- Common viruses interact with endocytotic receptors to enter target cells, and eventually escape the endosomal pathway.
  - pH-mediated change in conformation of a viral protein enables the virus to disrupt phospholipid membranes at late endosomal pH (< 6.2)

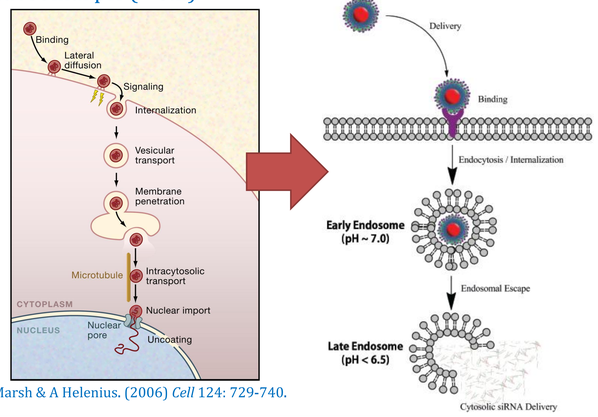

- M Marsh & A Helenius. (2006) *Cell* 124: 729-740.

Objectives

- Physicochemical characterization of the nanoparticles.
- Evaluate nanoparticle-mediated siRNA delivery to CD206-expressing macrophages *in vitro* and *in vivo*.

Mannosylated Polymeric Nanoparticles (ManNPs)

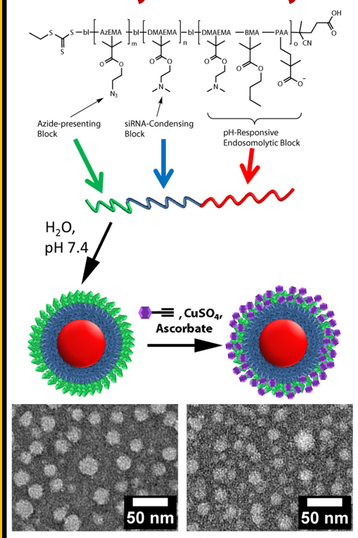

FIGURE 1. Smart Polymeric Nanoparticles for Macrophage-Specific Cytosolic Delivery of siRNA. Schematic representation of the triblock copolymers developed in this work, and resulting, multi-functional nanoscale siRNA delivery vehicles. The blocks include (red) a pH-responsive block that is capable of disrupting endosomes at low pH, (blue) a cationic block for condensation of nucleic acids, and (green) an azide-displaying block for conjugation of targeting motifs (purple) via 'click' chemistry. The pH-responsive block is hydrophobic at pH 7.4, enabling the formation of micelles. At pH < 6.2, protonation of this block produces a net cationic charge, resulting in disassembly of the micelles. (Bottom) Transmission electron micrographs of (bottom left) micelles of non-targeted diblock copolymers, and (bottom right) ManNPs. Scale bars = 50 nm.

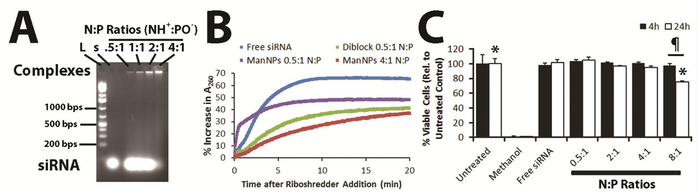

FIGURE 2. ManNPs Effectively Complex and Protect siRNA from Local Nuclease Activity, and Exhibit Negligible Cytotoxicity to THP-1 Macrophages. (A) Gel retardation assay of siRNA-loaded ManNPs at various N:P ratios. Control samples included the DNA ladder (L; numbers indicate # base pairs) and free, Cy3-labeled siRNA (s). (B) Micelle/ siRNA complexes were incubated with RNAse cocktails. RNAse-mediated degradation of siRNA was characterized by a hyperchromic effect at 260 nm. (C) Cell viability assay of human THP-1 leukemic macrophages treated with ManNPs/siRNA at varying N:P ratios for 4-24 h show minimal cytotoxicity for N:P < 8:1, relative to untreated cells.

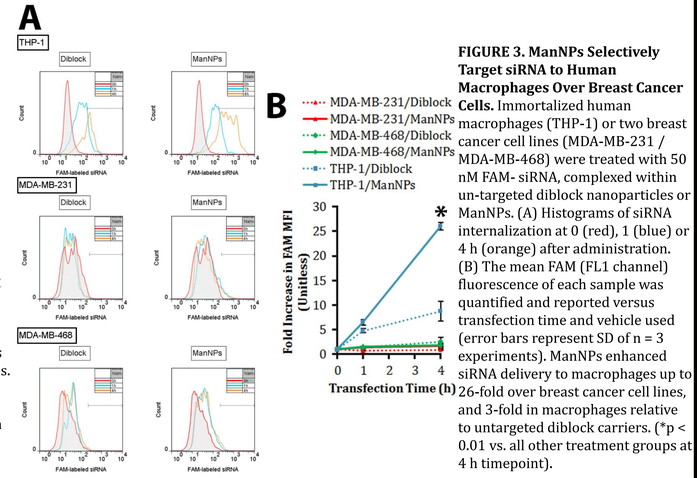

FIGURE 3. ManNPs Selectively Target siRNA to Human Macrophages Over Breast Cancer Cells. Immortalized human macrophages (THP-1) or two breast cancer cell lines (MDA-MB-231 / MDA-MB-468) were treated with 50 nM FAM- siRNA, complexed within un-targeted diblock nanoparticles or ManNPs. (A) Histograms of siRNA internalization at 0 (red), 1 (blue) or 4 h (orange) after administration. (B) The mean FAM (FL1 channel) fluorescence of each sample was quantified and reported versus transfection time and vehicle used (error bars represent SD of n = 3 experiments). ManNPs enhanced siRNA delivery to macrophages up to 26-fold over breast cancer cell lines, and 3-fold in macrophages relative to untargeted diblock carriers. (*p < 0.01 vs. all other treatment groups at 4 h timepoint).

ManNPs Enhance siRNA Delivery and Gene Knockdown in Primary Murine Macrophages

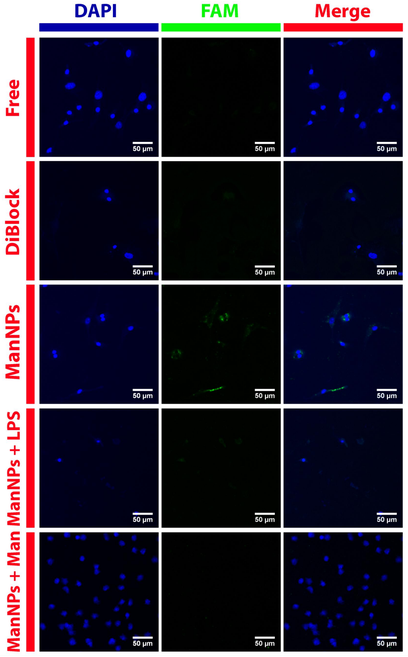

FIGURE 4. Improved Targeting of Primary Macrophages via ManNPs and Specificity for Mannose Receptor (CD206). Following 4h of transfection with FAM-siRNA (green; free or complexed into nanoparticles), BMDMs were fixed and imaged via confocal microscopy. Some BMDMs were pre-treated with LPS prior to administration of siRNA-loaded ManNPs, in order to down-regulate CD206 expression. Co-administration of the ManNPs with free D-mannose also blocks uptake of siRNA.

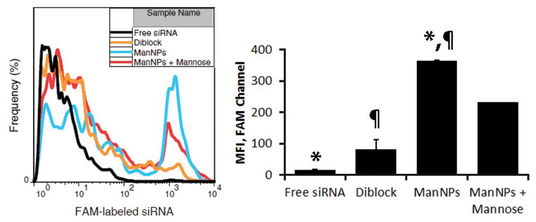

FIGURE 5. Improved Targeting of BMDMs via ManNPs. Flow cytometry confirms enhanced delivery of FAM-siRNA into BMDMs via ManNPs (blue) relative to untargeted nanoparticles (orange) or free siRNA without vehicle (black) within 4 h of administration. Co-administration of free mannose with the ManNPs reduces delivery of siRNA into BMDMs (red). (Left) FAM histograms for gated BMDMs, and (right) corresponding mean fluorescence intensity versus treatment. Error bars represent SD from 2 independent experiments (*,¶ p < 0.01).

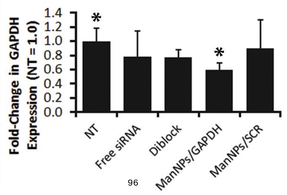

FIGURE 6. ManNPs Enhance siRNA-Mediated Knockdown of GAPDH Expression in BMDMs within 4 h of Administration. qRT-PCR confirmed ManNPs carrying anti-GAPDH siRNA mediated 40 ± 10% decrease in GAPDH expression, relative to non-transfected (NT) cells. Error bars represent standard deviation of 2-3 independent experiments (*p < 0.05).

ManNPs Selectively Target CD206-Expressing Cells in Murine Tumors *In Vivo*

Mouse Model

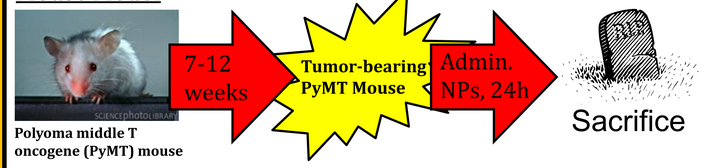

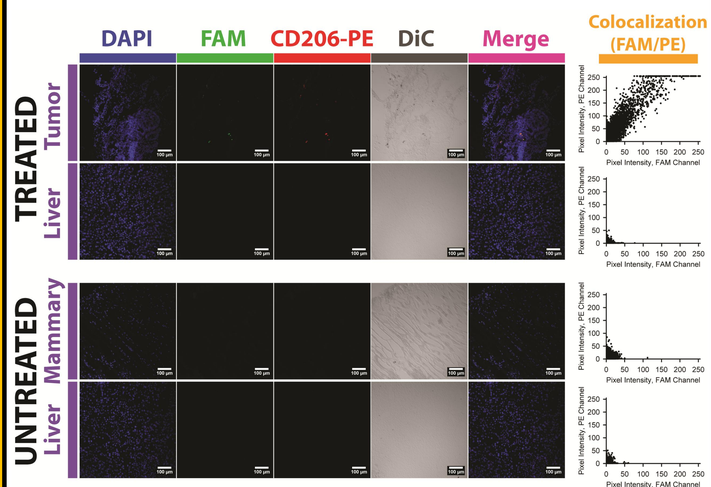

FIGURE 7. ManNPs/siRNA Co-localize with CD206 Staining in Tumor Frozen Sections. (Above) The expression of the PyMT oncogene in FVB mice results in the natural development of mammary epithelial tumors in these mice at 7-12 weeks after birth. We treated tumor-bearing PyMT mice with nanoparticles for 24 h prior to the collection and preservation of various organs. (Below) ManNPs deliver FAM-labeled siRNA to a select number of cells in the tumors of the treated mice, while showing low levels of clearance through the liver. Further, FAM-labeled siRNA colocalizes with CD206 staining in tumor sections of the treated mice, suggesting that siRNA delivery is specific for cells expressing CD206 in the tumor. (Scale bar = 100 µm)

Conclusions

- ManNPs form micelles that electrostatically complex siRNA and protect the siRNA from nuclease-mediated degradation.
- ManNPs deliver siRNA to BMDMs in a CD206-dependent manner, and enhance siRNA-mediated knockdown of the expression of a model gene.
- ManNPs selectively deliver siRNA to CD206-expressing cells in tumors of PyMT mice.

Acknowledgments

This work is supported through a Concept Award through the Department of Defense CDMRP Breast Cancer Research Program (#W81XWH-10-1-0684). Bone marrow-derived macrophages and in vivo work was supported through a multi-investigator, collaborative IDEA Award through the Department of Defense CDMRP Breast Cancer Research Program (#W81XWH-11-1-0344 & #W81XWH-11-1-0242). CML acknowledges partial support through a fellowship from the Vanderbilt Undergraduate Summer Research Program (VUSRP). Portions of this work were performed at the Vanderbilt Institute of Nanoscale Science and Engineering, using facilities renovated under NSF ARI-R2 DMR-0963361. Confocal microscopy (Zeiss LSM 710) was supported in part by the NCI Cancer Center Support Grant #P30 CA068485, utilizing the Vanderbilt University Medical Center Cell Imaging Shared Resource. The Vanderbilt University Medical Center Cell Imaging Shared Resource is also supported by NIH grants CA68485, DK20593, DK58404, HD15052, DK59637 and EY08126. qRT-PCR was performed in the laboratory of Prof. David G. Harrison (Division of Clinical Pharmacology, Vanderbilt University Medical Center).

References

1. A.E. Dirkx, M.G. Oude Egbrink, J. Wagstaff, A.W. Griffioen. (2006) *Monocyte/macrophage infiltration in tumors: modulators of angiogenesis*. J Leukoc Biol **80** (6), 1183-96.
2. M. Marsh & A. Helenius. (2006) *Virus entry: open sesame*. Cell **124** (4): 729-40.
3. S.S. Yu, C.M. Lau, W.J. Barham, H.M. Onishko, C.E. Nelson, H. Li, F.E. Yull, C.L. Duvall, & T.D. Giorgio. (2012) *Macrophage-Specific RNAi Targeting via 'Click', Mannosylated Polymeric Micelles*. (Submitted).

Yu SS, Lau CM, Barham WJ, Onishko HM, Nelson CE, Li H, Yull FE, Duvall CL, and Giorgio TD: In Vivo, Macrophage-Specific RNAi Targeting via "Click", Mannosylated Polymeric Micelles. Society for Biomaterials, Memphis, TN, February 2012.

Macrophages represent an important therapeutic target, because their activity has been implicated in the progression of common, debilitating diseases such as cancer and atherosclerosis. However, macrophage-specific drug delivery within pathologic sites is a significant challenge, as non-specific drug delivery may lead to side effects and undesired interference with molecular mechanisms in healthy tissues. Because CD206 (mannose receptor) is almost exclusively expressed on macrophages and dendritic cells, and upregulated in tumor-associated macrophages, we designed and characterized pH-responsive, mannosylated polymeric micelles in order to achieve CD206-targeted drug delivery. The glycoconjugates improved siRNA delivery into primary murine macrophages by fivefold relative to a non-targeted carrier. Internalization of these constructs can be blocked by co-incubation with mannose or suppressed by downregulation of CD206 via LPS. The delivered siRNA retained its activity following delivery, resulting in 40±10% knockdown of a model gene within 4h of delivery. Additionally, the glycoconjugates were avidly recognized and internalized by human macrophages, and facilitated the delivery of 13-fold more siRNA into these cells relative to model cancer cell lines. Preliminary results also show that the glycoconjugates co-localize with CD206 in murine breast tumors in vivo, suggesting that these vehicles may become an enabling technology to target macrophage activity in tumors.

Memphis Biomaterials Day
February 17, 2012

VANDERBILT
School of Engineering

In Vivo, Macrophage-Specific RNAi Targeting via 'Click', Mannosylated Polymeric Micelles

Shann S. Yu, Cheryl M. Lau, Whitney J. Barham, Halina M. Onishko, Christopher E. Nelson, Hongmei Li, Fiona E. Yull, Craig L. Duvall, & Todd D. Giorgio

The following
61/597,280 (
CM Lau, & CL

Fullscreen

Awakening the Immune System to Address Metastatic Cancer

Fullscreen

The Presence of Tumor-Associated Macrophages (TAMs) is Associated with Poor Prognoses

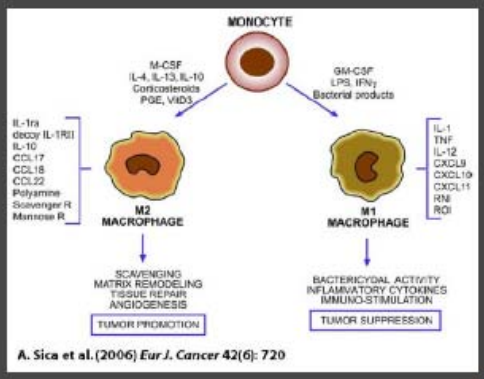

Fullscreen

CENTRAL OBJECTIVE

TAM-specific siRNA-mediated silencing of master genes regulating activities.

IMMEDIATE OBJECTIVE

Design and characterize new vehicles for TAM-specific siRNA delivery.

Fullscreen

How to Transfect a Macrophage: Lessons from Nature

- Common animal viruses are able to interface with receptors on cell surface
- To access cellular machinery for viral replication, virus escapes from vesicle
- Viral macromolecule is optimized for cytosolic delivery of active virus

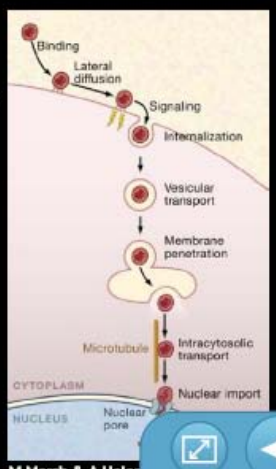

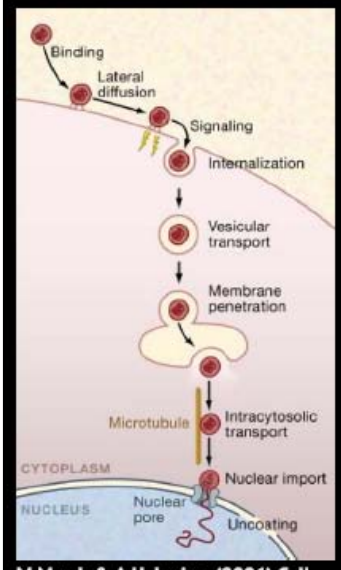

M Marsh & A Helenius. (2006) Cell.

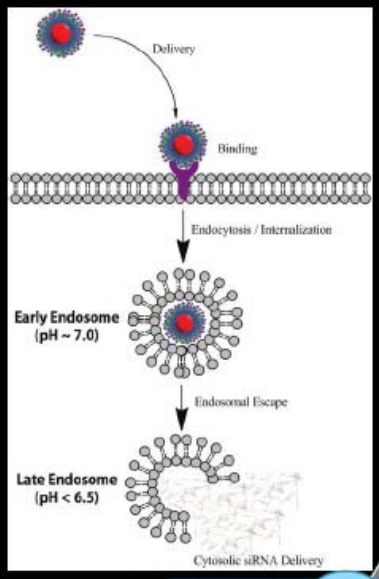

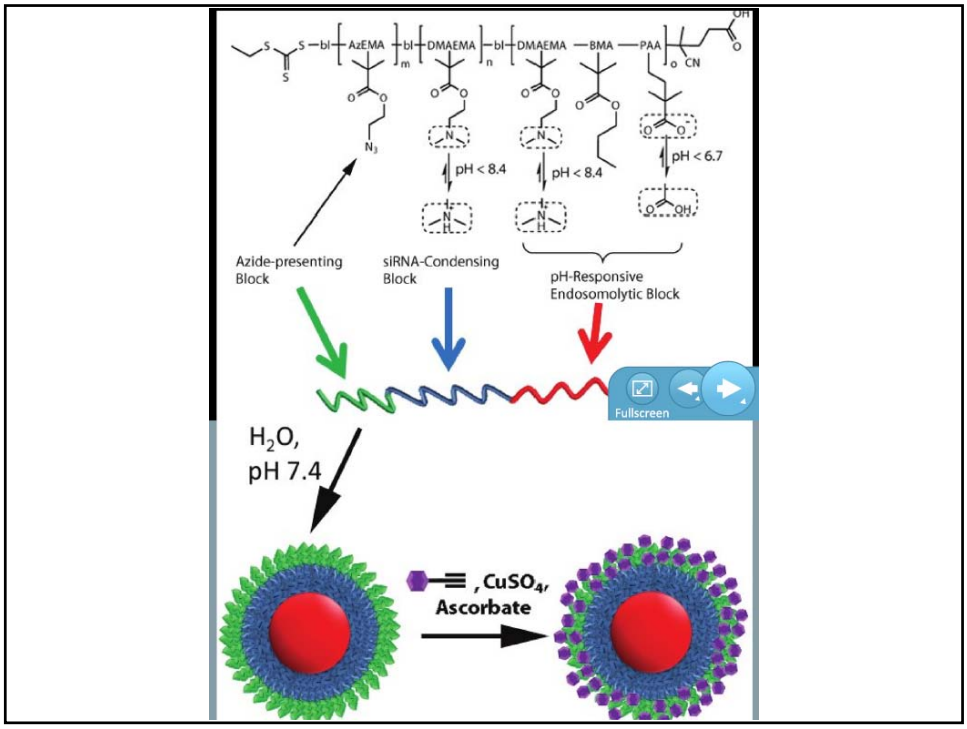
AzEMA
DMAEMA
DMAEMA
BMA
PAA
pH < 8.4
pH < 8.4
pH < 6.7
Azide-presenting Block
siRNA-Condensing Block
pH-Responsive Endosomolytic Block
Fullscreen
H_2O, pH 7.4
, $CuSO_4$, Ascorbate

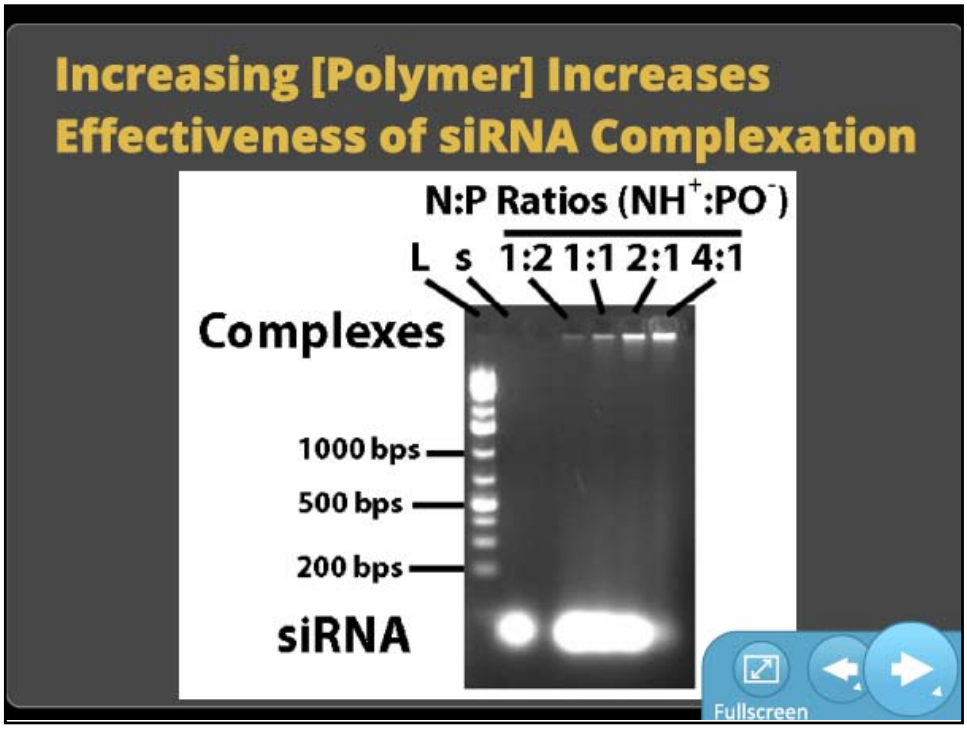
Increasing [Polymer] Increases Effectiveness of siRNA Complexation
N:P Ratios (NH^+:PO^-)
L s 1:2 1:1 2:1 4:1
Complexes
1000 bps
500 bps
200 bps
siRNA
Fullscreen

Polymers for siRNA Delivery form Micellar Nanoparticles

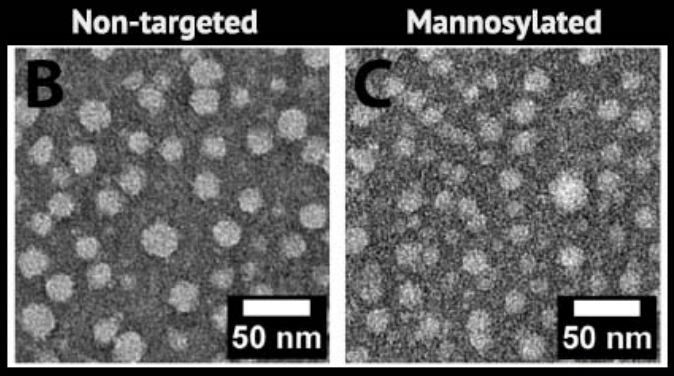

Micelles in water were dried onto TEM grids, and counterstained with uranyl acetate.

Fullscreen

ManNPs Enhance siRNA Delivery to Primary Murine Macrophages

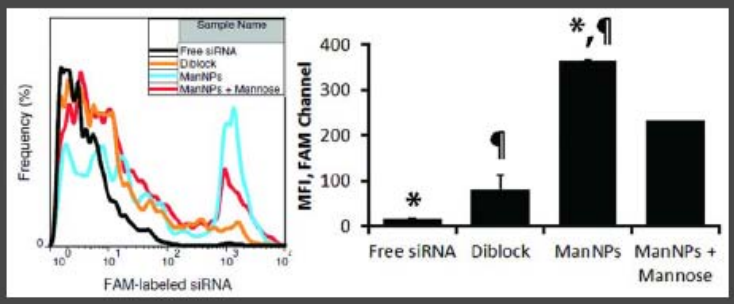

Cell line: Bone marrow-derived macrophages (BMDMs; FVB Background)
siRNA Used: FAM-labeled siRNA
*,¶ $p < 0.01$, Student's t-test

Fullscreen

ManNPs Enhance siRNA Delivery to Primary Murine Macrophages

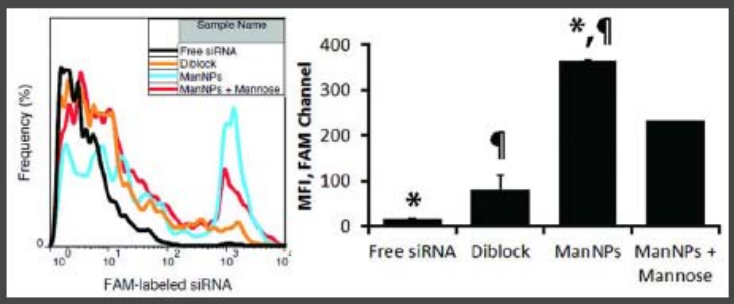

Cell line: Bone marrow-derived macrophages (BMDMs; FVB Background)
siRNA Used: FAM-labeled siRNA
*,¶ $p < 0.01$, Student's t-test

Fullscreen

BMDMs Rapidly Internalize siRNA Delivered via ManNPs

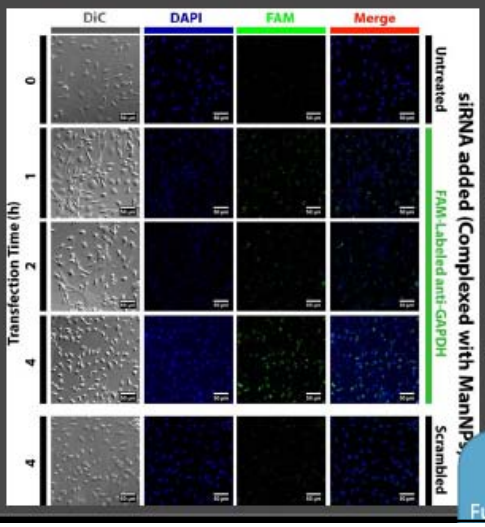

Fullscreen

ManNP-Delivered siRNA Knocks Down Target Gene in BMDMs

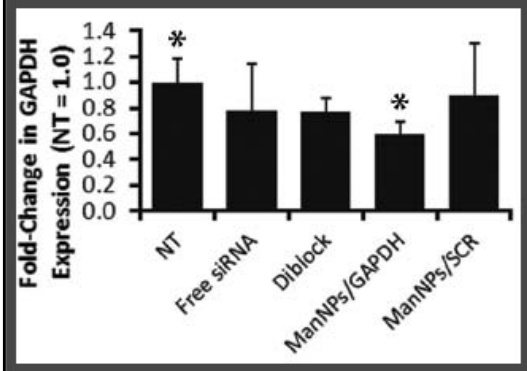

- *p < 0.05, n = 3
- 4 h transfection time
- NT = non-transfected
- SCR = scrambled siRNA

Fullscreen

ManNPs Selectively Target siRNA to Human Macrophages over Breast Cancer Cells

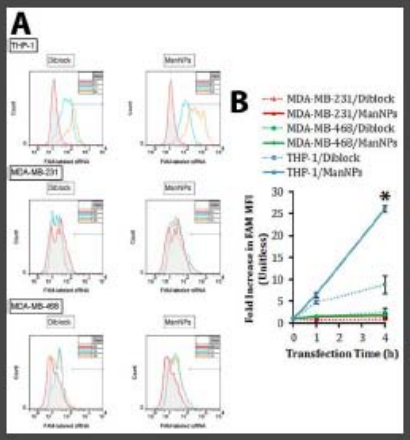

- *p < 0.01 vs. all other treatments at 4h
- THP-1: human leukemic macrophages

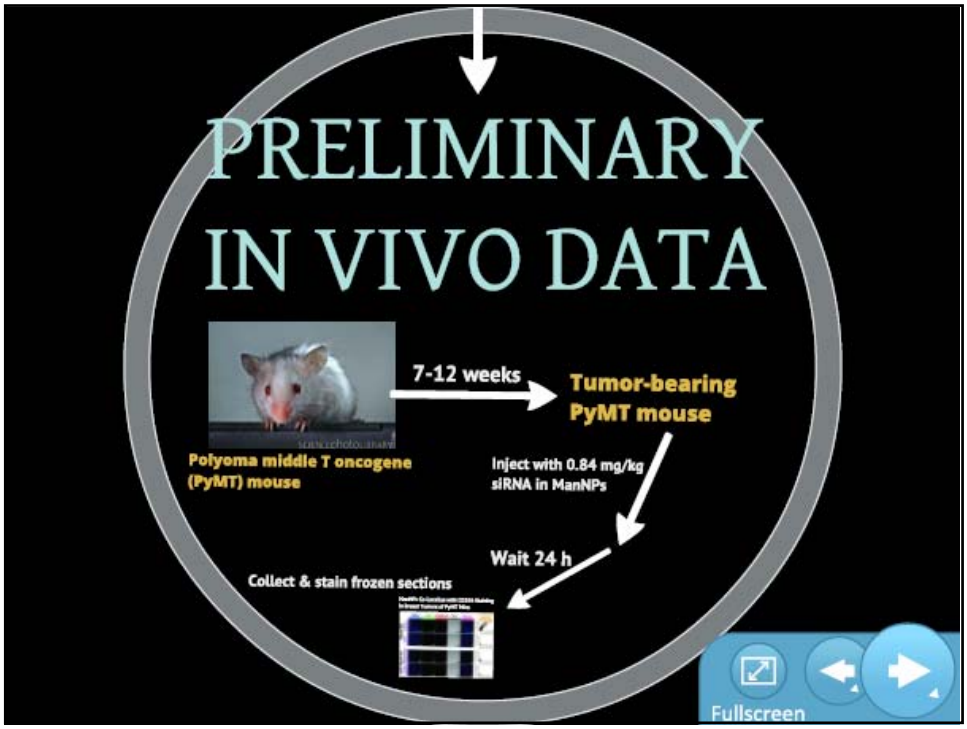
PRELIMINARY
IN VIVO DATA
7-12 weeks
Tumor-bearing
PyMT mouse
Polyoma middle T oncogene
(PyMT) mouse
Inject with 0.84 mg/kg
siRNA in ManNPs
Wait 24 h
Collect & stain frozen sections
Fullscreen

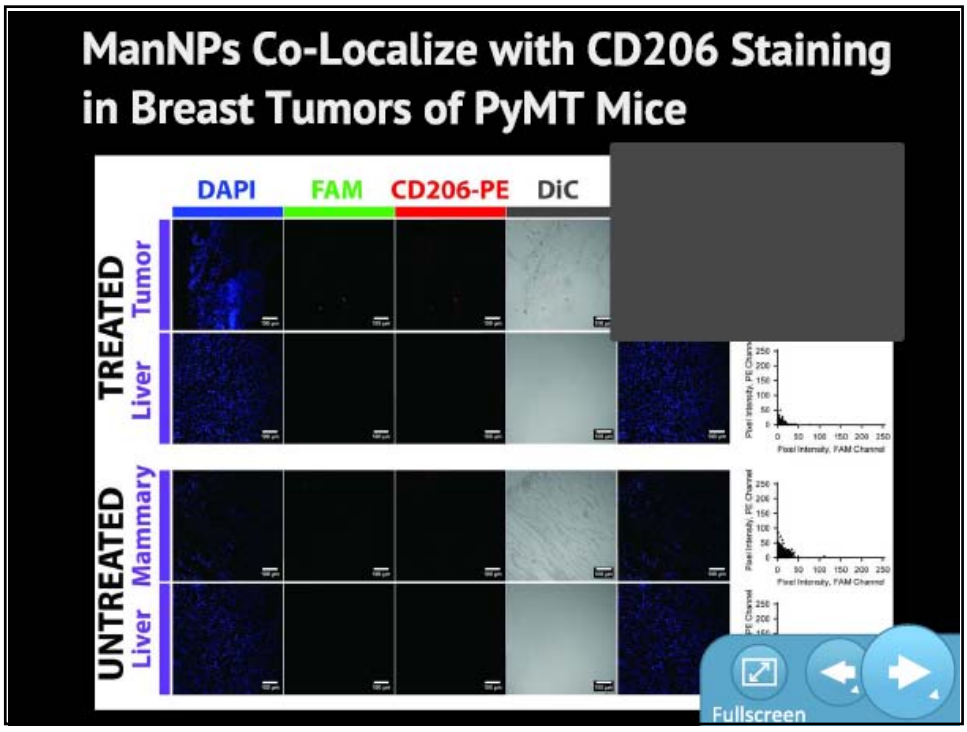
ManNPs Co-Localize with CD206 Staining
in Breast Tumors of PyMT Mice
DAPI
FAM
CD206-PE
DiC
TREATED
Tumor
Liver
UNTREATED
Mammary
Liver
Fullscreen

Conclusions

- Design, synthesis and characterization of a CD206-directed siRNA delivery agent
- Ongoing biodistribution studies to confirm site-specific and cell-specific siRNA delivery in PyMT mouse model

Fullscreen

ACKNOWLEDGMENTS

Funding Sources

- Department of Defense CDMRP-BCRP W81XWH-10-1-0684
- Department of Defense CDMRP-BCRP W81XWH-11-1-0344
- Department of Defense CDMRP-BCRP W81XWH-11-1-0242

Dissertation Committee Members

- Todd D. Giorgio (BME, ChBE, Cancer Bio)
- Hak-Joon Sung (BME)
- Craig L. Duvall (BME)
- Fiona E. Yull (Cancer Bio)
- David G. Harrison (Clinical Pharm)

Co-Authors

- Cheryl M. Lau
- Whitney J. Barham
- Halina M. Onishko
- Christopher E. Nelson
- Hongmei Li

Consultants

- Jared LeBoeuf (Histology)
- Becca Thomason / David Bader (Cryosections)
- Kwangho Kim (Chemical Synthesis)

Core Laboratory Facilities

- Vanderbilt Institute of Nanoscale Science & Engineering
- Cell Imaging Shared Resource

Fullscreen

VU Cancer Biology Research Hour
15 February 2012

Environmentally-Responsive Nano-Carriers for the Intracellular Delivery of RNAi Therapeutics into Tumor-Associated Macrophages

Shann S. Yu
Predoctoral Graduate Student
Laboratory of Todd D. Giorgio
Department of Biomedical Engineering

Awakening the Immune System to Address Metastatic Cancer

Fullscreen

The Presence of Tumor-Associated Macrophages (TAMs) is Associated with Poor Prognoses

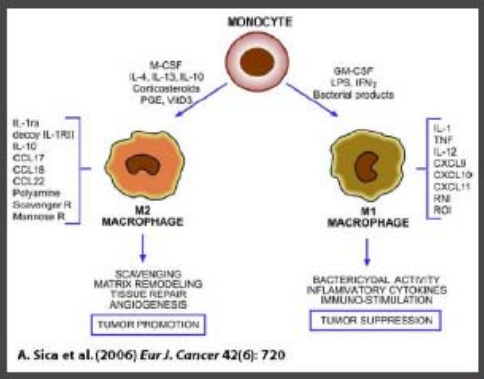

A. Sica et al. (2006) *Eur J. Cancer* 42(6): 720

Fullscreen

CENTRAL OBJECTIVE

TAM-specific siRNA-mediated silencing of master genes regulating activities.

IMMEDIATE OBJECTIVE

Design and characterize new vehicles for TAM-specific siRNA delivery.

Fullscreen

How to Transfect a Macrophage: Lessons from Nature

- Common animal viruses are able to interface with receptors on cell surface
- To access cellular machinery for viral replication, virus escapes from vesicle
- Viral macromolecule is optimized for cytosolic delivery of active virus

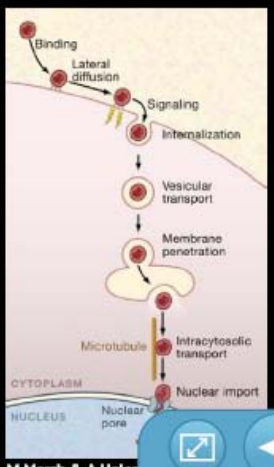

M Marsh & A Heler

Fullscreen

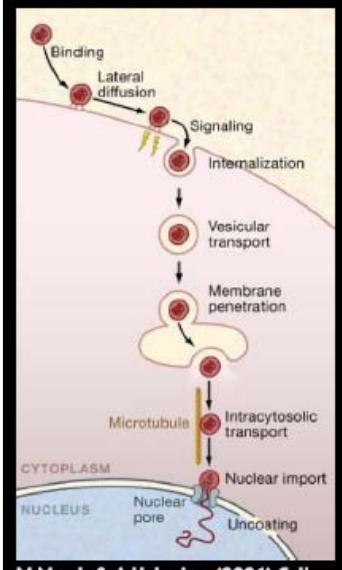

M Marsh & A Helenius. (2006) Cell.

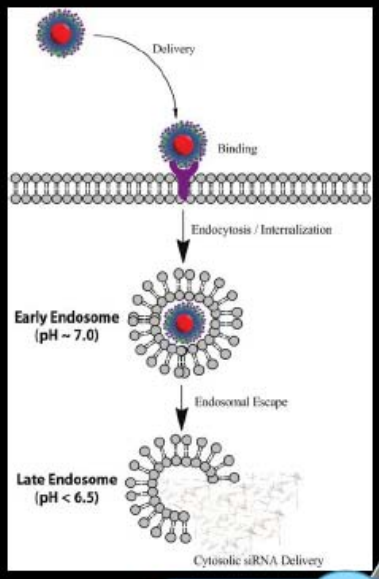

Fullscreen

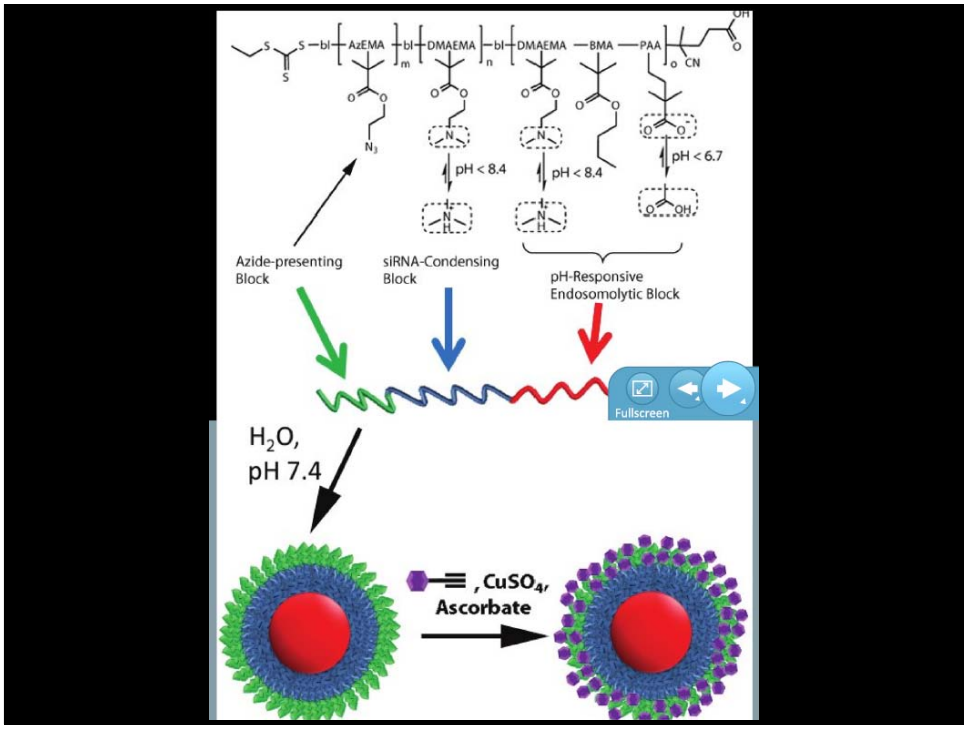
AzEMA
DMAEMA
DMAEMA
BMA
PAA
CN
pH < 8.4
pH < 8.4
pH < 6.7
Azide-presenting Block
siRNA-Condensing Block
pH-Responsive Endosomolytic Block
Fullscreen
H_2O, pH 7.4
, $CuSO_4$, Ascorbate

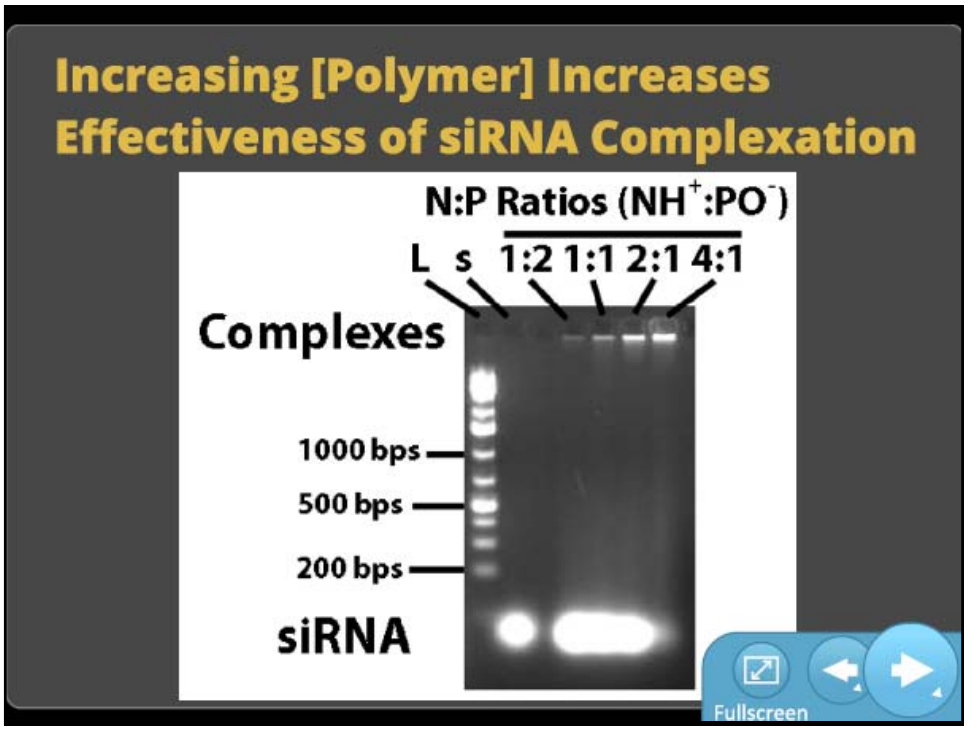
Increasing [Polymer] Increases Effectiveness of siRNA Complexation
N:P Ratios (NH^+:PO^-)
L s 1:2 1:1 2:1 4:1
Complexes
1000 bps
500 bps
200 bps
siRNA
Fullscreen

Polymers for siRNA Delivery form Micellar Nanoparticles

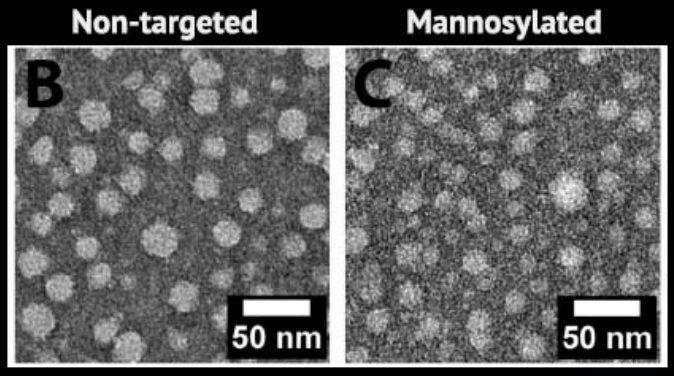

Micelles in water were dried onto TEM grids, and counterstained with uranyl acetate.

Fullscreen

ManNPs Enhance siRNA Delivery to Primary Murine Macrophages

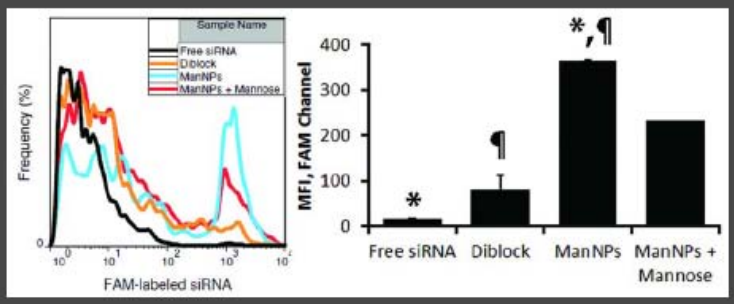

Cell line: Bone marrow-derived macrophages (BMDMs; FVB Background)
siRNA Used: FAM-labeled siRNA
*,¶ $p < 0.01$, Student's t-test

Fullscreen

ManNPs Enhance siRNA Delivery to Primary Murine Macrophages

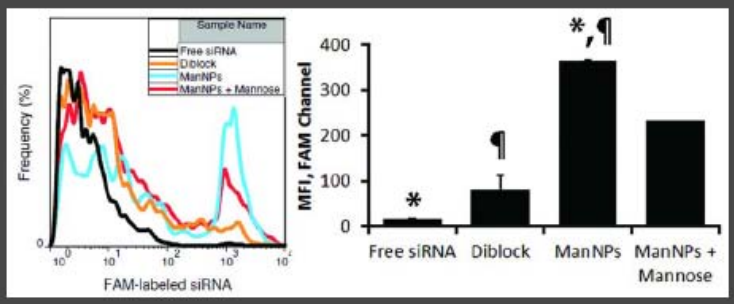

Cell line: Bone marrow-derived macrophages (BMDMs; FVB Background)
siRNA Used: FAM-labeled siRNA
*,¶ $p < 0.01$, Student's t-test

Fullscreen

BMDMs Rapidly Internalize siRNA Delivered via ManNPs

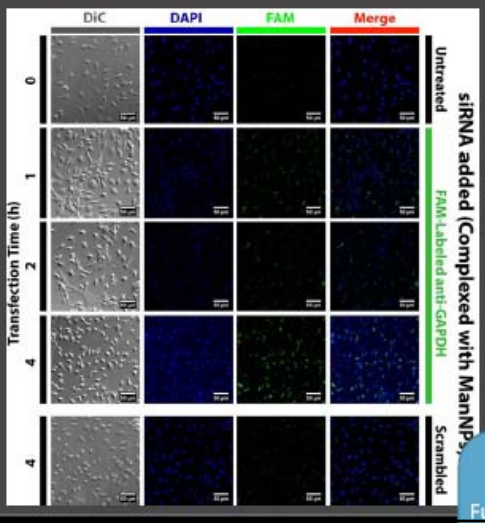

Fullscreen

ManNP-Delivered siRNA Knocks Down Target Gene in BMDMs

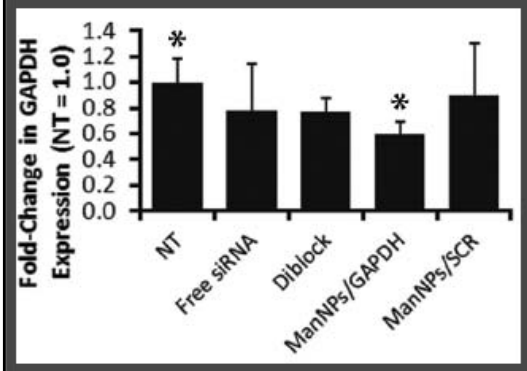

- *p < 0.05, n = 3
- 4 h transfection time
- NT = non-transfected
- SCR = scrambled siRNA

Fullscreen

ManNPs Selectively Target siRNA to Human Macrophages over Breast Cancer Cells

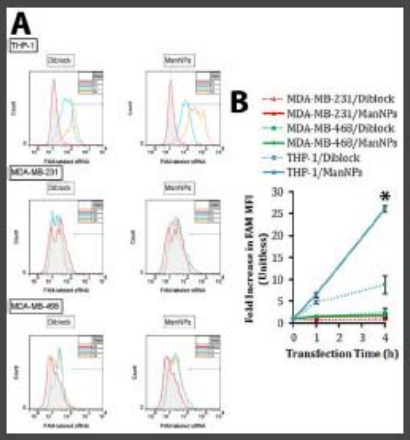

- *p < 0.01 vs. all other treatments at 4h
- THP-1: human leukemic macrophages

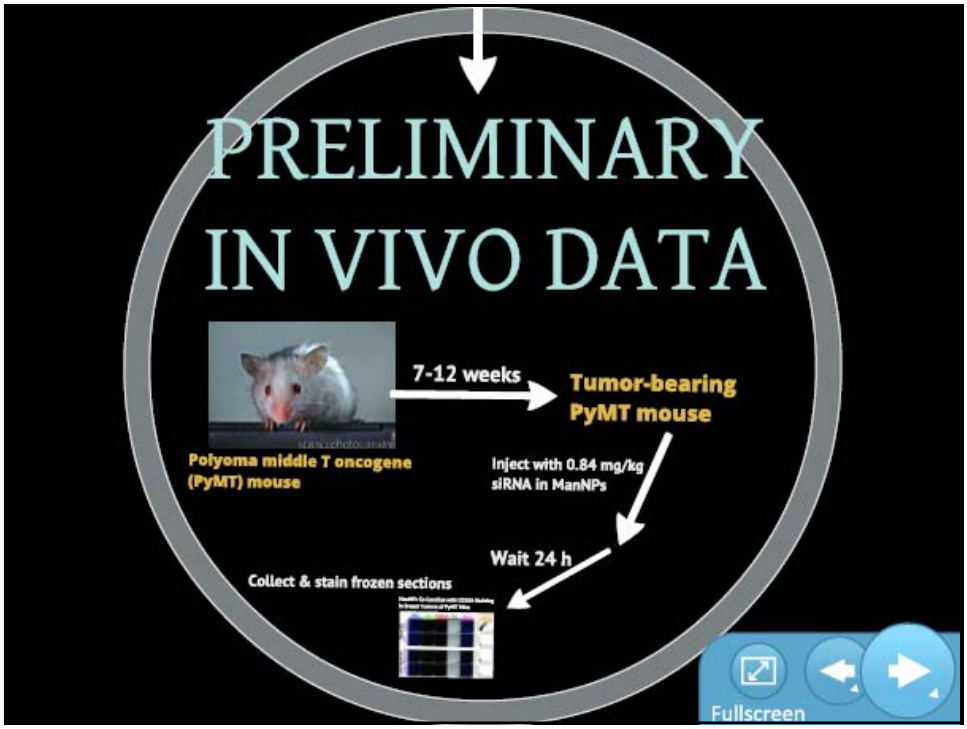
PRELIMINARY
IN VIVO DATA
7-12 weeks
Tumor-bearing
PyMT mouse
Polyoma middle T oncogene
(PyMT) mouse
Inject with 0.84 mg/kg
siRNA in ManNPs
Wait 24 h
Collect & stain frozen sections
Fullscreen

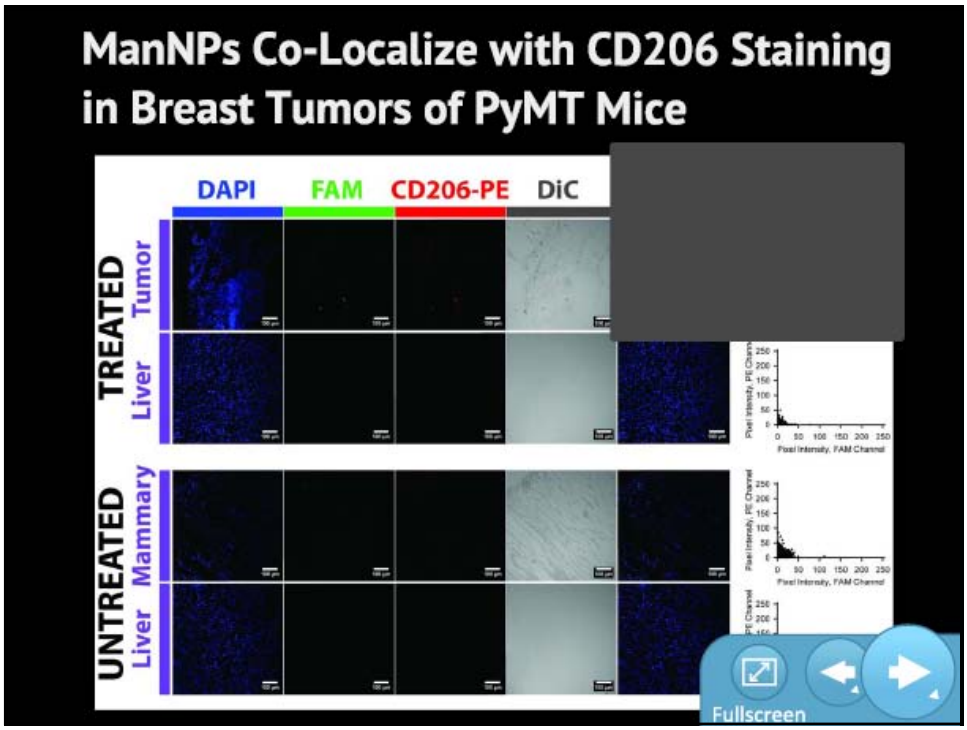
ManNPs Co-Localize with CD206 Staining
in Breast Tumors of PyMT Mice
DAPI
FAM
CD206-PE
DiC
TREATED
Tumor
Liver
UNTREATED
Mammary
Liver
Fullscreen

Conclusions

- Design, synthesis and characterization of a CD206-directed siRNA delivery agent
- Ongoing biodistribution studies to confirm site-specific and cell-specific siRNA delivery in PyMT mouse model

Fullscreen

ACKNOWLEDGMENTS

Funding Sources

- Department of Defense CDMRP-BCRP W81XWH-10-1-0684
- Department of Defense CDMRP-BCRP W81XWH-11-1-0344
- Department of Defense CDMRP-BCRP W81XWH-11-1-0242

Dissertation Committee Members

- Todd D. Giorgio (BME, ChBE, Cancer Bio)
- Hak-Joon Sung (BME)
- Craig L. Duvall (BME)
- Fiona E. Yull (Cancer Bio)
- David G. Harrison (Clinical Pharm)

Co-Authors

- Cheryl M. Lau
- Whitney J. Barham
- Halina M. Onishko
- Christopher E. Nelson
- Hongmei Li

Consultants

- Jared LeBoeuf (Histology)
- Becca Thomason / David Bader (Cryosections)
- Kwangho Kim (Chemical Synthesis)

Core Laboratory Facilities

- Vanderbilt Institute of Nanoscale Science & Engineering
- Cell Imaging Shared Resource

Our Crew in Stevenson Center 5,

Fullscreen

Targeted siRNA Delivery to Tumor-Associated Macrophages for Cancer Therapy

Cheryl Lau[1], Shann S. Yu[1], Whitney Barham[2], Halina M. Onishko[2], Fiona E. Yull[2], Craig L. Duvall[1], & Todd D. Giorgio[1].

[1]Department of Biomedical Engineering, Vanderbilt University, Nashville, TN 37235 [2]Department of Cancer Biology, Vanderbilt-Ingram Cancer Center, Nashville, TN 37232

Introduction

- Macrophages have two states:
  - M1 – proinflammatory, cytotoxic
  - M2 – angiogenic, tissue remodeling
- siRNA – short interfering RNAs that are complementary to genes of interest – bind to those genes and prohibit protein expression

Challenge: Deliver siRNAs to tumor associated macrophages (TAMs), possibly induce their transition from an M2 phenotype to an anti-tumor M1 state.

Targeting Tumor-Associated Macrophages

- Tissue macrophages express the **mannose receptor**
- Target siRNA condensing micelles to macrophages by attaching mannose to end of polymer via click chemistry

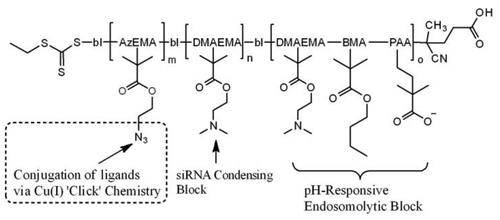

Figure 1. Composition of polymer forming siRNA-condensing micelles.

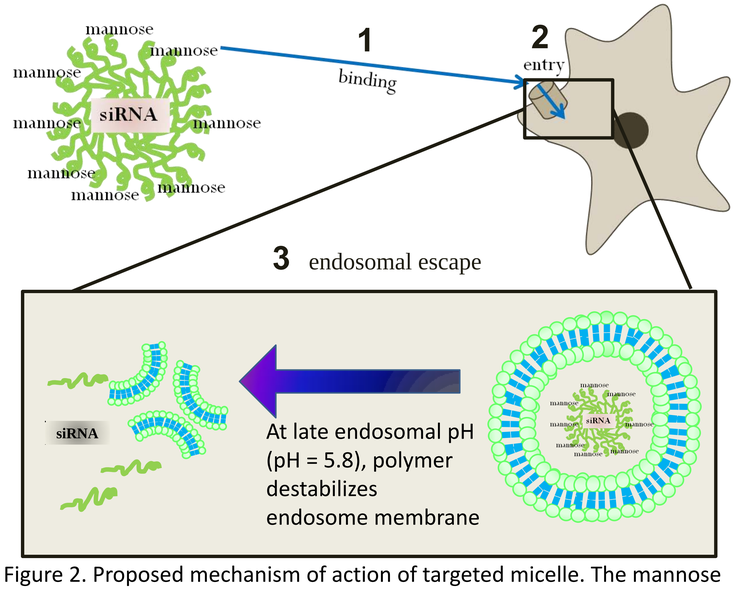

Figure 2. Proposed mechanism of action of targeted micelle. The mannose binding facilitates receptor-mediated endocytosis. The pH responsive copolymer destabilizes the membrane at late endosomal pH allowing for delivery of siRNA into cytoplasm of cell.[1]

Mannosylated Nanoparticles Enhance Delivery of siRNA into Primary Macrophages

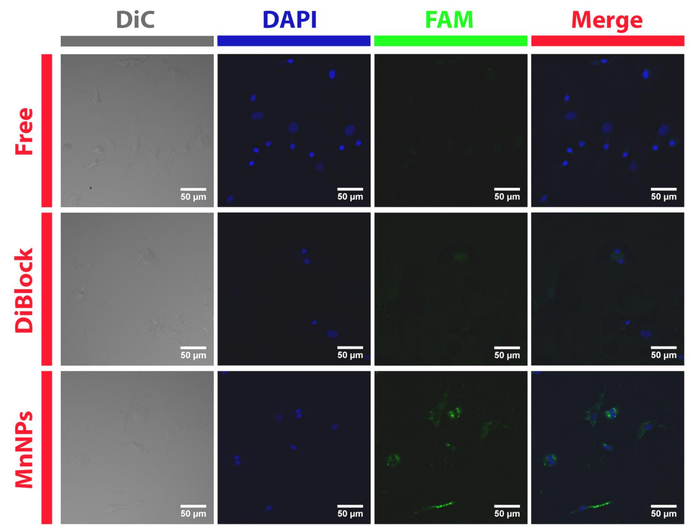

Figure 3. Confocal microscopy comparing internalization of FAM-labeled siRNA in the following conditions: a) Free siRNA, b) Untargeted diblock polymer micelle, c) Mannosylated diblock copolymer micelles.

Polymeric Micelles Effectively Complex siRNA

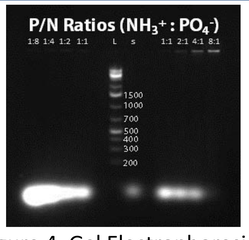

Figure 4. Gel Electrophoresis of various P:N ratios

- Positive charges from DMAEMA layer (P)
- Negative charges from siRNA (sugar phosphate backbone) (N)
- Gel Electrophoresis of siRNA loaded nanoparticles in the shown ratios
- 8:1 NP:siRNA ratio gives highest siRNA loading (band at top due to siRNA migration impedance because siRNA is protected by micelles)

Mannosylated Nanoparticles Protects siRNA from being Degraded

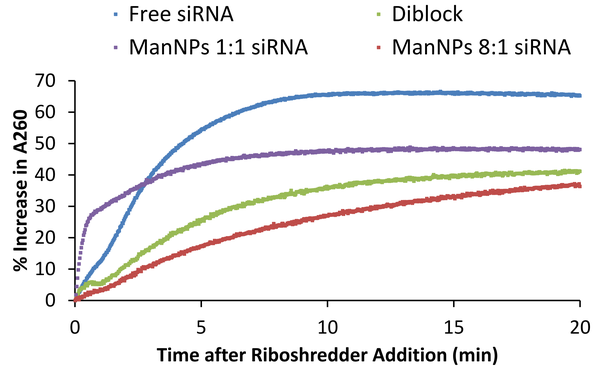

Figure 5. Comparison of RNA degradation for free siRNA vs. NPs+siRNA. Measurements were made via UV-Vis, absorbance at 260nm.

- A problem with delivering free siRNA is degradation by RNAases
- Riboshredder is a blend of potent RNAases that completely degrades RNA
- Degraded RNA will display a higher absorbance due to hyperchromic effect [2]
- 8:1 Mannose NPs :siRNA ratio protected siRNA from degradation

Micelles Exhibit Monodispersity and Cationic Surface Charge

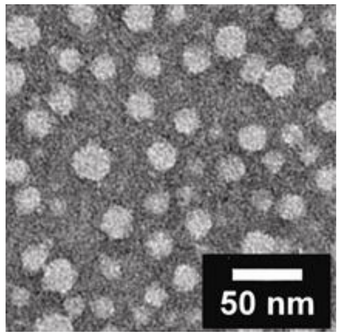

Figure 6. Transmission electron micrographs of micelles composed of mannosylated triblock copolymers. Micelles were stained with uranyl acetate for imaging

- Mannosylated tri-block micelles have a zeta potential of **19.6 ± 11.7 mV**

Conclusions / Future Work

- Mannosylated micelles deliver siRNA effectively to macrophages
- Future experiments include: cytotoxicity assay of micelles +siRNA, flow cytometry for quantification of siRNA uptake, evaluate GAPDH knockdown *in vitro*
- *In vivo* biodistribution imaging and macrophage collection.

References

1. AJ Convertine, DSW Benoit, CL Duvall, AS Hoffman, and PS Stayton. Development of a novel endosomolytic diblock copolymer for siRNA delivery. Journal of Controlled Release. 2009 Feb 10;133(3):221-9.

2. Kieleczawa, J. DNA sequencing II: optimizing preparation and cleanup, Volume 2. pp. 299.Jones & Bartlett Learning, 2006

Acknowledgments

This work is supported by an intramural Discovery Grant through Vanderbilt University (#4-48-999-9132), a Department of Defense CDMRP grant (#W81XWH-08-1-0502), and a Department of Defense IDEAS Award (#W81XWH-05-1-0306). In addition, the Harrison and Yull labs at the Vanderbilt Medical Center were invaluable with providing resources and guidance. Protocols for isolation of macrophages from mice were approved by the Vanderbilt University Institutional Animal Care and Use Committee (IACUC.)